Development of Exosome-Based Anti-Cancer Therapeutics

A thesis submitted by

Hanin Mohammed A. Alyamani

Strathclyde Institute of Pharmacy and Biomedical Sciences

University of Strathclyde
Glasgow, UK

Presented in fulfilment of the requirements for the degree of
Doctor of Philosophy
June 2020

Declaration

This thesis is the result of the author's original research. It has been composed by the author and has not been previously submitted for examination which has led to the award of a degree.

Signed: Hanin Alyamani

Date: 16/7/2020

Acknowledgments

First and foremost, I would like to express my appreciation and my sincere gratitude to my supervisors: Dr. Valerie Ferro and Dr. Rothwelle Tate for their excellent support, invaluable insights, enthusiasm, and constructive criticism during the entire period of this research. They are welcoming to offer help on any level, either emotionally or professionally. I would say I had great luck to work with them as determined scientists or as compassionate, and kind personalities.

My acknowledgements also go to my mother and father for supporting me emotionally and financially, particularly in the first year of my PhD studies. Significantly, I would immensely acknowledge and thank the Ministry of Education in Saudi Arabia for accepting me in their scholarship programme and sponsoring me during my studies which allowed me to achieve my goal in completing my doctorate degree.

Special thanks to the best brother ever and the best flatmate, Abdullah, for his support, help, and his encouragement to achieve my goals on every level. I wish him all the best in finishing his doctorate degree.

I would like to thank my siblings back home for reassuring me emotionally during my PhD journey.

Abstract

Hepatocellular carcinoma (HCC) exosomes are found to be responsible for cancer progression, metastasis, and angiogenesis via cellular communications. However, studying cancer derived exosomes *in vitro* is limited, due to the way cell lines are grown in medium supplemented with foetal bovine serum (FBS) that contains naturally occurring exosomes. Bovine-derived exosomes can cause artefacts and interfere with interpretation of results. The aim of this study was to investigate the release of exosomes from human liver cancer cell line HepG2 (HepG2-Exo) under different conditioned media with modified FBS to deliver the best approach for exosome production. Thus, two media were developed for growing HepG2 cell line which are M1 and M2 using dulbecco's modified eagle medium (DMEM), where M1 supplemented with 10 % (v/v) FBS, and M2 with 10 % (v/v) exosome depleted FBS (Dep-FBS). However, after cells reached confluency, those two media were removed and replaced with serum free media (only DMEM), to create M3 and M4, respectively. This resulted in collecting four categories of media: M1, M2, M3, and M4. Consequently, four groups of exosomes were obtained (Exo(M1), Exo(M2), Exo(M3), and Exo(M4). In regard to cell culture, findings confirmed that M2 was the best approach for cultivating HepG2 and collecting exosomes, as cell viability was enhanced and contamination with FBS-exosomes was minimal, compared to M1. However, analysis of the different HepG2-Exo groups showed significant difference in protein concentration, percentage of fluorescence, exosome marker detection, tetraspanins expression, particle count, metabolic and lipidomic profiling, RNA sequencing, and gene expression. This difference indicates that the effect of media composition is inevitable on cell-derived exosome which may cause misinterpretation of the effect of the exosomes of interest. Consequently, biological assessment and metabolomic profiling of HepG2-Exo effect on different cancer and

normal cell lines was carried out: A375 (melanoma), A549 (lung cancer), and PNT2A (normal prostate epithelium). The biological assays revealed that HepG2-Exo induced the proliferation, migration, adhesion, and invasion of A549 at 50 μg/ml. While metabolome analysis showed that HepG2-Exo at 100 μg/ml, induced significant changes in the cell metabolome of A375. The outcomes of this project provided an effective approach in developing successful cell culture for exosome collection without concern over contamination from FBS-derived exosomes and brought attention to the critical effect of media in exosome studies. Moreover, this project has highlighted the effect of HepG2-Exo on other cell lines and the potential of HepG2-Exo to be applied to the development of future lung cancer therapeutics.

Publications

- **Exosomes: Fighting cancer with cancer.** Hanin Alyamani, Mohammad A Obeid, Rothwelle J Tate, Valerie A Ferro**.** Therapeutic Delivery. 2018 Dec https://doi.org/10.4155/tde-2018-0051

- **Microfluidic manufacturing of different niosomes nanoparticles for curcumin encapsulation: Physical characteristics, encapsulation efficacy, and drug release.** Mohammad A. Obeid, Ibrahim Khadra, Abdullah Albaloushi, Margaret Mullin, Hanin Alyamani, Valerie A. Ferro. https://www.beilstein-journals.org/bjnano/articles/10/177

- **Melanoma Methods and Protocols.** Springer Nature's**.** Mohammad A. Obeid, Alaa Aljabali, Hanin Alyamani, Valerie A. Ferro. **Book Chapter** (**Submitted**)**.**

- **Optimisation of HepG2-exosomes production using different conditioned media.** Hanin Alyamani, Abdulmalik M. Alqarni, Mohammed Alrofaidi, Rothwelle J Tate, David G. Watson, Valerie A Ferro. (**To be submitted**)**.**

- **The Influence of HepG2-exosomes on cancer and normal cell lines.** Hanin Alyamani, Abdulmalik M. Alqarni, Mohammed Alrofaidi, Rothwelle J Tate, David G. Watson, Valerie A Ferro. (**To be submitted**).

Table of Contents

List of Figures

List of Tables

List of Abbreviations

>	More than
%	Percentage
˚C	Celsius
<	Less than
µg/ml	Microgram per mililitre
ACT	Adoptive cell therapy
Aex	Autologous ascites-derived exosomes
ALIX	(ALG-2)-interacting protein X
AML	Acute myeloid leukaemia
ANOVA	Analysis of variance
APCs	Antigen presenting cells
ATPase	Adenosine triphosphatase
BBB	Blood brain barrier
BCA	Bicinchoninic acid
BMDCs	Bone marrow DCs
BMMSCs	Bone marrow mesenchymal stem cells
BSA	Bovine serum Albumin
CAFs	Cancer associated fibroblasts
CCL	CC chemokine ligands
CD	Cluster of differentiation
CHMP4C	Charged multivesicular body protein 4C
CLL	Chronic lymphocytic leukaemia
CO_2	Carbon dioxide
CRC	Colorectal cancer
CSC	Cancer stem cell
CTL	Cytotoxic T lymphocytes

CV-ANOVA	Cross-validated residuals-ANOVA
CXCL12	C-X-C motif chemokine ligand 12
DCs	Dendritic cells
DC-SIGN	DC-specific intercellular adhesion molecule-3-grabbing non-integrin
DDR2	Discoidin domain receptor 2
Dep-FBS	Exosome-depleted foetal bovine serum
DKK1	Dickkopf-related protein 1
DMEM	Dulbecco's modified eagle medium
DNA	Deoxyribonucleic Acid
ECL	Enhanced chemiluminescence
ECM	Extracellular matrix
EE	Early endosome
EGFR	Epidermal growth factor receptor
ELISA	Enzyme-linked immunosorbent assay
EMT	Epithelial-to-mesenchymal transition
ER	Endoplasmic reticulum
ESCC	Esophageal squamous cell carcinoma
ESCRT	Endosomal sorting complexes required for transport
ESI	Electrospray ionisation
EVs	Extracellular vesicles
FACS	Fluorescence-activated cell sorting
FasL	Fas Ligand
FBS	Foetal bovine serum
GC	Gastric cancer
GM-CSF	Granulocyte–macrophage colony-stimulating factor
GNP	Gold nanoparticles
h	Hour
HBE	Human bronchial epithelial

HBSS	Hanks' balanced salt solution
HCC	Hepatocellular carcinoma
HFBRs	Hollow-fiber bioreactors
HGF	Hepatocyte growth factor
HNSCC	Head and neck squamous cell carcinoma
HPLC	High-performance liquid chromatography
Hrs	Hepatocyte growth factor-regulated tyrosine kinase substrate
HSP70	Heat shock protein 70
HUVECs	Human umbilical vein endothelial cells
ICAMs	Intercellular adhesion molecules
IGF1	Insulin like growth factor 1
IL-	Interleukin-
ILVs	Intraluminal vesicles
iNOS	inducible nitric oxide synthase
ISEV	International society for extracellular vesicles
kDa	Kilodaltons
KITL	kit ligand
KRAS	Kirsten rat sarcoma
LBPA	Lysobisphosphatidic acid
LC-MS	Liquid chromatography–mass spectrometry
LDH	Lactate dehydrogenase
LE	Late endosome
LFA-1	Lymphocyte function-associated antigen-1
lncRNAs	Long non-coding
Mac-1	Macrophage-1 antigen
MDR	Multiple drug resistance
MFG-E8	Milk fat globule factor 8 protein
MHC	Major histocompatibility complex

min	Minute
miRNA	Micro ribonucleic acid
MISEV	Minimal information for studies of extracellular vesicles
MM	Multiple myeloma
MMPs	Matrix metalloproteinases
mRNA	Messenger RNAs
MSC	Mesenchymal stem cell
MVBs	Multivesicular bodies
MWCO	Molecular weight cut off
NEAA	Non-essential amino acids
NK	Natural killer
NKG2D	NK (group 2D, member D)
NPC	Nasopharyngeal carcinoma
NSCLC	Non-small lung carcinoma
OSCC	Oesophageal squamous cell carcinoma
OVA	Ovalbumin
OXPHOS	Oxidative phosphorylation
PBMCs	Peripheral blood mononuclear cells
PBS	Phosphate buffered saline
PC	Phosphatidylcholine
PC	Pancreatic cancer
PCA	Principal component analysis
PCP	Planar cell polarity
PCR	Polymerase chain reaction
PDAC	Pancreatic ductal adenocarcinoma
PD-L1	Programmed cell death ligand 1
PE	Phosphatidyl-ethanolamine
PEG	Polyethylene glycol

PI3K–AKT	Phosphatidylinositol 3-kinase-protein kinase B
PI	Phosphatidylinositol
pi-RNAs	Piwi-interacting ribonucleic acids
PPI	Proton pump inhibitor
PS	Phosphatidylserine
PTEN	Phosphatase and tensin homolog
PVDF	Polyvinylidene fluoride
RIPA	Radioimmunoprecipitation assay
RNA	Ribonucleic acid
ROS	Reactive oxygen species
RT	Room temperature
Rt	Retention time
RT-qPCR	Real-time quantitative polymerase chain reaction
SD	Standard deviation
SDS	Sodium dodecyl sulphate
SDS-PAGE	Sodium dodecyl sulphate-polyacrylamide gel electrophoresis
SEC	Size exclusion chromatography
sE-cad	Soluble E-cadherin
SF	Serum free
SPH	Sphingomyelin
STAM1	Signal transducing adaptor molecule-1
TACSTD2	Tumour-associated calcium-signal transducer 2
TAMs	Tumour associated macrophages
TBST	Tris-buffered saline with tween
TCA	Tricarboxylic acid
TEIR	Total Exosome isolation reagent
TEX	Tumour derived exosome
TGF-β	Transforming growth factor beta

TGS	Tris/Glycine/SDS
TGX	Tris Glycine eXtended
Th1	Type I helper T cells
TIRF	Total internal reflection fluorescence
TNBC	Triple negative breast cancer
TPM	Transcripts per million
Treg	Human regulatory T cells
tRNAs	transfer RNA
TSG 101	Tumour susceptibility gene 101
UK	United Kingdom
uPA	Uroplasminogen activator
USA	United States of America
VASN	Vasorin
VCP	Valosin-containing protein
VEGF	Vascular endothelial growth factor
VPS4	Vacuolar protein sorting-associated protein 4
VPS4B	Vacuolar protein sorting-associated protein 4B
VTA1	Vacuolar protein sorting-associated protein VTA1 homolog
YB-1	Y-box1

List of Materials

Consumables/ Equipment /Software	Supplier/ Manufacturer
1 M glycine	Sigma-Aldrich, UK
10% Mini protein Tris Glycine eXtended Precast protein gel	Bio-rad, UK
4x Laemmli sample loading buffer	Bio-rad, UK
Accela HPLC system	Thermo Fisher Scientific, Germany
Accutase	Sigma-Aldrich, UK
ACE 5 C18-AR (150 × 4.6 mm, 3 µm)	HiChrom, UK
ACE C4 (150 × 3.0 mm, 3µm)	HiChrom, UK
Acetonitrile	Fisher Scientific, UK
Aldehyde/Sulphate Latex Beads, 4% (w/v), 4 µm	Life Technologies, UK
Automatic X- Ray Film Processor-Model JP-33	JPI Healthcare Solutions, USA
BD CompBead Anti-Mouse Ig, κ/Negative Control Particles Set	Fisher Scientific, UK
Bovine serum albumin	Sigma-Aldrich, UK
Cell culture flasks	Sigma-Aldrich, UK
Cell proliferation Kit I	Sigma-Aldrich, UK
Chloroform	Fisher Scientific, UK
Corning®Bottle-top vacuum filter system (0.22 µm)	Sigma-Aldrich, UK
CytoSelect™ 24-well Cell Migration and Invasion Assay (8 µm), Colorimetric - Combo Kit	Cambridge Bioscience, UK
CytoSelect™ 48-Well Cell Adhesion Assay (Collagen I-Coated, Colorimetric Format)	Cambridge Bioscience, UK

Dulbecco's Modified Eagles medium- High glucose (D6429)	Sigma-Aldrich, UK
Electrophoresis tank, and power pack	Bio-rad, UK
Exactive Orbitrap mass spectrometer	Thermo Fisher Scientific, Germany
Exosome-depleted FBS (A2720801)	Life Technologies, UK
ExoView R100	NanoView, USA
ExoViewTM platform	NanoView, USA
FBS	HyClone, UK
Flow Cytometer (Canto)	BD Biosciences, UK
Gibco™ RPMI 1640 Medium	Invitrogen, UK
Goat anti-mouse IgG H&L secondary antibody (Alexa Fluor® 488)	Abcam, UK
GraphPad Prism software version 5.00	San Diego, USA
Haemocytometer	Sigma-Aldrich, UK
Hanks' Balanced Salt solution	Sigma-Aldrich, UK
HPLC grade water	Fisher Scientific, UK
Human hepatocellular carcinoma (HepG2)	ATCC® HB-8065™, USA
L-glutamine	Sigma-Aldrich, UK
Methanol	Fisher Scientific, UK
Micro BCA Protein Assay kit	Life Technologies, UK
Microscopy	Olympus, Japan
MZMatch software	SourceForge, USA
NanoViewer 2.8.9	NanoView Biosciences, USA
Nitrocellulose membrane	GE Healthcare Life Sciences, UK
Non-essential Amino Acids	Sigma-Aldrich, UK
NScan v2.8.9	NanoView Biosciences, USA
Penicillin–Streptomycin	Sigma-Aldrich, UK
Phosphate-buffered saline	OXOID, UK
Pierce™ enhanced chemiluminescence	Life Technologies, UK

Primary monoclonal mouse anti-CD63	Abcam, UK
Primary monoclonal mouse anti-CD81	Life Technologies, UK
Protease inhibitor	Cambridge Bioscience, UK
Rabbit anti-mouse IgG (H+L) HRP secondary antibody	Life Technologies, UK
Radioimmunoprecipitation assay buffer	Cambridge Bioscience, UK
Sigma Centrifuge 1K15	Philip Harris Scientific, UK
SIMCA-P software v.14.1	Umetrics, Sweden
Sodium Pyruvate	Sigma-Aldrich, UK
SpectraMax M5 plate reader	Molecular Devices, USA
StepOne Plus Real-Time PCR System	Applied Biosystems, UK
TaqMan™ Advanced miRNA Assays: mir-21-5p (Assay ID: 477975_mir), mir-23a-3p (Assay ID: 478532_mir), mir-26a-5p (Assay ID: 477995_mir), and mir-423-5p (Assay ID: 478090_mir)	Life Technologies, UK
TaqMan™ Advanced miRNA cDNA Synthesis Kit	Life Technologies, UK
TaqMan™ Fast Advanced Master Mix	Life Technologies, UK
Tetraspanin Exoview kit	NanoView Biosciences, USA
Total Exosome Isolation reagent	Life Technologies, UK
Total Exosome RNA and Protein Isolation Kit	Life Technologies, UK
Tris/Glycine buffer	Bio-rad, UK
Tris/Glycine/SDS buffer	Bio-rad, UK
Tris-buffered saline	Sigma-Aldrich, UK
Trypan blue dye	Sigma-Aldrich, UK
Tween 20	Sigma-Aldrich, UK
Universal vacuum system	Thermo Fisher Scientific, Germany
Vacuum centrifuge -SPD SpeedVac	Thermo Fisher Scientific, Germany

Xcalibur 2.1.0 software	Thermo Fisher Scientific, Germany
X-Ray Film	Thermo Fisher Scientific, Germany
ZIC-pHILIC (150 × 4.6 mm, 5 μm)	HiChrom, UK

Chapter 1

Introduction and literature review of exosome-based anti-cancer therapeutics

Abstract

Exosomes are nanovesicles secreted by many cells, including cancer cells. Extensive research has been carried out to validate potential applications of exosomes and to evaluate their efficiency in a wide range of diseases, including cancer. In this chapter, the current knowledge on the origin, biogenesis and composition of exosomes will be described, followed by a review on cancer derived exosomes and their role in cancer progression and the most applicable exosomal therapeutic approaches. After that, the current challenges in large scale-exosome production will be highlighted. In addition, the most common techniques in exosome isolation and their limitations along with exosome characterisation methods followed in this project, will be reviewed.

Keywords: Exosomes, cancer, miRNA, progression, therapeutic, diagnostic, nucleic acid, angiogenesis, immunosuppression, immune system.

1.1. Introduction

Cellular communications are carried out through delivering and receiving chemical and mechanical signals that induce a particular response in the recipient cells. These signals are found primarily in the form of extracellular vesicles (EVs). These EVs are divided into three subtypes according to their size range and origin: (1) apoptotic bodies (50 nm-5 µm); (2) microvesicles or ectosomes (50 nm–1 µm); and (3) exosomes (30–150 nm), the smallest group of vesicles in dimensions compared to other vesicles [1–3].

Exosomes are secreted to maintain normal physiological functions. While in response to pathological conditions, exosomes are found to be secreted in high numbers reflecting any alterations in parent cell composition. Therefore, exosomes found to play a major role in cancer progression and metastasis via mediating intercellular communications and modulating immune responses [4–8].

Thus, the aim of this chapter is to focus on the role of cancer-derived exosomes in promoting cancer progression, metastasis, and immune system modulation, starting with reviewing their biogenesis, structure and composition, then analysing the challenges of generating large scale production of exosomes. After that, exosome isolation techniques and their limitations followed by characterisation methods of exosomes are discussed.

1.2. Discovery of exosomes

In the 1970s, fragments of plasma membrane were discovered circulating in biological body fluids such as serum, blood, and urine that had been shed from viable human cells such as liver cells, *in vivo* and *in vitro* [9–12]. However, during the 1980s, laboratories of Stahl and Johnstone reported their observations regarding the secretion of EVs that were found to be involved in the uptake and the release of transferrin during the maturation cycle of reticulocytes in blood [13–17]. Briefly, they noticed that EVs formed by inward

budding inside intracellular endosomes lead to the formation of multivesicular bodies (MVBs) that were released into the extracellular space by exocytosis [14–18]. By 1987, the term “exosome” was used for the first time to describe these tiny membrane vesicles [17,18].

1.3. Exosome biogenesis

In the endo-lysosomal system, the formation of endosomes starts with invagination of the membrane, to sort the early endosomes (EEs). The content of EEs is mainly derived from the plasma membrane during the sorting process of endosomes. Subsequently, EEs mature into late endosomes (LEs). During the maturation process, a large number of intraluminal vesicles (ILVs) are formed in LEs. Hence LEs are commonly named MVBs (Figure 1.1) [19–21]. The biogenesis of exosomes starts during the formation of ILVs which is thought to be driven by CD9 and CD63 tetraspanins and the endosomal sorting complexes required for transport (ESCRT) [22,23].

ESCRT are made up of four multimeric protein units: ESCRT-0, ESCRT-I, ESCRT-II and ESCRT-III. Generally, they work collectively in this subunit machinery in a unique way to deform membranes surrounding the endosome through particular interactions [21,24]. Briefly, ESCRT-0 is used to cluster cargo through, in a ubiquitin-dependent manner. ESCRT-I and ESCRT-II are both stimulate budding, and ESCRT-III induces vesicle splitting. In addition, there are accessory proteins that contribute to the ESCRT machinery, which are the vacuolar protein sorting-associated protein adenosine triphosphatase (4VPS4 ATPase), tumour susceptibility gene 101 (TSG101), and (ALG-2)-interacting protein X (ALIX). For instance, VPS4 ATPase has a role in dissociating and recycling the ESCRT complex, to assist in the final stages of ILV formation [21,22]. On the other hand, the removal of ESCRT-0 associated proteins hepatocyte growth factor-regulated tyrosine kinase substrate (Hrs)

and TSG101, and signal transducing adaptor molecule-1 (STAM1) protein of ESCRT-I, decrease exosome secretion [25,26]. In contrast, the suppression of associated proteins of ESCRT-III such as charged multivesicular body protein 4C (CHMP4C), vacuolar protein sorting-associated protein 4B (VPS4B), VTA1 and ALIX results in an increase in exosome production. Therefore, the presence and the absence of these accessory proteins plays a critical role in exosome secretion and biogenesis [25,26].

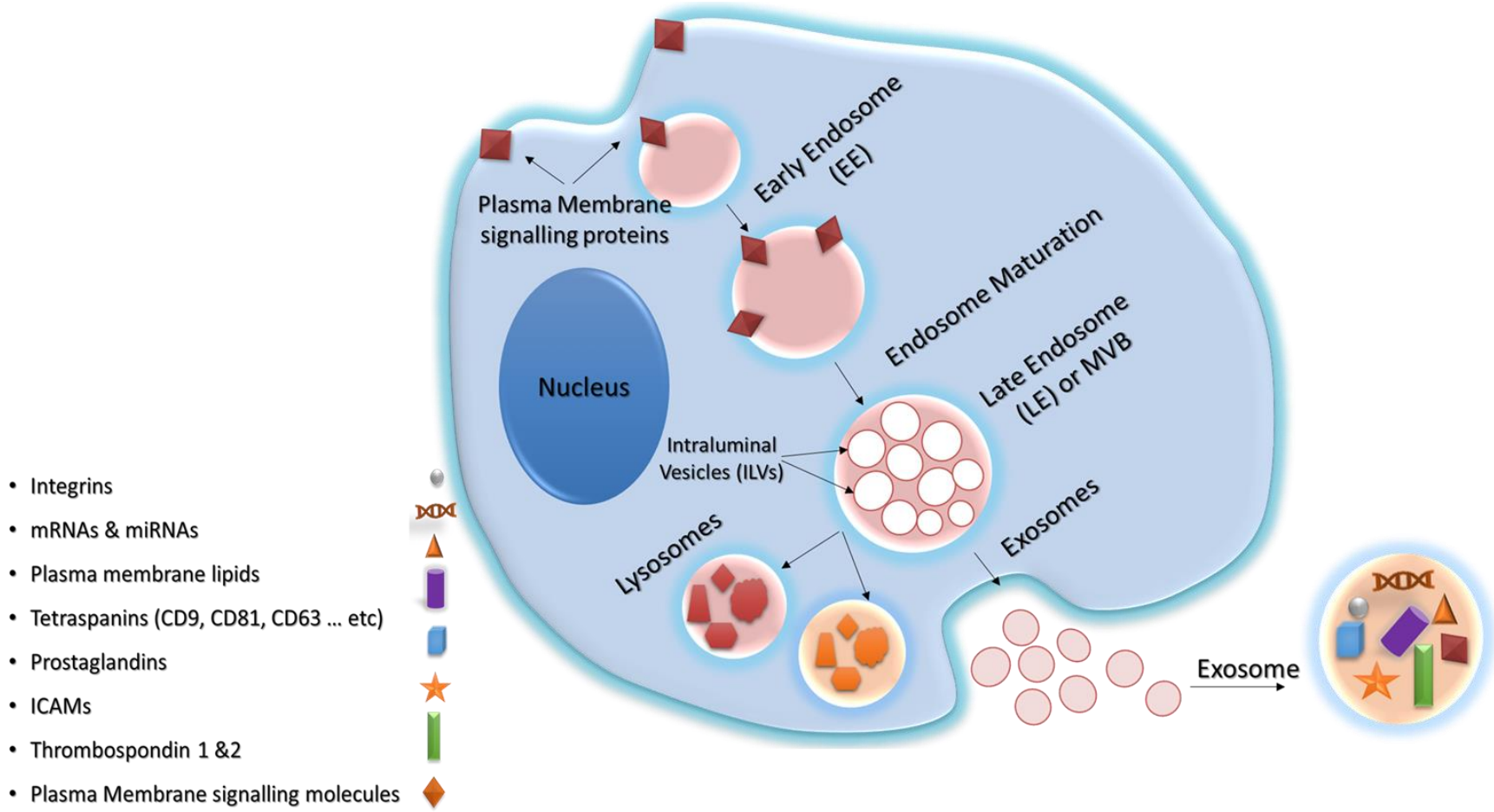

Figure 1.1: Schematic illustration of exosome biogenesis and release.

Endocytosis process starts through the invagination of cell membrane and its substance (proteins, lipids, proteins, fluids, electrolytes, microorganisms, and macromolecules), to form a vacuole i.e. early endosome (EE). EE matures into late endosome (LE) where intraluminal vesicles (ILVs) start to be formed. LE are known as multivesicular body (MVB) which contains the exosomes. The exosomes release into the extracellular environment, maintain the parent cell membrane properties, and carry cell-specific cargos of proteins, lipids, and genetic materials.

1.4. Structure and composition of exosomes

Due to the extensive investigation and increasing interest in exosomes and EVs structure and composition, two databases were developed to co-ordinate all the efforts on the characterisation and identification of their structure and content. EV structure characterisation is summarised in the Vesiclepedia database (http://microvesicles.org). While proteomic and genetic information of exosome content, are collected in ExoCarta (http://www.exocarta.org), which is a regularly updated database [27–29]. A summary of the key components of exosomes are described below.

1.4.1. Lipids

1.4.1.1. Prostaglandins and lysophophatidic acid

Exosomes were found to be enriched with many lipids such as prostaglandins which are known for their role as cell signalling mediators [30]. Another important lipid is lysobisphosphatidic acid (LBPA) which is considered an exosomal lipid that has been found abundantly in MVB internal membranes. Also, LBPA and ALIX were found to play a role in internal vesicle budding to form ILVs within MVBs, which consequently contributes to the process of exosome production. Moreover, low LBPA levels results in reduced numbers of ILVs formed within MVBs [31].

1.4.1.2. Plasma membrane lipids

The exosome lipid bilayer is mainly composed of plasma membrane lipids such as sphingomyelin (SM), phosphatidyl-ethanolamine (PE), phosphatidylserine (PS), ganglioside GM3 and phosphatidylinositol (PI) [32]. Recently, these lipids were found to be asymmetrically distributed in the exosome bilayer membrane. For instance, SM and other sphingolipids are expected to be located in the outer layer, while the other lipid classes are mainly distributed in the inner layer. This asymmetrical distribution of lipid classes can be

changed under the influence of different enzymes such as flippases, floppasses and scramblases [33]. The presence of these lipids varies depending on the origin of the exosomes. For instance, reticulocytes contain phosphatidylcholine (PC), forming half of the exosomes' lipids [34]. While exosomes originating from mast cells and dendritic cells (DCs), consist of less than one third of PC in their overall lipid content [35].

1.4.2. Proteins

Exosome-associated proteins are involved in regulatory processes and induce cellular responses. Exosomal proteins play a functional role in inhibiting interactions with extracellular components and facilitate entry to target cells [36]. Key proteins are described below:

1.4.2.1. Tetraspanins

CD9, CD63, CD81 and CD82 are exosomal transmembrane proteins that are known as tetraspanins. Often, they are used as markers for exosomes [37–39]. Some of these tetraspanins are detected in high concentrations in exosomes compared to their parent cells. For instance, exosomes derived from DCs are found enriched in CD9 compared to cells they originate from [40]. Whereas exosomes released from B lymphocytes are found heavily enriched in CD37, CD63, CD81 and CD82 [39,41]. While CD81 is specifically present in high levels in trophoblast-derived exosomes, in contrast, CD63 is not detected in either exosomes or their parent cells [42].

The relatively small size of tetraspanins (20–30 kDa) and their limited interaction between ligand and receptor makes them difficult to investigate; hence, biochemical or immunological detection is not successful [43]. However, total internal reflection fluorescence (TIRF) microscopy, a super resolution microscopy, has been used to study the dynamics of tetraspanin CD9 web, a network of molecular interactions [44]. Therefore,

techniques include super resolution microscopy and the analysis of tetraspanins dynamics can provide essential insights into the function of these molecules [45].

1.4.2.1.1 Role of tetraspanins

It is believed that tetraspanins work as mediators of fusion, cell migration, cell to cell adhesion and signalling [46]. Furthermore, they have a fundamental action in ESCRT-independent pathways, particularly with regard to the differences between cell types [39]. For instance, in mice with CD9 deficiency, exosome production is affected in bone marrow (BM) DCs (BMDCs) [47]. In contrast, the deficiency of CD81 in lymphocytes does not affect the production of exosomes [48]. In addition, tetraspanins are involved in cargo selection, targeting and uptake, target cell reprogramming and antigen presentation [39,49]. CD9, CD63, CD81 and CD82 tetraspanins also play a role in DCs migration [37,38]. These tetraspanins are considered as regulators for antigen presenting cells (APCs) including DCs, monocytes, and B cells. They are also involved in regulating efficient immune responses [50]. Moreover, exosomal tetraspanins are found to be involved in meditating metastasis through regulating the communication of stromal and cancer cells, and altering the extracellular matrix of the host [49].

1.4.2.2. Adhesion molecules

1.4.2.2.1. Integrins

By referring to the ExoCarta database, integrins are classified as exosomal proteins, that have been found abundantly, specifically in tumour and immune cell-derived exosomes [51]. They are found as heterodimers (α and β subunits) and 24 different heterodimers have been observed in vertebrates. β_1, β_2 integrins, and αv containing integrins represent the largest categories. They work as adhesion molecules and organise binding of cells to the extracellular matrix (ECM) [52,53]. In exosomes, these integrins play a role in guiding the vesicles to fuse to the desired target cells [54]. Moreover, in cancer cell-derived

exosomes, integrins and their ligands are found to be involved in cancer progression through targeting tissues and inducing integrin mediated signalling pathways, in order to initiate the formation of metastatic niche [55]. It was also suggested that exosomal integrins and their ligands can be utilised to develop exosome based diagnostics and therapeutics [55].

1.4.2.2.2. Thrombospondin 1 and 2

Thrombospondin 1 is classified as an adhesion molecule, found in exosomes that has been demonstrated particularly in healthy volunteers' physiological fluids such as urine and saliva [56–59]. Additionally, patients with cancer in general, show exosomes contain thrombospondin 1 and 2 [60,61]. Recently, Cen *et al*. (2019) confirmed the role of thrombospondin 1 expressed in cancer-derived exosomes in facilitating the migration of breast cancer cells, to promote metastasis [62].

1.4.2.2.3. Intercellular adhesion molecules (ICAMs)

The intercellular adhesion molecules (ICAMs) family is considered one of the adhesion molecule classes involved in cell adhesion and leukocyte trans-endothelial migration [63]. ICAM-1 and ICAM-3 have been demonstrated in exosomes derived from immune cells [41,64–67].

1.4.2.2.3.1 Role of ICAMS

ICAMS are considered significant mediators during immune responses. For instance, ICAM-1 is meant to be a ligand for integrin α_L β_2 lymphocyte function-associated antigen-1 (LFA-1) and macrophage-1 antigen (Mac-1). Moreover, it induces leukocyte adhesion [68]. Interestingly, ICAM-1 is detected abundantly in exosomes derived from mature DCs compared to exosomes derived from immature DCs. It has been stated that mature DC-derived exosomes are more potent than immature DC-derived exosomes to stimulate T cell activation *in vitro*. It has been suggested that mature exosomes enriched with ICAM-1

play a role in exosome adhesion to trigger APCs, through priming naive T cells [69]. A follow up study has revealed that exosomes bearing high levels of ICAM-1 trigger stronger immunity responses, *in vitro* and *in vivo*. It has been demonstrated that the adhesion of exosomes to immune cells is mediated through the expression of ICAM-1 on exosomes, and LFA-1 ligand on recipient CD8+ cells *in vivo* [70]. Moreover, ICAM-1 is found to be enriched in myeloid leukaemia-derived exosomes, that is responsible for the modulation of the neovascularisation process [71]. While ICAM-2 and ICAM-3 were found to be attached to DC-specific intercellular adhesion molecule-3-grabbing non-integrin (DC-SIGN), ICAM-2 on endothelial cells and ICAM-3 on T lymphocytes, were found to contribute to trans-endothelial migration of DCs and the formation of DCs-T cell synapse (C), respectively [72]. In terms of exosomes, ICAM roles are still under examination [73].

1.4.2.3. Other membrane proteins

Another protein considered to be important is lactadherin (also known as Epidermal Growth Factor (EGF)-factor VIII or Milk Fat Globule factor 8 protein (MFG-E8)) [40]. Lactadherin has specifically been found in immune cell-derived exosomes and fibroblasts [40,74–76]. It has been found that the C1C2 domain of lactadherin influences antigen expressing tumours when combined with a protein of interest. For instance, a vaccine consisting of chicken ovalbumin (OVA) encoded in a DNA vector bound to the C1C2 domain, showed slower growth in tumours expressing OVA antigen, compared to vaccination with OVA vector only [77–79].

1.4.3. Nucleic acid

miRNA and messenger RNAs (mRNA), are significant components of exosomes in healthy and disease conditions. These exosomal RNAs are either encoding protein or silencing targeted genes, and transferred between cells, respectively. Exosomal RNA is found to be involved in several biological processes such as immune system activation or inhibition,

cancer progression, angiogenesis, and metastasis [80–87]. Other types of RNA have been found in exosomes, such as viral RNAs, Y-RNAs, fragments of transfer RNAs (tRNAs), small nuclear RNA, small nucleolar RNA, piwi-interacting (pi-RNAs), and long non-coding (lncRNAs). Around 764 microRNAs (miRNAs) and 1639 mRNAs have been discovered in these nanovesicles arising from different tissues [88–91]. The loading mechanism of these RNA species into exosomes are not fully known [27].

1.5. Biological functions of exosomes

Exosomes originate from different cell types and can be present in biological fluids such as urine, breast milk, synovial fluid, blood, saliva and amniotic fluid [92]. For this reason, exosomes appear to play a significant role in cell-to-cell and initiate important physiological responses such as coagulation, angiogenesis, immune system activation or suppression and inflammation [93]. Exosomes were initially found to be involved in the maturation cycle of the cell to remove unnecessary proteins [94]. Exosome functions also vary based on their origin or parent cell [93]. Platelet-derived exosomes, are involved in the inflammation reaction due to the presence of prostaglandin in these exosomes [95]. Furthermore, in cancer, exosomes contribute into developing a tumour microenvironment through delivering mutated genetic material and misfolded proteins [96–99].

In this review, the biological role of cancer derived-exosomes will be discussed in the next section 1.6 to provide a better understanding of the critical role of exosomes released from cancer tissues.

1.6. Cancer-derived exosomes

Cancer derived exosomes involved in cancer pathogenesis through influencing the recipient cells biological process such as proliferation, migration, adhesion, and invasion [100]. These biological processes will be reviewed in detail in chapter 3, section 3.1.

However, this section will focus mainly on cancer-derived exosomes role in cancer progression, major signalling pathways, immune system modulation, and angiogenesis.

1.6.1. The role of cancer-derived exosomes in cancer progression

In pathological conditions, cancer stem cells and mesenchymal stem cells (MSCs) are considered tumour microenvironment regulators, therefore, it is believed that their secretion of exosomes contributes to their regulatory function through cell-to-cell communication [101]. It has also been found that exosomes exert an endocrine effect which means that they can migrate to distant cells and induce cell transformation. Hence, cancer cell derived exosomes are considered tissue modulators due to their role in tumour growth and cell progression. Also, these exosomes named as ''oncosomes'' due to their ability to travel to distant tissues, develop a pre-metastatic niche, and stimulate the migration of tumour cells to a conditioned tumour microenvironment [102,103]. For instance, a recent study was carried out by Kumar *et al.* (2018), to reveal the pathogenesis process of acute myeloid leukaemia (AML). It has been found that AML-derived exosomes induce Dickkopf-related protein 1 (DKK1) expression in BM stromal cells which suppress normal haematopoiesis and osteogenesis, causing loss of osteoblasts. Moreover, tumour derived exosomes (TEX) cause downregulation of supporting genes of haematopoietic stem cells in BM such as C-X-C motif chemokine ligand 12 (CXCL12), kit ligand (KITL) and insulin like growth factor 1 (IGF1), which affect the normal haematopoiesis process [104]. Recent studies by Zheng *et al.* (2018), and Nakamura *et al.* (2019), discussed in depth the roles of TEX in promoting the progression of non-small cell lung cancer (NSCLC) and ovarian cancer [105,106].

In normal conditions, the immune system is considered to induce apoptosis and suppress aggressive progression. For instance, exosomes secreted from APCs induce the expression of major histocompatibility complex (MHC) class I and II on the cell surface, which are

followed by specific immune reactions through the activation of CD8+ and CD4+ [54,107,108]. While in the case of tumour progression, immunosuppression is promoted by cancer-derived exosomes through stimulating the production of suppressor cells, or inhibiting cytotoxic T cell production, natural killer cells (NK) and APCs [109]. It has to be noted that DCs are considered professional APCs due to their antigen presenting capacity, and their ability to prime and initiate T cells responses [110]. Furthermore, It has been found that the maturation process of DCs can be inhibited via the uptake of cancer-derived exosomes [111]. It has previously been reported by Valenti *et al.* (2006) that the production of DC is affected by TEX that resulted in low expression of DC co-stimulator molecules and secretion of inhibitory cytokines, due to insufficient priming of T-cell by DCs [112].

Tumour cells escape being destructed by cytotoxic T cells through expressing low levels of MHC-I, however, tumour cells are still recognised by NKs [113]. Nevertheless, exosomes are still able to avoid destruction by NKs. For instance, Hedlund *et al*. (2011) observed that NK (Group 2D, member D) (NKG2D) receptor was found to be expressed on exosomes which caused an impairment of NKG2D mediated NK-cell cytotoxicity, resulting in immune evasion of leukaemia/lymphoma cells [114].

1.6.1.1. Exosomal signalling pathways in cancer microenvironment

TEX found to be associated with multiple signalling pathways that play a key role in tumour initiation and progression, however, the role of these exosomes is not fully elucidated in these pathways [115]. For instance, TEX found to induce the expression of transforming growth factor beta (TGF-β) receptors I and II, and TGF-β-related signalling pathways in recipient cells [116] which found to be mainly involved in the generation and maintenance of tumour stroma and the initiation of epithelial-to-mesenchymal transition (EMT) [97]. In breast cancer, TEX found to stimulate the TGF-β receptor-mediated signalling pathway in MSCs promoting their differentiation to myofibroblasts, which are major components of

tumour stroma [117]. Moreover, exosomes containing TGF-β1 can induce immune suppression by impairing the lymphocytes response to interleukin (IL-)2 [118].

Exosomal tetraspanins, CD82 and CD9 found to regulate the Wnt signalling pathway via the discharge of β-catenin from exosome [47] where Wnt-β-catenin pathway plays a key role in normal development and in cancer [47,119]. For instance, fibroblast-derived exosomes were found to be containing autocrine Wnt-11 that was found to induce invasiveness in breast cancer cells via the Wnt-planar cell polarity (PCP) signalling pathway [120].

TEX found also to be loaded with phosphatase and tensin homolog (PTEN) which induce phosphatase activity in recipient cells, causing reduction in cellular proliferation [121]. PTEN function through regulating phosphatidylinositol 3-kinase-protein kinase B (PI3K-AKT) signalling, cell growth and cell survival [122].

Furthermore, Notch signalling, a survival pathway deregulated in tumours, found to be influenced by exosomes [121,123,124]. For instance, in pancreatic tumour, TEX interact with target cells which in turn supress Notch-1 survival pathway and stimulate apoptosis [125].

1.6.1.2. Immune system activation and suppression

Cancer progression is induced through several biological processes including the activation of immune suppressor cells, defective antigen presentation, and the induction of T-cell apoptosis that results in insufficient immune response [113,126].

Modulation of immune responses in cancer, is found to be influenced by surface proteins and genomic content of exosomes [127].

In terms of immune system activation, several studies have shown that T cells can be activated directly and indirectly by exosomes [128–130]. For instance, in direct activation, exosomes produced by APCs such as DCs exhibit MHC class I and II peptides, co-stimulators and adhesion molecules. The presence of these molecules on exosome surfaces facilitate the activation of T cells (CD8+ and CD4+) in order to induce a prominent immunogenic response [54,107,131]. Indirectly, DCs transduced with tumour peptides, produce immunogenic exosomes that cause a significant anti-tumour response through activation of T cells (CD8+) [54]. Furthermore, NK cells and macrophages can be activated by the presence of heat shock protein 70 (HSP70) on the exosomal surface [132]. It has been found that exosomes released from cancer cells subjected to heat stress induce stronger anti-tumour immune response compared to non-heat stressed cancer cell-derived exosomes [133]. Exosomes derived from immune cells (e.g. NK) have an immune function. NK-derived exosomes contain perforin molecules which are known as effector molecules. It has been suggested that perforin molecules can trigger cell death through exosome uptake by the target cells with consequent release of perforin inside the target cell. These exosomes work as mediators of anti-tumour activities [134].

However, TEX can work as immune system suppressants [108]. Exosomes modulate immune system responses through several processes such as changing the gene expression and the function of human regulatory T cells (Tregs) through signalling with cell surface receptors [135]. Also, It has been noted that nasopharyngeal carcinoma (NPC) or TEX

modulate the phenotype of Tregs and induce their suppressive function [136,137]. Furthermore, TEX have been found to induce the production of prostaglandin E2, IL6, and TGF-β from MDSCs that resulted in forming a immunosuppressive environment [138,139]. Another example is demonstrated by NK cells that can be suppressed by TEX expressing a NKG2D receptor [118]. Moreover, in a recent study, circulating plasma exosomes of patients with AML were found to carry immunosuppressive antigens and inhibitory molecules that suppress activated immune cells and interfere with adoptive cell therapy (ACT). This was investigated through the administration of activated NK cells into AML patients with pre-therapy plasma. This resulted in immunological dysfunction which included NK cell deficiency and suppressed activity, high levels of Tregs, and dysregulated cytokines which could result in leukaemia relapse [140].

TEX can also play an indirect role in favour of disease progression through influencing monocytes and macrophages to exhibit immunosuppressive molecules such as dysregulated cytokines. For instance, in chronic lymphocytic leukaemia (CLL), TEX contain a noncoding Y RNA, an exosomal miRNA called hY4. This hY4 was found to possess a pro-tumourigenic effect that was able to induce the production of phenotypically CLL associated monocytes expressing programmed cell death ligand 1 (PD-L1). This study has indicated that the transfer of TEX or hY4 to monocytes, induced inflammatory related cancer reactions and immune escape via the expression of PD-L1 [141]. Macrophages are normally originated from monocytes released from bone marrow [142,143], and differentiated into two polarised types: type 1 macrophages (M1) and type 2 macrophages (M2) [144]. Tumour associated macrophages (TAMs) are found to possess high degree of phenotypic plasticity, where M1 and M2 are found to be inducing two extreme different reactions in tumour microenvironment, where M1 expressing inducible nitric oxide synthase (iNOS), reactive oxygen species (ROS), and producing type I helper T cells (Th1)-associated cytokine IL-12 which elicit a strong immune response and cause tumour

suppression [145], and M2 expressing high levels of IL-10, arginase 1, and the CC chemokine ligands (CCL)17 and CCL22 which induce tumour progression through promoting angiogenesis and tissue repair [144,146]. In gastric cancer (GC), released exosomes were found to enable monocytes to produce TAMs expressing PD-L1 with M2-like surface phenotypical characteristics that inhibit anti-tumour immunity and induce tumour progression [147].

Immune cell-derived EVs including exosomes, are considered factors that facilitate the metastasis of HCC, via lncRNAs shuttle between immune cells and human liver cancer cell-derived EVs (exosomes) that can result in metastatic phenotypical acquisition in the immune cells mediated through their EVs [148].

1.6.1.3. Angiogenesis

TEX are found to be strongly involved in the angiogenic process through their role in cell-to-cell communication, and their genetic and proteomic cargo that may induce upregulation or down-regulation of significant proteins and genes in normal tissue, enhance tube formation, and increase cell proliferation [149]. Several studies have demonstrated significant effects of TEX on tumour progression and angiogenesis, summarised in Table 1.1.

Table 1.1: Summary of several cancer studies that confirmed the role of TEX in tumour progression, metastasis, and angiogenesis.

Cancer	Cancer cell line - derived exosomes/ EVs	Exosome Role	Recipient cell line	Outcomes
Human renal cancer stem cells (CSCs)	Renal CSCs expressing CD105 (Human).	Twenty-four exosomal miRNAs found to be responsible for regulating significant biological processes such as transcription, metabolic processes, proliferation, nucleic acid binding and cell adhesion molecules. Also, contain pro-angiogenic genes such as vascular endothelial growth factor (VEGF), fibroblast growth factor (FGF), angiopoietin1, ephrin A3 (EFNA3), matrix metalloproteinase 2 (MMP-2), and MMP-9 and growth factors.	Human umbilical vein endothelial cells (HUVECs)	Development of lung pre-metastasis niche, and stimulation of the angiogenesis process [150].

HCC	Huh-7 liver cancer cell line expressing CD90 (Human).	High levels of lncRNA H19 found in exosomes that induce the modulation of endothelial cell phenotype with more angiogenic properties and to induce the adhesion of CD90+ cells to endothelial cells through overexpression of ICAM-1 in HUVECs.	HUVECs	Promoting tube formation (angiogenesis) and cell adhesion [151].
Head and neck squamous cell carcinoma (HNSCC)	PCI-13 and UMSCC47 cell lines (Human).	Exosomes containing proangiogenic proteins such as uroplasminogen activator (uPA), coagulation factor III, IGFBP-3, endostatin, and MMP-9.		Tumour angiogenesis [152].
Leukeamia	K562 cell line (Human).	High levels of exosomal miR-210 induce angiogenic activity in endothelial cells.		Promoting tube formation (angiogenesis) [153].
Multiple Myeloma (MM)	RPMI8226, KMS-11, and U266.	Upregulation of miR135b in exosomes derived under hypoxic conditions.		Induced endothelial tube formation and angiogenesis [154].

Oesophageal squamous cell carcinoma (OSCC)	ECA109, KYSE410 and HET-1A cell lines (Human).	Upregulation of mRNAs expressed in exosomes that are responsible for cell proliferation and migration, and cell pathways under normoxic and hypoxic conditions.	HUVECs	Modification of the phenotypic profile of HUVECs. Stimulation of HUVECs proliferation, migration, invasion and tube formation, was mainly induced by hypoxic exosomes [155].
Lung cancer	Transformed human bronchial epithelial (HBE) cell line (Human).	Activation of STAT3 in transformed cells, found to induce the production of exosomes with high levels of mir-21, which caused an increase in VEGF levels in normal HBE cells, and induce angiogenesis.		Promoting angiogenesis and tube formation [156].

NPC	C666-1 cell line (Human).	Upregulation of pro-angiogenic cell adhesion proteins in exosomes such as ICAM-1 and CD44v5 1, and downregulation of TSP-1, an angio-suppressive protein.	HUVECs	Stimulation of angiogenesis through inducing tube formation, migration and invasion [157].
Ovarian cancer	Caov-3 and OV-90 cell lines (Human).	Exosomes containing high levels of soluble E-cadherin (sE-cad) which promotes tumour angiogenesis.		Enhancement of angiogenesis, stimulation of migration and tube formation in HUVECs [158].
Pancreatic cancer (PC)	PK-45H cell line (Human).	Exosomes involved in stimulating phosphorylation of Akt and ERK1/2 signalling pathway molecules and tube formation via dynamin-dependent endocytosis in HUVECs.		Promoting angiogenesis [159].

HCC	HepG2 cell line (Human).	Exosomes expressing HSP70, which are responsible for endothelial cell migration and lumen formation via the PI3K-AKT pathway. Also, upregulation of miR-145 and miR-27 was observed.	HUVECs	Angiogenesis [160].
Ovarian cancer	CAOV3 cell line (Human).	Exosomes containing potential proteins related to angiogenesis, such as ATF2, MTA1, ROCK1/2.		Angiogenesis [161].
HCC	HepG2 cell line (Human).	Exosomes expressing Vasorin (VASN), that mediates the communication between tumour cells and endothelial cells.		Promoting the migration of HUVECs and stimulating the angiogenesis process [162].

Mentioned studies in Table 1.1 have suggested the use of cancer-derived exosomes, their upregulated genes, and protein as therapeutic approaches in the future to suppress angiogenesis and prevent cancer progression.

However, in order to employ exosomes in therapeutic applications, production of exosomes on a large scale is required in such applications as tissue regeneration and immune response modulation [163]. However, there are challenges to overcome harvesting exosomes that will be discussed in section 1.7.

1.7. Challenges in large scale -exosome production

Exosome production levels and cargo are found to be strongly influenced by cell culture conditions such as culture containers, cell type, medium composition, hypoxia, and treatment of cells [164]. For instance, it has been demonstrated that the analysis of exosomes derived from cells cultured in conventional cell culture dishes *versus* two-chamber bioreactors, revealed that exosomes produced in both containers were similar in terms of morphology, size distribution and surface markers, however, two-chamber bioreactors yielded exosomes that were more than 100 times higher compared to dishes. In addition, significant differences were detected by metabolomic analysis using non-targeted LC–MS metabolite profile analysis [165] Also, another study employed hollow-fibre bioreactors (HFBRs) for culturing human adipose-derived MSCs (hMSCs) while control cultures were grown in T225 flasks, for comparison purposes. Findings showed that exosome yield was significantly increased in HFBRs compared to the flasks. Moreover, continuous production of exosomes was maintained during 10 weeks of harvesting with no requirement to subculture the cells, where the phenotype of the cells remained constant [166].

However, cell seeding density play a significant role in exosome production and their purity. For instance, cells seeded at different densities (low, medium, and high) during a 72h incubation period, cells reached sub confluency in low density cell cultures, and reached confluency in medium density cell cultures after 36h, however, both were found to produce

a sufficient yield of exosomes with a minimal contamination with proteins. While high density cell cultured cells reached confluency after 12h and were found to inhibit exosome production per cell with increased contamination with medium-derived proteins. Therefore, it is necessary to stabilise and standardise the same cell seeding protocol to maintain the production of exosomes of the same constancy in terms of levels and cargo [167].

Moreover, the composition of medium used for cell culturing and exosome recovery were found to play an important role in exosome production. For instance, Burger *et al*. (2017) found that high glucose levels in culture media induced EVs production and the generation of bigger vesicles (250 nm). They reported that proteomic analysis showed molecular composition of EVs had changed. These exosomes were found to express exosomal proteins that were involved in stimulating molecular pathways in recipient cells. However, EVs produced under lower glucose levels were found to activate different molecular pathways, compared to EVs derived from cells cultured with higher glucose levels [168]. Earlier on, Rice *et al*. (2015), reported that exosome production had increased under high glucose levels and the bioactivity of exosomes had altered, when compared to exosomes isolated from low glucose level medium [169]. In contrast, glucose deprivation was found to also induce exosome secretion, and change their protein content [170].

In order to minimise contamination from foetal bovine serum (FBS) derived EVs or exosomes, it has been suggested that cells be cultivated in the absence of serum using platelet lysates, pituitary extracts, bile salts or synthetic factors as a substitute [171]. However, Zhou *et al*. (2017) found that growth factors exert an effect on regulating exosome production, as they found that exosome production was significantly decreased after treating cells with epidermal growth factor (EGF), and increased after treating cells with epidermal growth factor receptor (EGFR) inhibitor, gefitinib [172].

Furthermore, hypoxia is considered a major factor that influences exosome production, as it was demonstrated that under hypoxic conditions, exosome secretion increased and their tetraspanins expression (exosomal markers) changed [152,167]. Moreover, the exosome cargo was found to be affected under hypoxic conditions [99].

Moreover, some drug treatments of cells were found to affect exosome secretion. For instance, Datta *et al*. (2018) tested a total of 4580 pharmacologically active compounds, 22 compounds were found to either stimulate or reduce exosome production [173].

Oxidative stress was also found to stimulate exosome production. For example, Atienzar-Aroca *et al*. (2017) exposed cells to increasing concentrations of ethanol to induce oxidative stress; a two-fold increase in exosome production was observed [174].

Thus, more advanced equipment is required to minimise the effect of these factors on exosome secretion and to induce exosome secretion on a large scale. For instance, the HFBR system was found to be an efficient platform for maintaining successful and constant cell culture, and large scale consistent production of pure exosomes [165,166] The major benefits of employing HFBR over flask-based methods, it ensures the stability and constancy of cell culture, and maintains high scalable consistent exosome secretion, compared to T-flask exosome production. Moreover, it offers successful cell culture in serum free media, in order to avoid the interference with FBS endogenous exosomes. Furthermore, it reduces apoptosis and cellular debris, which makes the exosome purification process easier [166]. Therefore, HFBRs are considered a promising platform for large-scale production of exosomes for therapeutic applications [166].

In this project in order to have a greater understanding of the factors that affect exosome production, the flask method was used instead of HFBRs as a cost-effective option. To

provide greater insight into isolation methods and their effect on exosome yield, the most common isolation techniques and their limitations are discussed in sections 1.8 and 1.9.

1.8. Exosome isolation techniques

Different methods for exosome isolation have been developed, to obtain an exosomal fraction of high purity, and to be applicable with exosomes isolated from different biological fluids or cell cultures [21]. These methods have exploited specific characteristics of exosomes such as their size, shape, density, and surface proteins [17]. However, each method has its pros and cons in terms of recovery, purity, required sample volume, and time required for isolation; determined based on sample source, intended use, and the downstream analysis of exosomes [17,21,175]. Thus, commonly used methods are outlined below in more detail:

1.8.1. Ultracentrifugation

Ultracentrifugation or differential centrifugation is the most commonly applied method used to isolate exosomes from all types of human samples [176,177]. The principle of this method is to precipitate, and isolate exosomes, and remove any contaminants such as residual cells, large vesicles, cellular debris, and macromolecular proteins through numerous centrifugation steps accompanied by gradual increase in centrifugation forces and duration at low temperature (4°C) to obtain an enriched sediment of pure exosomes [17,176,178,179].

1.8.2. Sucrose density gradient centrifugation

Sucrose density gradient centrifugation is an ultracentrifugation method, used to separate exosomes from other vesicles based on their floatation densities ranging from 1.08 to 1.22 g/ml, by applying centrifugal force, and using a pre-constructed density gradient of sucrose

built in an ultracentrifuge tube; called a sucrose gradient [17,175,180–183]. Exosome samples are then placed at the top of this sucrose gradient consisting of overlapping lower concentrations of sucrose on higher concentrations, ranging from 20% to 70% sucrose, from top to bottom in the centrifuge tube. After that, exosomes are collected by fractionation [17,175,181–184].

1.8.3. Exosome precipitation

Precipitation of exosomes is achieved using commercial reagents, such as ExoQuick (System Bioscience) [185], the Total Exosome Isolation kit (Invitrogen) [186], Exo-spin (Cell Guidance System) [187] that enables exosome enrichment [21]. These reagents consist of polyethylene glycol (PEG), a water excluding polymer, therefore, after adding the reagent to the sample, water molecules are tied-up and exosomes and other particles are precipitated out of solution. This is followed by centrifugation to pellet down the precipitated vesicles [188].

1.8.4. Immunoaffinity capturing

The principle of immunoaffinity capture-based techniques is to capture exosomes using specific antibodies, that are capable of binding an antigen expressed on the exosome surface. Selected antibodies for a specific antigen of interest can be used in different experimental sets [189]. For instance, enzyme-linked immunosorbent assay (ELISA) can be used for isolating exosomes via immobilising exosomal antibodies on the surface of a microplate to allow capture of exosomes via their expressed antigens [190]. Another immunoaffinity technique, is magneto-immunoprecipitation which works by the attachment of specific antibodies against the antigen of interest, to streptavidin coated magnetic beads. This is followed by incubation with exosome samples to allow the antibody-antigen binding, hence, exosome capture occurs [178,189].

1.8.5. Size exclusion chromatography (SEC)

Size exclusion chromatography (SEC) is used to separate proteins of different sizes, however, this approach can be utilised to separate exosomes from other EVs based on their size. This separation is achieved using columns packed with a porous stationary phase that allows small particles to penetrate the pores and be eluted after the larger particles. Purification of exosome samples using SEC is usually followed after performing ultracentrifugation of the sample, to allow the enrichment of the sample [191,192].

1.8.6. Ultrafiltration

Ultrafiltration is a technique used for separating exosome particles based on their size and molecular weight cut off (MWCO) of the membrane being used. Thus, particles larger than the MWCO are retained by the filter and the smaller ones pass through [178,189].

1.9. The advantages and the limitations of techniques used for exosome isolation

Techniques used for isolating exosomes have been developed to separate exosomes from other EVs and molecules as described in section 1.9. However, these techniques suffer from different challenges that affect the purity of the exosome fraction, quality of produced exosomes, the recovery level, the time consumed for preparation, the volume of sample (i.e. biological fluid or cell culture), equipment affordability, technical expertise and downstream analysis. An overview of the advantages and the limitations of each technique is described in Table 1.2.

Table 1.2: Overview of the advantages and the limitations of each isolation technique.

Technique	Advantages	Limitations
Ultracentrifugation	• Little technical expertise required. • No sample pre-treatment. • Equipment affordability (i.e. only one ultracentrifuge) to be used over a prolonged period for several applications and different experiments [189].	• Time consuming. • Co-precipitation of protein molecules, other EVs with exosomes (low purity). • Large starting volume required. • Low exosome recovery. • Instrument-dependent [175,181,184,189,193,194].
Sucrose density gradient centrifugation	• Exosome fraction of high purity. • Preserves the integrity and biological activity of exosomes [175,184,195].	• Time consuming. • Preparation of sucrose gradient. • Low exosome yield [175,184,195].

Exosome precipitation	• Fast and easy processing. • High yield of exosomes. • Little technical expertise required. • Equipment affordability (no special instrument required). • Small volumes of sample can be processed [178,189,196].	• Lack of selectivity. • Preparation step is required (i.e. ultracentrifugation or filtration). • Co-precipitation with other particles (EVs and protein molecules) [178,188,197,198].
Immunoaffinity capturing	• High specificity and purity (i.e. isolation of exosome of specific source. • The ability to be highly selective, where a specific exosomal biomarker is identified [61,188,194,199].	• Capturing only expressed surface antigen. • Low exosome yield. • Antibody-assay determined. • Prior enrichment required using ultracentrifugation or ultrafiltration [61,178,197].

Size exclusion chromatography (SEC)	• Maintaining the physiological and biochemical properties of the exosomes (i.e. structure, integrity, and biological activity). • High purity [192].	• Time consuming. • Preparatory step required (i.e. ultracentrifugation). • Hard to be scalable [192].
Ultrafiltration	• Fast and effective isolation of exosomes of large volumes. • High purity. • High exosomes yield. • Equipment affordability [184,188].	• Filter clogging with trapped vesicles may lead to loss of exosomes. • Deformation, or lysis of exosomes, due to the shear force [189,200].

Due to inconsistency in the outcomes of these methods (Table 1.2), method standardisation is required to deliver exosomes of high yield and greater purity [184], as lack of standardisation was found to cause an overlap of protein profiles and the physiochemical and biochemical properties of exosomes and other EVs [201,202]. Furthermore, the proteomic profiling of EVs was also found to be dependent on the isolation technique [201].

Another challenge of exosome isolation in cell cultures, is the contamination of cell derived exosomes with serum supplementation components, such as FBS derived exosomes or EVs and proteins. It has been revealed that there is high resemblance in terms of homologous proteins between human and bovine exosomes, consequently, this masks the detection and analysis of exosome components of low-abundance [203,204]. Therefore, serum deprivation was followed to deplete FBS from cell culture, however, this has resulted in significant inhibition in cell viability, and subsequently exosome production [204].

However, in order to employ isolated exosomes in downstream analysis, a panel of different characterisation methods is required to identify the properties of exosomes of interest. Thus, in section 1.10, a brief description of the methods used in this study is discussed.

1.10. Exosome characterisation methods

Several common methods are used to visualise, determine the biophysical and molecular properties of exosomes following purification. Exosome characterisation in this project was carried out using the following techniques: ExoView platform, Micro BCA, Western blot, flow cytometry, liquid chromatography-mass spectrometry (LC-MS), RNA isolation, and real-time quantitative polymerase chain reaction (RT-qPCR). These methods are outlined below in more detail:

1.10.1. ExoView characterisation platform

NanoView Biosciences has developed silicon chips with an array of antibodies against exosome surface markers. This method allows differentiation of exosome subpopulations with a very small sample volume, according to the most expressed marker on their surface. Exosome samples are incubated with the chips overnight. After that, chips are rinsed with PBS on a shaker and air dried. Captured exosomes are identified via single particle interferometric reflectance imaging sensor technology [205].

1.10.2. Micro BCA

A micro BCA kit has been developed by Thermo Scientific to measure diluted samples of protein (0.5-20µg/mL) using bicinchoninic acid (BCA) as the detection reagent for copper (Cu) reduction from Cu^{+2} to Cu^{+1}, by protein in alkaline environment. This resulted in forming visible purple-coloured reaction and strong absorbance detected at 562 nm that is linear with increasing protein concentrations [206,207]. Micro BCA have been used to determine protein content in exosomes [208,209].

1.10.3. Western blotting

Western blotting or immunoblotting is used to detect the antigen (protein) of exosome particles by interaction with targeted antibodies. This analysis is carried out by lysing exosome particle and denaturing their proteins. After denaturation, exosome samples are separated by sodium dodecyl sulphate-polyacrylamide gel electrophoresis (SDS-PAGE). After that, the gel of the separated samples is transferred to a nitrocellulose or polyvinylidene fluoride (PVDF) membrane. This membrane is blocked with protein (non-fat milk) then incubated with a specific antibody against an antigen of interest. After that, the membrane is incubated with secondary antibody, which is developed against the host of the primary antibody used for binding to the specific antigen. The secondary antibody

is detected either by its fluorescent tag, or by insoluble substrate to horseradish peroxidase/alkaline phosphatase conjugated to the secondary antibody [175,210].

1.10.4. Flow cytometry

Flow cytometry is a method of analysis that allows the detection of exosomes using their protein composition [175]. However, the resolution limit of standard flow cytometers lies between 300 and 500 nm while exosomes fall below this range. This makes exosomes difficult to be detected. Therefore, a method was developed by attaching exosomes to aldehyde/sulphate-latex beads and incubating them for 15 min with continuous rotation. Then glycine and bovine serum albumin (BSA) were added to stop the reaction. This is followed by washing the exosome-bound beads with PBS and blocking them with BSA. Then primary antibody and fluorescence-conjugated secondary antibodies are added for detection of specific exosomal surface markers using a flow cytometer [205]. This technique allows the quantification and identification of exosomes according to their surface expressed antigen or protein [211].

1.10.5. LC-MS

Metabolomics analysis is carried out using LC-MS, which is used to identify and detect the widest range of proteins or lipids within a sample. This technique starts by first analysing an exosome sample using a high-performance liquid chromatography (HPLC) column then processing the data by mass spectroscopy. This is followed by processing the data using specialised software to obtain information of the sequence of amino acids and fatty acids detected, in order to identify proteins and lipids present in a sample [175,212–215].

1.10.6. Nucleic acid analysis

RNA extracted from exosomes using an RNA isolation kit, containing reagents and filters that allow the separation of miRNAs from other RNAs. These extracted miRNAs are sequenced using a bioanalyser. The expressed miRNAs profiles were investigated by RT-

qPCR applying an array of reference miRNAs. This process is usually carried out by reverse-transcribing, then pre-amplifying the miRNA following the manufacturer's instructions [205,216,217].

1.11. Project aims

To contribute to the knowledge of collecting, isolating exosomes and maintaining their native composition without causing changes that may mask their potential function in therapeutic approaches by:

- Developing efficient approaches to optimise cell culturing methods in order to maintain successful cell culture, maximise native exosome yield and minimise contaminants such as FBS derived EVs or exosomes, and to deliver the highest and purest exosome yield. These approaches were then evaluated by visually observing cells under the microscope and quantitively assessing their cell viability using a Trypan Blue dye exclusion assay. This was followed by identifying and characterising changes in cancer cell-derived exosomes using multiple techniques: ExoView, Western blotting, micro BCA, flow cytometry, LC-MS, RNA analysis, and qRT-PCR (**Chapter 2**).
- Demonstrating the influence of cancer cell-derived exosomes on cancer and normal cell line behaviour by applying: MTT cell proliferation assay, migration, adhesion, and invasion assays, then applying LC-MS, to study the metabolome of the affected cells. (**Chapter 3**)

Thus, the aim was to identify if harvesting exosome of the same cell line, in different media combination had any effect on exosome surfaces and composition. Also, to assess if adding HepG2-Exo on other cell lines, induce or inhibit the biological process of these cells.

Chapter 2

Optimisation of HepG2-exosome production using different conditioned media

Abstract

Introduction: Research into exosomes has gained interest due to their efficiency as nanoparticles in signaling, delivering, and transferring protein, lipid, and genetic material. However, there is a major challenge that still exists in terms of producing exosomes with no or minimal contamination from external sources. For instance, cell cultures are normally carried out in the presence of FBS, which is an essential supplement required for cell attachment, growth, and proliferation. On the other hand, FBS is considered a source of contamination in exosome studies, as they contain naturally occurring EVs or exosomes, high protein, and RNA content. Therefore, the aim of this study was to harvest HepG2-Exo, optimise their production, and investigate their composition through culturing the human HepG2 cell line in a specific growth medium supplemented with different preparations of FBS. In the present study, HepG2 cell line was cultivated using 2 different approaches to produce exosomes. These approaches consisted of using DMEM as the growth medium and either 1) standard FBS as M1, or 2) Dep-FBS as M2, to grow cells for 72 h. This was followed by serum starvation for 48 h, to collect M3 and M4, respectively. Four categories of collected media were obtained: M1, M2, M3, and M4. Exosomes isolated from these media were classified accordingly, Exo(M1), Exo(M2), Exo(M3), and Exo(M4), respectively.

Methods: Cell viability under growth conditions M1, M2, M3, and M4 was assessed using a trypan blue dye exclusion assay and light microscopy. HepG2-Exo samples: Exo(M1), Exo(M2), Exo(M3), and Exo(M4) were produced, characterised and distinguished applying the following techniques: Micro BCA evaluation for determining protein content, flow cytometry for quantifying exosome content, Western blotting for detecting exosomal markers, ExoView chip analysis for characterising exosome subpopulations based on their

tetraspanins expression using capturing and fluorescence particle count, LC-MS for analysing exosome composition, RNA isolation for extracting and sequencing RNA, and RT-qPCR for validating the expression of specific gene of interest using reference genes.

Results: Cell viability, cell morphology, and size results, demonstrated that all growth media influenced HepG2 cell line viability, where M2 was found to be the best medium to cultivate HepG2, maintain its viability and offer minimum contamination with FBS, compared to the other media. The characterisation of HepG2-Exo groups demonstrated an overall variation between groups starting with Micro BCA where the protein concentration of Exo(M1) was significantly ($p < 0.05$) the highest compared to all groups. This suggested that FBS content (bovine exosomes and protein) in M1 media, was added up to the actual content of Exo(M1). Similarly, flow cytometry also showed that Exo(M1) significantly *($p < 0.05$)* recorded the highest percentage of fluorescence compared to the other groups, confirming the micro BCA results and altogether indicating that FBS derived exosomes in M1 were misinterpreted as HepG2-Exo in Exo(M1). After that, the expression of CD63 and CD81 exosomal markers assessed by Western blotting, showed inconsistent bands of detection between groups which indicated that exosomal markers were affected by the media as well. Whereas the ExoView findings have also detected a significant *($p < 0.05$)* difference between groups, where Exo(M4) has recorded significantly ($p < 0.05$) the highest particle count expressing CD9 and CD63 tetraspanins, compared to all groups via ExoView. This indicated that the difference in expression between HepG2-Exo is due to the effect of the media used to grow the cells.

After that, LC-MS results showed a significant *($p < 0.05$)* separation between all groups using OPLS-DA model (SIMCA). Moreover, the calculated ratios of detected metabolites in each group showed a significant *($p < 0.05$)* difference, compared to the control group, Exo(M1). RNA-sequencing results revealed differences in the expression of hsa-miRNA

(identified) and predicted novel (non-identified) miRNAs between groups which proposed that media composition of each group has influenced and changed miRNA content of HepG2-Exo. After that, the verification of of hsa-mir21-5p expression using RT-qPCR, showed significant variation *($p < 0.05$)* in the fold change between exosome groups compared to the calibrator sample, Exo(M1) via RT-qPCR, which indicated that the expression of specific gene can be affected due the collection media used for exosomes. Overall, these results collectively confirmed that the variation between HepG2-Exo groups traits, count, and composition is highly influenced by the growth media.

Conclusion: Designing growth and collection media for exosomes studies require standarisation, where media combination, hypoxic conditions, and the duration of serum starvation are found to be significant factors for maintaining successful cell culture and inducing exosomes production. In terms of cell cultures, depleting media from FBS derived-EVs applying certain techniques or using commercially depleted FBS, found to induce certain effects in cell behaviour. However, applying serum starvation technique found to be inefficient as cell growth and viability were affected. In terms of produced exosomes, different characteristics and different proteins, lipids, and RNAs profiles were observed in each group of HepG2-Exo, influenced by its collection media and applied conditions.

Keywords HepG2, exosome, FBS, miRNA, CD63, CD81, serum starvation

2.1. Introduction

In the literature, multiple approaches have been carried out to optimise the extraction of exosomes from biological fluids and cell cultures using different isolation and purification methods such as ultracentrifugation, precipitation, separation, affinity reaction, and SEC [196]. One issue with *in vitro* cell culture-based studies is that they commonly use FBS as an essential supplement, as its constituents are vital for cell growth and division. However, FBS, as a natural blood product, contains its own endogenous exosome component that could influence and compromise any investigation into the action of exosomes on cell behaviour and function. Thus, in Chapter 1 section 1.11, FBS use is mentioned as one of the limitations in exosome studies that is associated with isolating exosomes from cell cultures.

To overcome this issue, several methods have been developed and applied to minimise FBS-exosome contamination: differential ultracentrifugation for 2–19 hours at 4˚C, is one of the most common approaches due to its simplicity and efficiency, which allows depletion of medium supplemented with 10-20% (50-100 ml) of FBS of its naturally occurring exosomes. This approach can be performed in most basic laboratories with no additional cost; however, it is not a robust method that is capable of eliminating FBS-derived exosomes totally. For instance, a comparative study of FBS depletion methods has revealed that overnight ultracentrifugation compared to ultrafiltration, commercially depleted FBS, and standard FBS, are not considered efficient methods to purify FBS from its EVs, due to high particle size distribution, detection of EVs via electron microscopy, distinctive protein pattern using silver staining, and RNA profiles of vesicular origin via bioanalyser [218]. Hence, commercial versions of Dep-FBS offer higher purity, but at a higher cost compared to standard FBS and other lab-based techniques. A 500 ml bottle of Dep-FBS costs twice that of standard FBS (500 ml). Moreover, the ultrafiltration method recently gained attention as it was found to be an efficient alternative technique for FBS

depletion as it provides serum of the highest purity compared to conventional ultracentrifugation and commercially depleted FBS, using products such as Amicon ultra-15 centrifugal filters to reduce the exosome content in FBS [218–220].

An indirect method to reduce *in vitro* contamination of cells with FBS-exosomes, is through a process that involves growing cells in medium supplemented with standard FBS, discarding this medium and replacing it with a serum-free alternative, followed by maintaining the cell culture for 24 to 48 h. This approach helps ensure the majority of the exosomes collected at the appropriate point in the study will be cell-derived exosomes [221,222]. However, this approach should be applied with caution as it may affect the cell behaviour. Alternatively, cells could be grown long-term in serum-free media where some companies have developed synthetic solutions to be used as replacement of FBS for certain cell lines, containing the essential supplements, growth factors, and proteins of standard FBS, to avoid using serum from animal sources [223]. Overall, these methods still require monitoring to analyse their impact on cell growth, morphology, function, and exosome production in comparison to conventional animal serum-supplemented media. For instance, Fang *et al*. (2017) found that cells of the same origin such as epithelium of head and neck might respond very differently to a specific type of alternative serum, hence, they recommended that each cell line should be assessed specifically, to be used with a specific serum alternative [224]. Also, it was reported that the requirements of cell culture basic components such as serum, amino acids, and the choice of cell culture media, are found to vary from one cell line to another. Therefore, cell culture media should be evaluated for each cell line [225].

Aim of this chapter: HepG2, liver carcinoma cells were grown under different conditions to see if the yield of exosomes could be maximised while minimising contaminants from FBS (e.g. bovine proteins and exosomes), using tailored approaches to deliver the highest

and purest exosome yield. HepG2 were grown in different media and an examination made of their influence on the composition of the exosomes produced.

2.2. Methodology

2.2.1. Preparation of HepG2 cell conditioned culture media

The human hepatocellular carcinoma (HepG2) cell line (passage no. 10) was cultured and maintained in Dulbecco's Modified Eagles medium (DMEM)- High glucose (D6429) contained with 4.5 mg/ml of glucose and supplemented with 0.584 mg/ml of L-glutamine, 0.11 mg/ml of sodium pyruvate, 3.7 mg/ml of sodium bicarbonate, and a mixture of amino acids as provided in the product information sheet by Sigma-Aldrich, UK. After that, a concentration of 100 I.U./mL penicillin and 100 (µg/mL) streptomycin was added. Cell culture was incubated at 37°C in the presence of a mixture of 95% air 5% CO_2 with 100% humidity. In addition, 10 % (v/v) standard FBS or 10 % (v/v) Dep-FBS, were added to the DMEM. Cells were seeded at a density of 1.09 $\times 10^6$ cells/ml into two 75 cm^2 cell culture flasks, one in DMEM supplemented with FBS and the other with Dep-FBS. When the cells reached confluency (80-90%), both DMEM-FBS and DMEM-Dep-FBS media were collected separately, labelled M1 and M2 respectively, and replaced with serum-free DMEM, after washing the cells with Hanks' Balanced Salt solution (HBSS) three times to remove any residues from the previous media (Figure 2.1). After 48 h of serum starvation, the media from both flasks were collected separately denoted M3 and M4, respectively (Figure 2.1). Thus, four samples of media were obtained: M1, M2, M3, and M4, consequently four groups of exosomes will be purified: Exo(M1), Exo(M2), Exo(M3), and Exo(M4) (Figure 2.1).

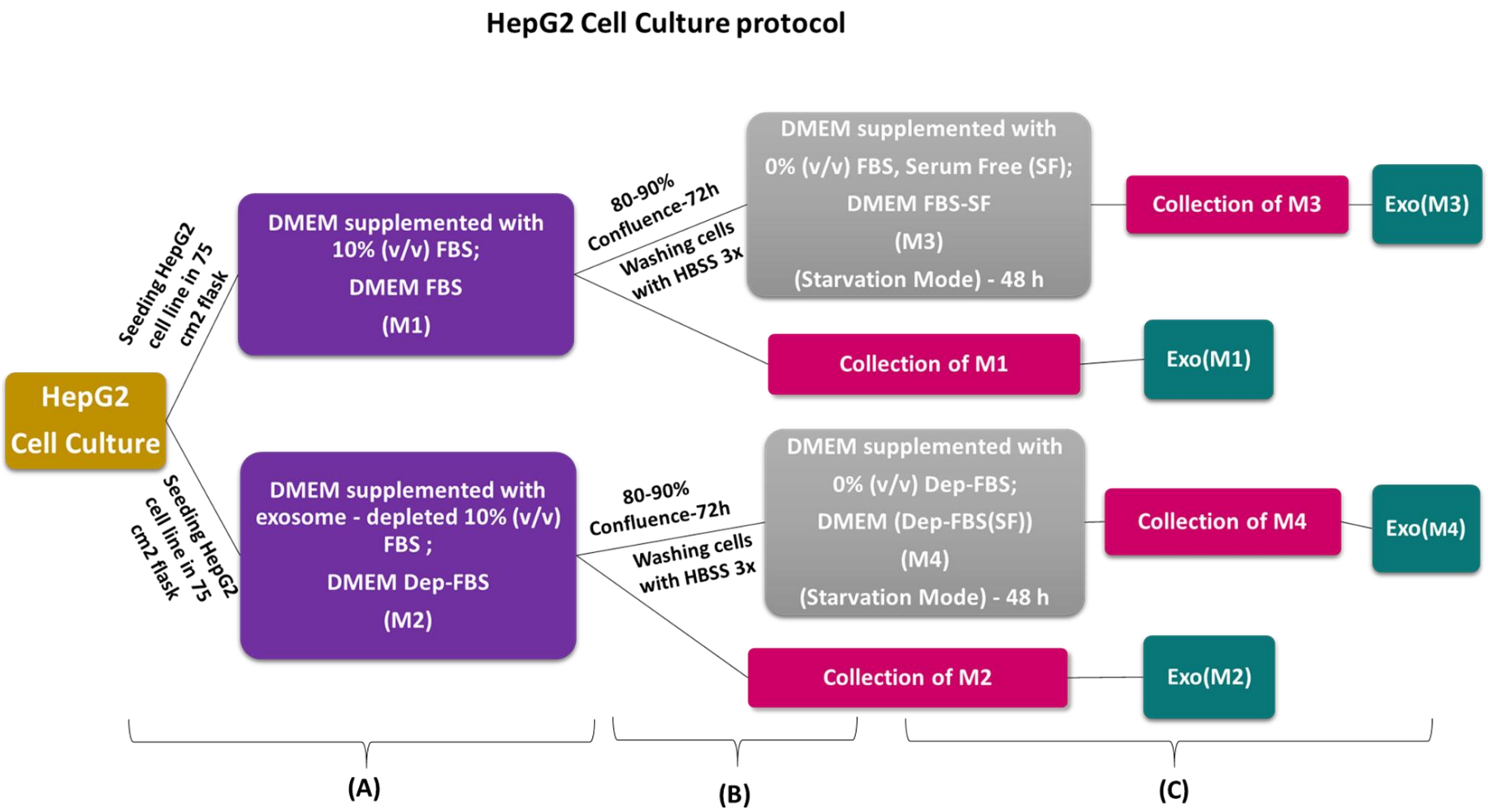

Figure 2.1 Schematic diagram of HepG2 cell culture method used for exosome collection.

(A) HepG2 cell line was seeded in two 75cm2 flasks at a density of 1.09×10^6 cells/ml. One flask was supplemented with M1 and the other with M2. (B) After cells have reached confluency, M1 and M2 were collected. Both cell cultures were washed with HBSS three times. (C) Serum free (SF) media were added to both flasks and maintained for 48 h. M3 and M4 media were collected. All media were filtered and centrifuged to collect four groups of HepG2- Exo that correspond to the harvesting media: Exo(M1), Exo(M2), Exo(M3), and Exo(M4).

2.2.2. Trypan blue dye exclusion

The effect of the four different media on cell viability, was assessed using a Trypan blue dye exclusion assay. Cells were seeded at a density of 1.09×10^6 cells/ml into four cell culture flasks of 75 cm^2 for 72 h, where two flasks were cultured with M1 media, the other two with M2. After cell reached confluency, media of each flask were collected, and one flasks of each media group was washed with HBSS 3x, and a fresh SF media were added to each flask to create M3 and M4 (Figure 2.1). While the other two flasks of each media, were washed with HBSS 2x then treated with 5 ml of Accutase and incubated for 5 min at 37°C for cell detachment. After that, DMEM media supplemented with FBS were added to each flask to stop Accutase action then transferred into 15 ml centrifuge tube and centrifuged for 5 min at 5000 × g to pellet the cells. After centrifugation, supernatants were discarded, and cell pellets were suspended with DMEM. For cell counting, 10 µl of cell suspension of each tube was mixed with 10 µl of Trypan blue. After that, 10 µl was aspirated and placed on clean haemocytometer and covered with a cover slip then placed under the microscope at 10x objective lens. Viability was determined by the number of cells retaining the blue dye (non-viable cells) versus unstained viable cells. The percentage of cell viability was expressed by the equation:

$$\% \text{ of cell viability} = \frac{\text{number of non-viable or viable cells x100}}{\text{total number of cells counted}}$$

2.2.3. Isolation and purification of HepG2-Exo

Enrichment of HepG2-Exo from the collected media was carried out using a Corning®Bottle-top vacuum filter system (0.22 µm). This was followed by a purification process using total exosome isolation reagent (TEIR). The required volume of cell-free filtered media was transferred into a new tube and 0.5 the volumes of TEIR was added (i.e. 5 ml of TEIR to be

added to 10 ml of cell culture media). Samples were vortexed with TIER and incubated at 4°C overnight. After incubation, samples were centrifuged at 10,000 × g for 1 hour at 3°C. Supernatants were discarded and exosome (non-visible) pellets were resuspended in a convenient volume of 1X PBS (i.e. if the starting volume of media was 10 ml, pellet can be resuspended in 100 µl–1 ml of PBS). Exosome samples were stored at 4°C for up to 1 week, or at ≤20°C for long-term storage. The TEIR volume used in each assay is depending on the downstream analysis that would be carried out. Four groups of exosomes were extracted from their harvesting media: Exo(M1), Exo(M2), Exo(M3), and Exo(M4) (Figure 2.1).

2.2.4. Total protein quantification

Estimation of total protein in purified exosome samples was calculated using a Micro BCA™ Protein Assay kit, following the manufacturer's instructions. Eight serial dilutions of albumin standard were prepared: 200, 40, 20, 10, 5, 2.5, 1, and 0.5 µg/ml, to create a standard curve. After that, 1 ml of each filtered medium sample was incubated with 500 µl of TEIR over 16 h. Samples were centrifuged at 10,000× g for 60 min at 4 ˚C, supernatants were discarded, and samples were diluted 1:5. One hundred µl of each sample were added to 96-well plates and incubated with the Micro BCA working reagent for 2 h at 37 ˚C and absorbance at 562nm read on a SpectraMax M5 plate reader. Corrected readings of samples were obtained by subtracting blank readings from the exosome sample readings.

2.2.5. Flow cytometry

HepG2-Exo groups: Exo(M1), Exo(M2), Exo(M3), and Exo(M4) were prepared by mixing and incubating them with 30µL Aldehyde/Sulphate Latex Beads, 4% (w/v), 4 µm for 15 min at RT. Phosphate-buffered saline (PBS) was added to each sample and incubated for 2 h at RT. Then 110 µl of 1 M glycine was added to the samples and incubated for 30 min at RT. The samples were centrifuged for 3 min at 3000 × g. The supernatant from each sample was discarded,

and the bead pellet resuspended with 1 ml 0.5% (w/v) BSA in PBS (PBS/0.5% BSA). This step was carried out a further two times to wash the samples. After that, the sample pellets were suspended in 500 µl of PBS/0.5% BSA. One hundred µL of each sample suspension was incubated with 200 µl of diluted primary monoclonal mouse anti-CD63 antibody in PBS/0.5% BSA (1:250) for 30 min at 4^{o}C. Each sample was washed twice with 200 µl of PBS/0.5% BSA. Then 100 µl of diluted goat anti-mouse IgG H&L (Alexa Fluor® 488) secondary antibody in PBS-BSA (1:500) was added to each sample and incubated for 30 min at 4^{o}C. The samples were washed twice with PBS/0.5% BSA and then resuspended in 1 ml PBS/0.5% BSA. BD CompBead Anti-Mouse Ig, κ/Negative Control Particles Set was used as a negative control. The samples and negative control were analysed on a Flow Cytometer (Canto) using Diva software. The method and the analysis steps were performed as described in [18]. The equation used for calculating the percentage of fluorescence was:

$$\% \text{ of fluorescence} = \frac{\text{number of fluorescent events}}{\text{total number of detected events}} \times 100$$

2.2.6. Western blotting

Exosome groups were prepared for gel electrophoresis by adding radioimmunoprecipitation assay (RIPA) buffer with protease inhibitor (1:100) and incubated at 4˚C for 15 min. The samples were heated for 10 min at 70 ˚C and diluted in 4x Laemmli sample loading buffer (1:1.5). Fifty µl (25µg/ml as determined in section 2.2.5) of each sample was loaded onto a 10% Mini protein Tris Glycine eXtended (TGX) Precast protein gel. The electrophoresis buffer used was 1x Tris/Glycine (TG) running buffer. The gel was run at 140V for 60 min in an electrophoresis tank connected to a power pack. The gel was transferred onto nitrocellulose membrane with 1x Tris/Glycine/SDS (TGS) buffer and blocked using BSA dissolved in Tris-Buffered Saline with (3% v/v) Tween (TBST) for 1 h at RT. The membrane was probed with primary monoclonal mouse anti-CD63 and CD81, and incubated overnight at 4˚C. Primary

antibodies were washed using TBST, then the membrane was incubated with rabbit anti-mouse IgG (H+L) HRP secondary antibody, for 1 h at RT. The membrane was incubated with Pierce™ enhanced chemiluminescence (ECL) for visualisation, using an Automatic X- Ray Film processor (Model JP-33). Densitometry was performed on the film to assess the difference between band intensities using Image J software from the National Institutes of Health (http://rsb.info.nih.gov/ij/).

2.2.7. Exosome characterisation using ExoView™

Exosome groups were characterised by the ExoView™ platform, using a Tetraspanin (CD81, CD9, and CD63) Exoview kit which includes 16 chips to test up to 8 samples in duplicate. This analysis was carried out by first diluting all exosome groups in manufacturer supplied buffer (1:20), solution A, and incubating them overnight at room temperature (RT) on ExoView Tetraspanin chips. The chips were washed three times in solution A, prior to incubation with fluorescent antibodies. Labelling antibodies consisted of anti-CD81 Alexa 555 (Green), anti-CD9 Alexa 488 (Blue), and anti-CD63 Alexa 647 (Red). Antibodies were diluted 1:1200 as per the manufacturer's instructions and incubated on the chips for 1 h at RT. Chips were then washed in kit supplied buffers, dried, and imaged by the ExoView R100 using nScan v2.8.9. Sizing was obtained by interferometry-based label-free measurements performed on each spot of the ExoView chip using the light scattering intensity of each particle. The mean was calculated from three spots for each capture antibody. Particle number was calculated using the number of particles detected in a defined area of the antibody capture spot (normalised particles). All obtained data was adjusted for dilution of the sample onto the chip and analysed using NanoViewer 2.8.9. Fluorescent cut offs that were set relative to the membrane immunoglobulin G (MIgG) control.

Histograms and fluorescent counts bar graphs were provided by NanoView while data analysis was carried out and represented via Graphpad Prism 5.00.

2.2.8. Liquid chromatography–mass spectrometry (LC-MS) analysis

2.2.8.1. Metabolite Extraction

Two-hundred and fifty µl of HPLC grade water was added to 200 µl (100 µg/ml) of purified exosomes together with 500 µl of chilled methanol. Samples were vortexed and incubated on ice for 15 min. Then 500 µl of chloroform was added to each sample. This was followed by centrifugation at 10,000 × g, at 4 ˚C for 10 min. The supernatant was transferred to a fresh tube, and 500 µl of acetonitrile was added and centrifuged at 10,000 × g at 4 ˚C for 10 min. The aqueous layer was transferred to a fresh tube, then the sample was dried and concentrated using a centrifuge connected to a universal vacuum system. Sequential extraction was followed starting with water (aqueous), methanol (semi-polar) and a non-polar solvent (chloroform) to optimise the detection of multiple metabolites. The resuspension solution was prepared with the following ratios methanol:acetonitrile:water 50:30:20, and 200 µl added to the dried extract. The samples were then ready for LC-MS analysis [19].

2.2.8.2. LC-MS conditions

An Accela HPLC system interfaced to an Exactive Orbitrap mass spectrometer was used. HPLC columns used were ZIC-pHILIC (150 × 4.6 mm, 5 µm), ACE 5 C18-AR (150 × 4.6 mm, 3 µm) and ACE C4 (150 × 3.0 mm, 3µm). Running conditions of samples using the ZIC-pHILIC column consisted of a mobile phase (A) of 20 mM ammonium carbonate dissolved in HPLC-grade water, and acetonitrile as the mobile phase (B). The solvent gradient had an A:B ratio of 20:80 (0 min), 80:20 (30 min), 92:8 (31–36 min), and 20:80 (37–45 min) at a flow rate of 0.3 mL/min.

For the ACE 5 C18-AR columns, the mobile phase consisted of (A) 0.1% (v/v) formic acid in water, pH 3 and (B) 0.1% (v/v) formic acid in acetonitrile, pH 3. The gradient elution of A:B was 95:5 (0 min), 0:100 (30 min), 0:100 (35 min), 95:5 (36 min), and 95:5 (46 min) at a flow rate of 0.3 mL/min.

For the ACE C4 column, the mobile phase was 1 mM acetic acid in water (A) and 1 mM acetic acid in acetonitrile (B). The solvent gradient of A:B was 60:40 (0 min), 0:100 (30–36 min) and 60:40 (37–41 min) at a flow rate of 0.4 mL/min.

The operating conditions for separation using the different columns were the same. This was carried out by employing the electrospray ionisation (ESI) interface in a positive/negative switching mode / dual polarity mode, with a spray voltage of 4.5 kV for positive mode and 4.0 kV for negative mode, while the ion transfer capillary temperature was set at 275˚C. To avoid degradation of the samples the instrument temperature was set to 4 ˚C.

Full scan data were obtained in the mass-to-charge ratio (m/z) between 75 and 1200 amu for both ionisation modes. The data were collected and processed using Xcalibur 2.1.0 software (Thermo Fisher Scientific, Germany).

2.2.8.3. Data extraction and analysis

MZMatch software was used to extract the obtained data, then a macro-enabled Excel Ideom file was then created for filtration and identification of the detected metabolites (http://mzmatch.sourceforge.net/ideom.php) [226]. Metabolites were manually evaluated by contemplating the quality of their peaks and by comparing their recoded retention times to those of authentic standard mixtures, run in the same sequences. Human Metabolome Data Base [227], KEGG (Kyoto Encyclopedia of Genes and Genomes [228], and lipid maps were used to carry out the identification of the metabolites within 3 ppm difference of their exact masses. Univariate comparisons were carried out between all groups of exosomes

versus Exo(M1) as a control group using Microsoft Excel and paired t-tests, calculated ratios were considered significantly different at $p < 0.05$. For multivariate analysis, SIMCA-P software v.14.1 was used to highlight any significant separation between all groups of exosomes according to the recoded peak area of detected metabolites, by fitting PCA-X and OPLS-DA models, and to apply cross-validated residuals-ANOVA (CV-ANOVA) on OPLS-DA model.

2.2.9. MicroRNA (miRNA) isolation

Total RNA isolation of purified exosomes was carried out using a Total Exosome RNA and Protein Isolation Kit. The manufacturer's protocol was followed to obtain and isolate small RNAs from large RNAs and total proteins from exosome samples. Samples were subjected to organic extraction of RNA to isolate proteins from RNA. The aqueous phase obtained containing total RNA, was transferred to a new tube. Then the enrichment for small RNA was accomplished by first immobilising large RNAs on the provided filter cartridge that was inserted into microcentrifuge tubes and by adding ethanol to each sample and collecting the flow-through containing mostly small RNA, after centrifugation. This flow-through was mixed again with ethanol and transferred into a fresh tube containing a new filter cartridge. This was followed by centrifugation, the flow-through was discarded, and the filter cartridge was washed twice with miRNA Wash Solution and Wash Solution 2/3 then centrifuged to discard the flow-through. The filter cartridge was transferred into a fresh collection tube, then small RNA was eluted with Elution Solution, and centrifuged. The elute containing small RNA was collected and stored at ≤ -20 ˚C. Exosome samples were subjected to deep sequencing by BGI-Tech company.

2.2.10. Real time - quantitative polymerase chain reaction (RT-qPCR)

RT-qPCR was performed to assess and validate the RNA-sequencing analysis. TaqMan™ Fast Advanced Master Mix, TaqMan™ Advanced miRNA cDNA Synthesis Kit, and TaqMan™ Advanced miRNA Assays: mir-21-5p (Assay ID: 477975_mir), mir-23a-3p (Assay ID: 478532_mir), mir-26a-5p (Assay ID: 477995_mir), and mir-423-5p (Assay ID: 478090_mir) were used following the manufacturer's protocol for RT-qPCR analysis. The fold change was calculated for each gene, applying the equation below:

$$\text{Fold Change} = 2^{-\Delta\Delta CT}$$

2.2.11. Statistical analysis

All experiment values are representative of at least three independent experiments and are displayed as mean ± SEM, where *p< 0.05, **p< 0.01, ***p< 0.001, n=3. One-way ANOVA followed by Tukey's multiple comparison test, and two-way ANOVA followed by Bonferroni post-tests, were used to assess statistical significance between the groups. The statistical analysis was performed using GraphPad Prism software version 5.00.

2.3. Results

2.3.1. The effect of different growth conditioned media on HepG2 cell viability

Cultivation of HepG2 in different growth medium combinations was carried out to optimise the best growing conditions, and to maximise the production of exosomes with the least contamination with FBS-derived exosome (Figure 2.2). Images of the HepG2 cell cultures were captured by light microscopy (objective lens 10×), during their cultivation in the four media (M1, M2, M3, and M4) (Figure 2.2.A). Cells maintained their size, morphology, and growing density during their cultivation period in serum supplemented media: M1 and M2, and during serum deprivation: M3 and M4 (Figure 2.2.A). However, under the microscope, after 48 h of serum starvation using M3 and M4, noticeable numbers of rounded and floating cells were visible in both cultures. Hence, the assessment of cell viability using trypan blue dye exclusion showed a significant *($p < 0.05$)* reduction in viable cell count and a significant *($p < 0.05$)* increase in non-viable cell count in SF (M3 and M4), compared to the serum supplemented (M1 and M2) growth conditions (Figure 2.2.B).

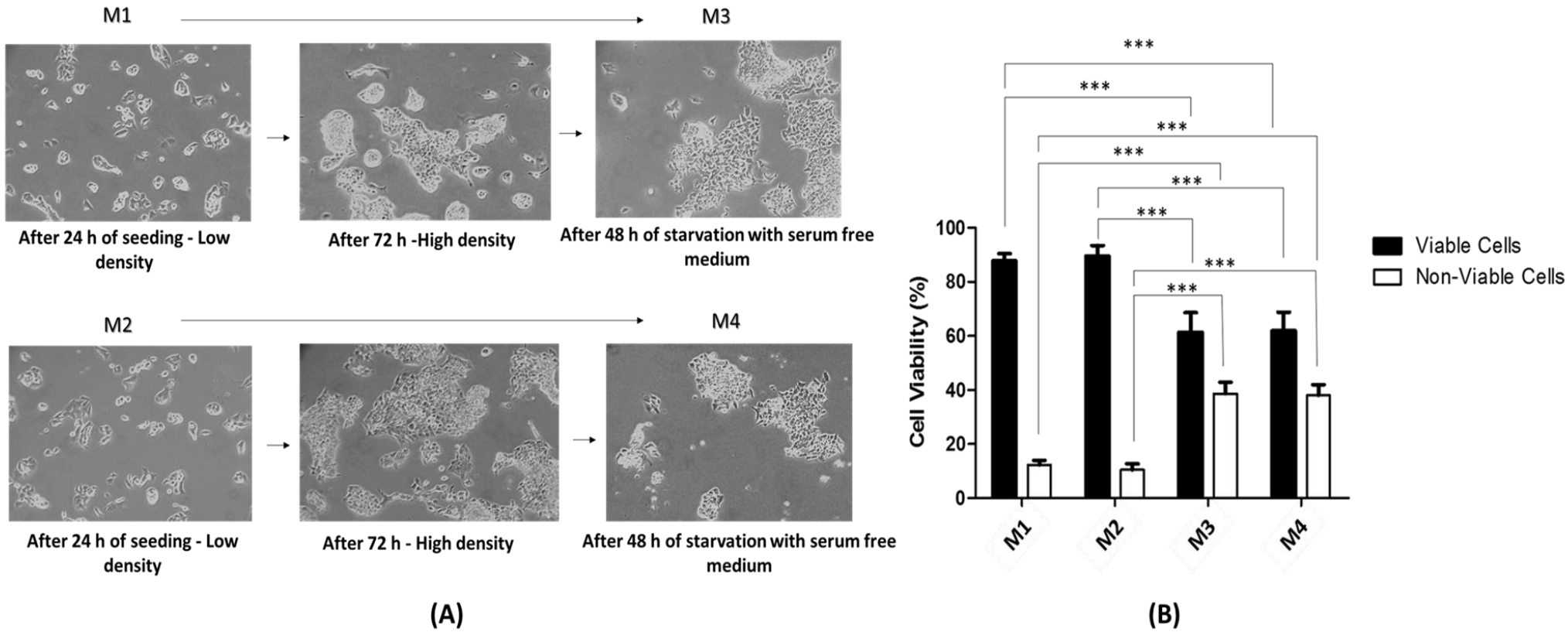

Figure 2.2: Optimisation of HepG2 cell culture using different DMEM media combinations.

(A) Captured images of the HepG2 cell line in all media (objective lens 10×) showed no changes in cells morphology and density, at different time points i.e. 24 h and 72 h. M1 and M2 are removed after 72 h and replaced with serum free (SF) DMEM media. After 48 h of serum deprivation, significant loss of HepG2 cells noticed in M3 and M4. (B) Bar graphs of HepG2 cell viability in M1, M2, M3, and M4 obtained by cell counting of viable and non-viable cells in each media. Significant decrease in cell count of M3 and M4 compared to M1 and M2. Data shown as mean ± SEM of triplicate cell cultures and are representative of three independent experiments; *** $p<0.001$.

2.3.2. Assessment of protein content of HepG2-Exo

Quantification of total exosomal protein was performed to assess the influence of different media combinations on exosome content using a Micro BCA assay kit. The total protein concentration was calculated from the albumin standard curve (Figure 2.3).

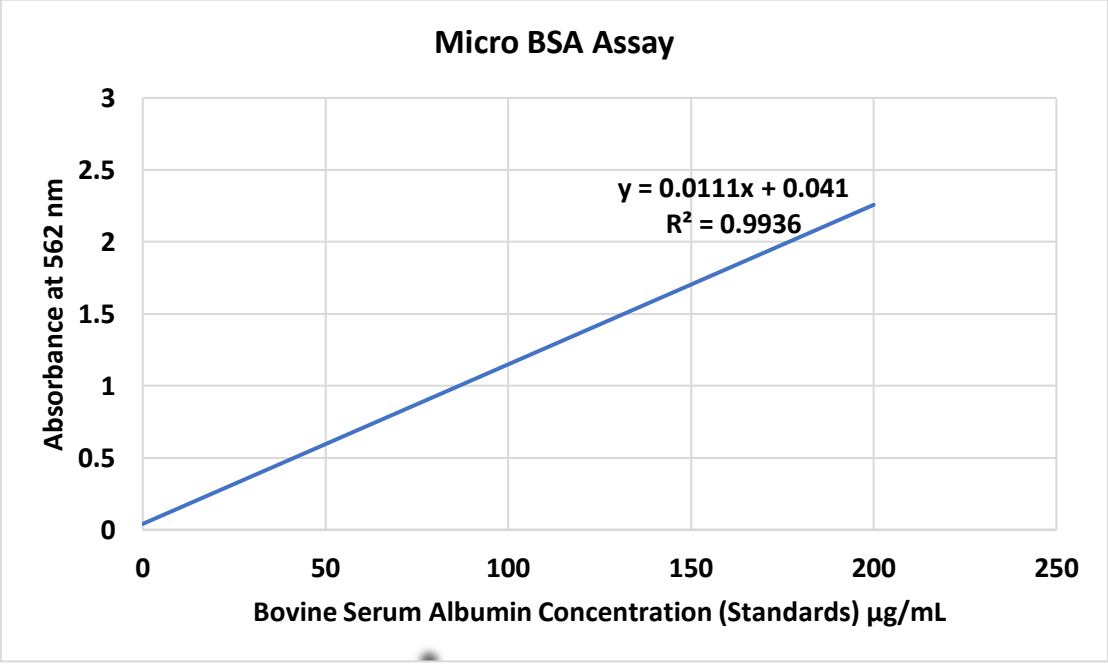

Figure 2.3: Albumin standard curve.

By applying the standard curve equation, the protein concentration of each group was calculated (Figure 2.4). Statistically, a significant increase *($p < 0.05$)* in protein concentration (µg/ml) of Exo(M1) was observed, compared to all exosome groups.

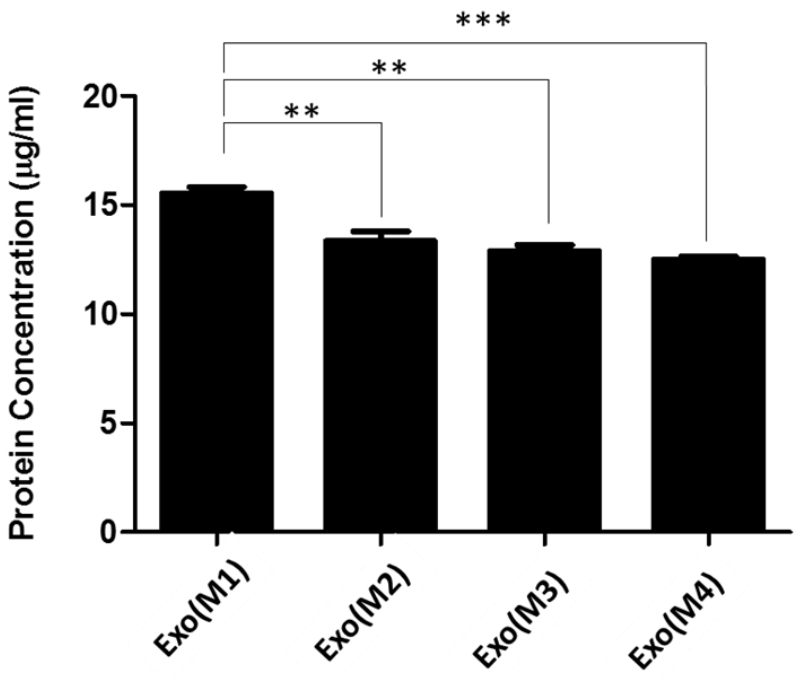

Figure 2.4: Total protein concentration of purified exosome samples using a Micro BCA assay kit.

This bar graph of HepG2-Exo groups showed significant variation in protein content compared to Exo(M1) which has recorded the highest concentration. All values are representative of mean ± SEM where **p< 0.01, ***p< 0.001 n=3.

2.3.3. Assessment of HepG2-Exo using flow cytometry

Flow cytometer analysis was performed to estimate exosome production under different growing conditions. Flow cytometry histograms were extracted from BD FACS Diva software (Figure 2.5.A). The calculated % of fluorescence of each group is shown in Figure 2.5.B., where Exo(M1) recorded the highest % of fluorescence and Exo(M4), the lowest. The statistical analysis showed a significant *($p < 0.05$)* difference in % of fluorescence in between all exosome groups (Figure 2.5.B).

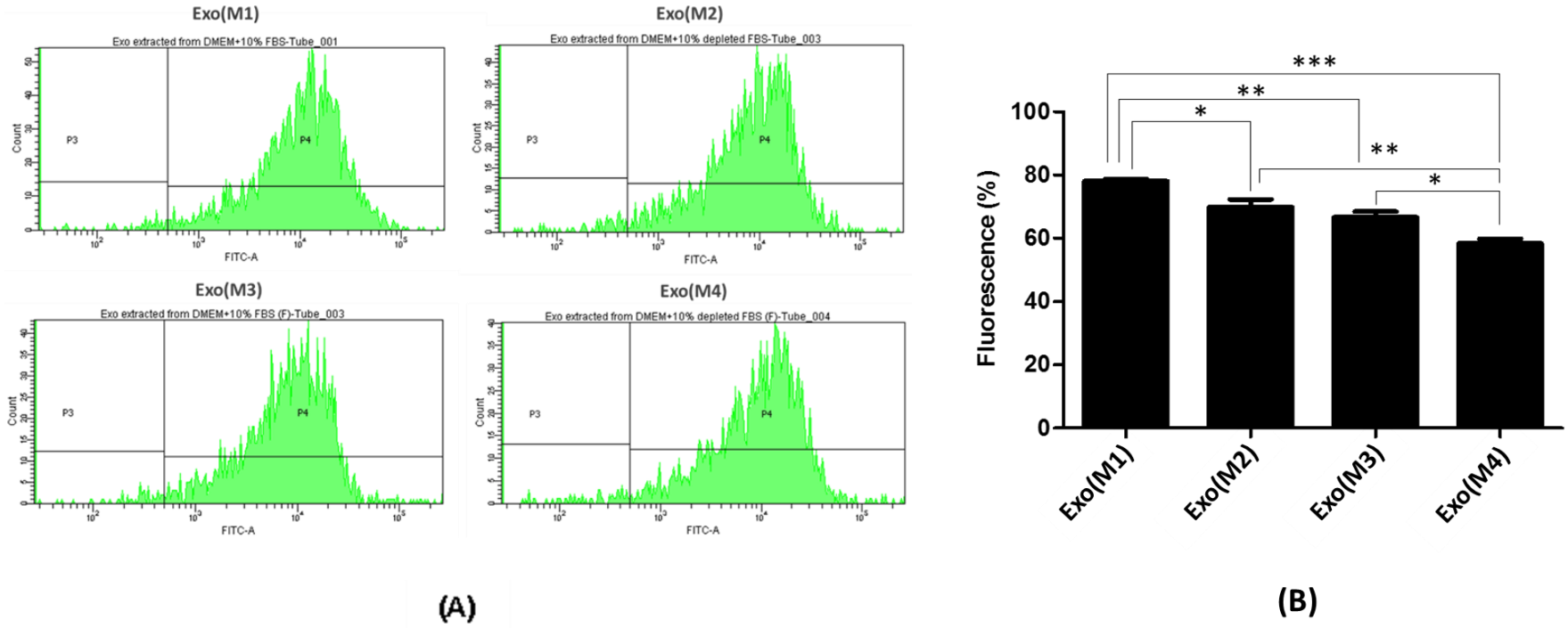

Figure 2.5: Flow cytometry analysis of exosome production.

(A) Flow cytometry histograms of all exosomes groups showed no significant difference. (B) Bar graph illustrating the % of fluorescence of each group of exosomes collected from different media revealed significant changes in number of fluorescent particles between groups. All values are representative of the mean ± SEM where *p < 0.05, **p< 0.01, ***p< 0.001 (n=3).

2.3.4. Assessment of the expression of exosomal markers using Western blotting

Western blotting was carried out to assess and evaluate the yield of HepG2-Exo from different groups of media. CD63 and CD81 were used as exosomal biomarkers to detect exosomes in these four groups. Processed films of expressed bands and % of expression using densitometry, are shown in Figure 2.6, where CD63 showed dark bands in all groups, however, CD81 showed variation between groups. Statistically, a significant *($p < 0.05$)* decrease in CD81 expression in Exo(M3) and Exo(M4) compared to Exo(M1), while no significant difference observed for CD63.

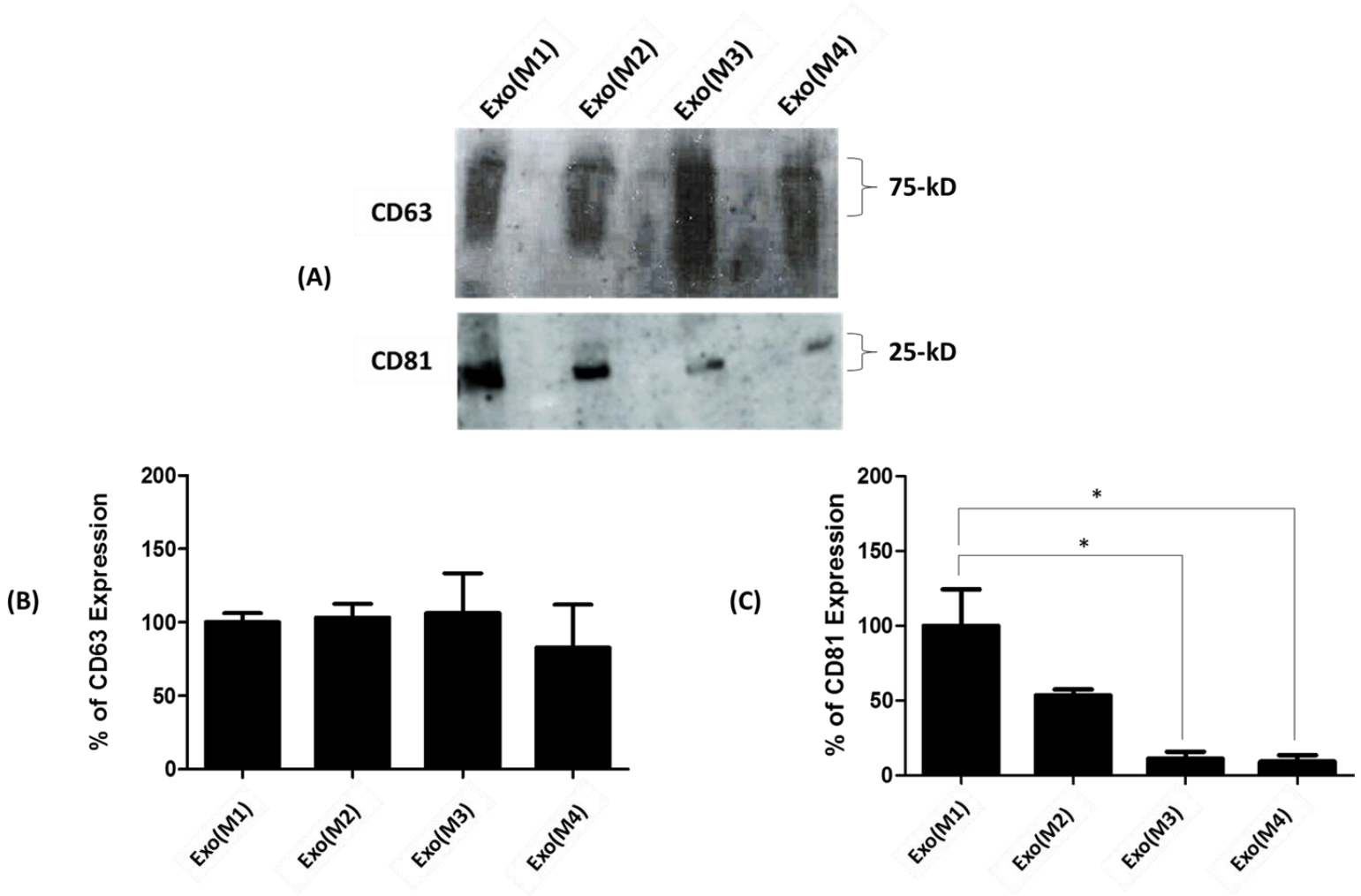

Figure 2.6: Western blotting of HepG2-Exo groups.

(A) Bands of varying intensities in between groups detected using CD63 and CD81. (B) A slight difference in the percentage of CD63 expression detected between groups. (C) A significant difference in the expression of CD81 observed between Exo(M1) and Exo(M3), and Exo(M4). Data shown as mean ± SEM of triplicate and are representative of three independent experiments; *$p < 0.05$.

2.3.5. Assessment of exosome subpopulations using ExoView™

Characterisation of exosomes using the ExoView™ platform was carried out, to allow the measurement of particle size using multiple capturing antibodies: CD81, CD63, and CD9, to determine particle counts using fluorescent detection by adding a cocktail of primary fluorescent conjugated antibodies against CD81, CD63, and CD9, and to study the effect of different conditioned media on exosome surface markers. Histograms showed that all exosomes groups captured CD63 and CD9 only (Figures 2.7) while fluorescent particles count bar graphs showed variation between all exosome groups in CD63 and CD9 capturing spots that bound to anti-CD63 and anti-CD9, fluorescent labelling antibodies (Figures 2.8). However, statistical analysis showed that Exo(M4) recorded significantly *($p < 0.05$)* the highest particle count where CD63 and CD9 capturing spots bound highly to both anti-CD63 and anti-CD9, compared to Exo(M1), Exo(M2), and Exo(M3) (Figure 2.8).

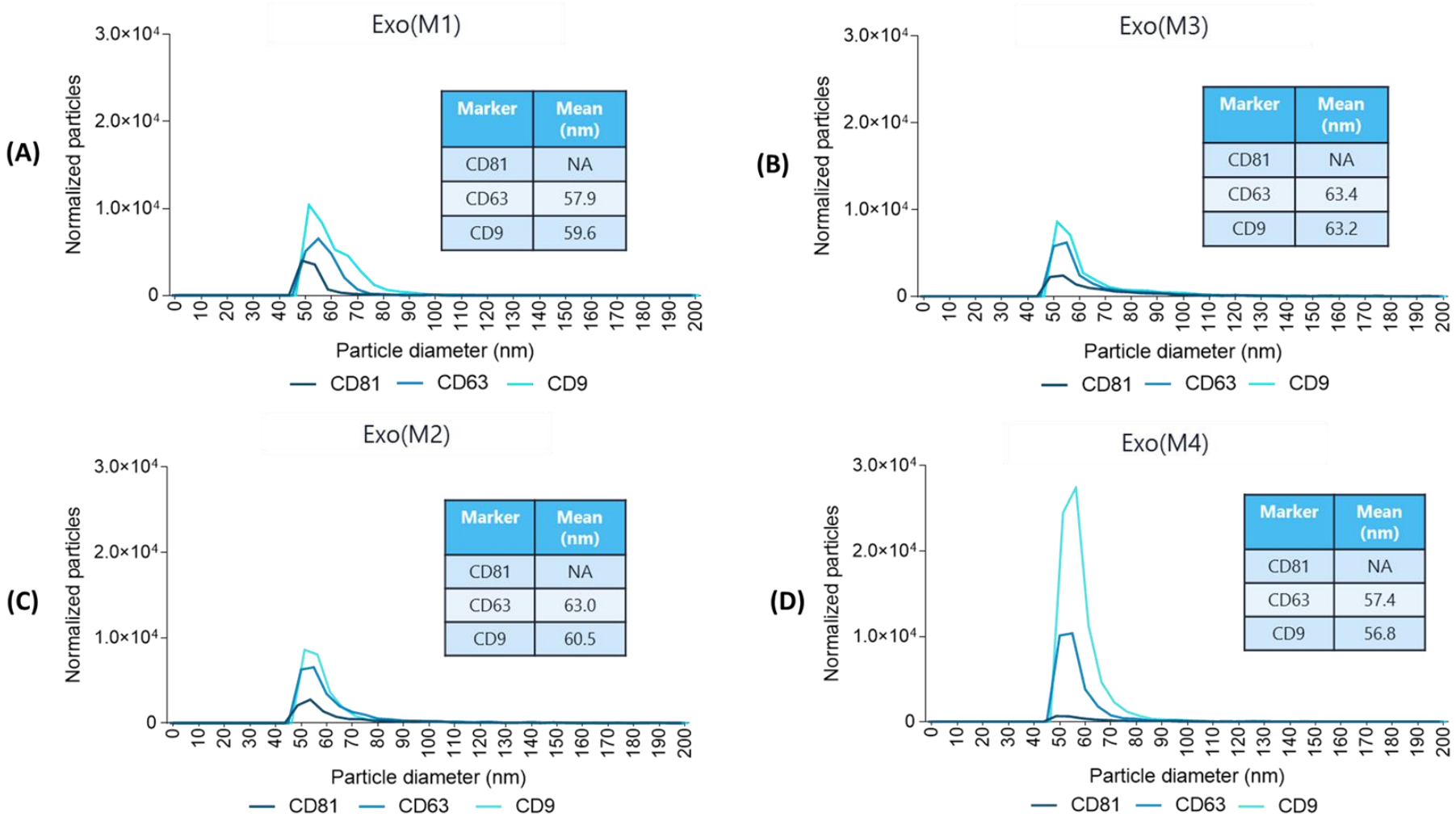

Figure 2.7: Particle size distribution histograms of HepG2-Exo groups incubated with captured antibodies (CD81, CD63, and CD9) on ExoView chip.

Slight variation in particle diameter mean of CD63 and CD9 were observed in-between groups, where no accurate size could be determined (NA) for CD81 in all groups. (A) Exo(M1), (B) Exo(M2), and (C) Exo(M3) showed similarity in particle counts while in (D) Exo(M4) particle count found to be highly elevated. HepG2- Exo particles exhibited higher affinity for capturing CD9 followed by CD63.

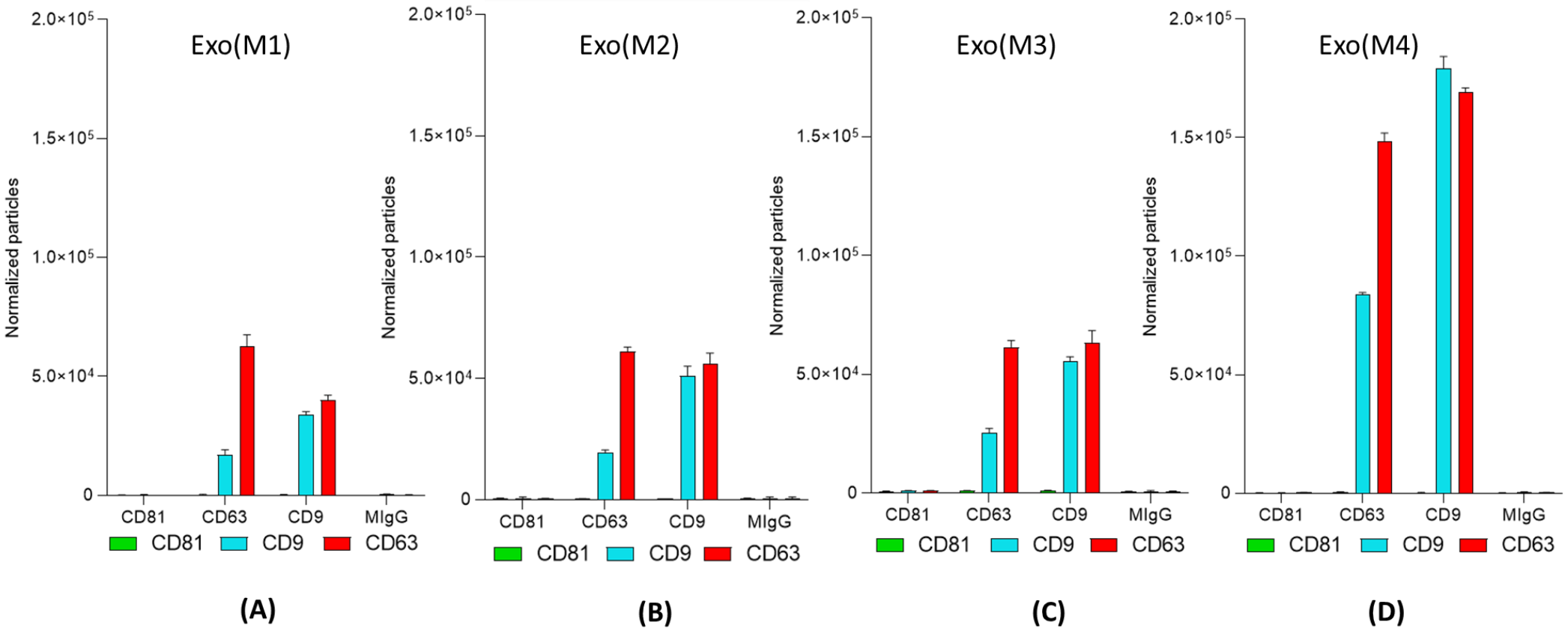

Figure 2.8: Fluorescent particle counts of all exosome groups.

Co-binding observed of anti-CD63 and anti-CD9 in (A) Exo(M1), (B)Exo(M2), (C)Exo(M3), and (D)Exo(M4), to CD63 and CD9 capture spots. (A), (B), and (C) showed similar count of particles. While (D) represented the highest particles count.

2.3.6. Metabolomic profiling of exosome using LC-MS

Metabolomic profiling was performed on all exosome groups using ZIC-pHILIC, C18-AR and C4 columns. The purpose of using different HPLC columns was to investigate and detect a broader range of produced metabolites under the different growth conditions. To study the efficiency of separation of each column and sample quality and deviation from others, two models were created by SIMCA software: Principal component analysis (PCA) and OPLS-DA. For the ZIC-pHILIC column, pooled samples (P) were clearly clustered at the bottom of the PCA model (Figure 2.9.A). This indicates that the column used was of a good quality, high selectivity, and stability. In the OPLS-DA model, a distinctive and significant separation between the HepG2-Exo groups was observed with *P* CV-ANOVA=0.002 (Figure 2.9.B). All detected metabolites, calculated ratio, and *p-value* can be found in Table 2.1.

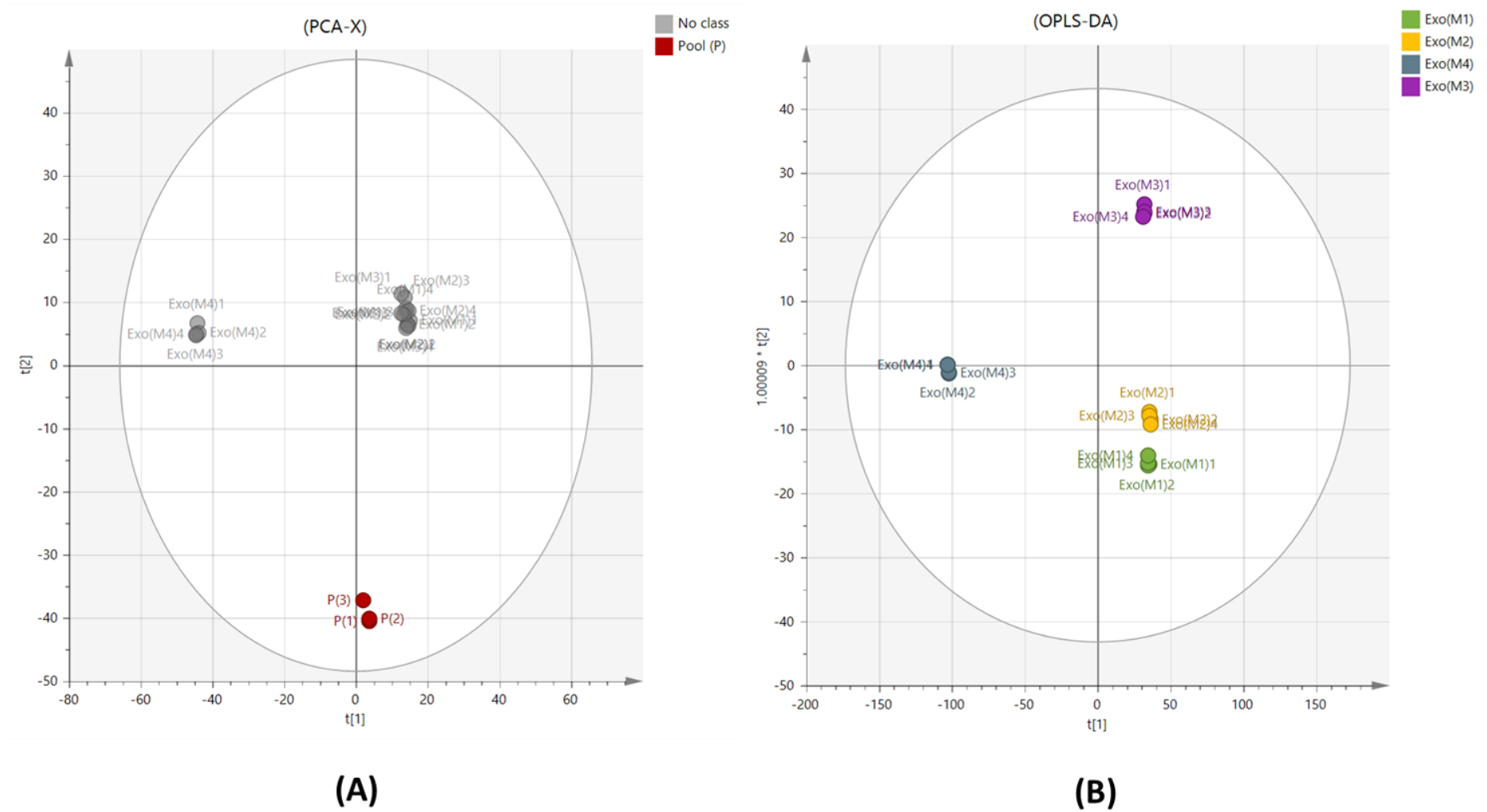

Figure 2.9: (A) PCA-X vs (B) OPLS-DA score plot of HepG2- Exo using ZICpHILIC.

(A)plot shows the clustering of pooled samples (P) compared to the rest of HepG2-Exo (grey-No class) isolated from different media, PCA-x score plot (A) has R2 = 0.889, Q2= 0.821. (B) plot shows a clear separation and distribution of 16 observations based on readings of 274 polar putative metabolites.The observations classified into four groups: Exo(M1), Exo(M2), Exo(M3), and Exo(M4), OPLS-DA score Plot (B) has R2 = 0.957, Q2=0.989.

Table 2.1: Significantly changed metabolites detected by ZICpHILIC column.

Mass	Retention Time (Rt)	Putative Metabolite	Exo(M1) vs Exo(M2)		Exo(M1) vs Exo(M4)		Exo(M1) vs Exo(M3)	
			Ratio	*p* value	Ratio	*p* value	Ratio	*p* value
		Arginine and proline metabolism						
129.04	15.17	4-Oxoproline	3.005	<0.001	00.00	<0.001	2.984	<0.001
129.09	26.40	4-Guanidinobutanal	2.164	0.000	2.492	<0.001	3.466	<0.001
240.12	16.30	Homocarnosine	0.670	0.000	0.0002	<0.001	0.022	0.003
145.08	15.43	4-Guanidinobutanoate	0.652	0.004	00.00	<0.001	0.392	<0.001
113.05	9.98	Creatinine	0.795	0.002	00.00	<0.001	0.019	<0.001
175.09	15.99	L-Citrulline	0.807	0.003	00.00	<0.001	0.323	<0.001
145.15	16.29	Spermidine	5.298	0.007	0.0002	<0.001	7.040	0.01
174.11	17.89	L-Arginine	1.280	0.0119	0.0005	<0.001	17.36	<0.001
132.08	22.12	L-Ornithine	0.884	ns	00.00	<0.001	0.390	0.0001
147.05	13.90	L-Glutamate	2.187	0.0004	00.00	<0.001	2.516	0.02
115.06	13.03	L-Proline	1.310	<0.001	00.00	<0.001	0.837	0.0007
133.03	14.65	L-Aspartate	2.293	<0.001	00.00	<0.001	0.383	0.004
146.06	15.17	L-Glutamine	3.141	<0.001	00.00	<0.001	3.143	<0.001
131.06	14.89	Creatine	0.722	0.0006	00.00	<0.001	0.081	<0.001
130.02	14.59	2,5-Dioxopentanoate	1.888	0.001	00.00	<0.001	0.712	0.012

246.13	14.40	N2-(D-1-Carboxyethyl)-L-arginine	2.131	<0.001	00.00	<0.001	1.190	0.016
		Pyrimidine metabolism						
126.04	11.55	Thymine	0.454	<0.001	00.00	<0.001	0.438	0.0001
112.02	11.87	Uracil	0.295	<0.001	00.00	<0.001	0.470	0.0001
128.05	15.00	5,6-Dihydrothymine	0.725	0.001	00.00	<0.001	0.358	<0.001
111.04	11.52	Cytosine	0.706	0.014	00.00	<0.001	0.310	<0.001
244.06	12.15	Pseudouridine	1.112	ns	0.153	<0.001	0.641	<0.001
		Purine Metabolism						
136.03	10.43	Hypoxanthine	0.401	<0.001	00.00	<0.001	1.399	<0.001
135.05	9.87	Adenine	0.779	0.001	00.00	<0.001	2.311	<0.001
284.07	15.93	Xanthosine	1.440	0.001	0.00	<0.001	0.00	<0.001
300.07	12.40	urate-3-ribonucleoside	0.766	0.040	0.00	<0.001	0.00	<0.001
		Tryptophan Metabolism						
160.09	10.45	Tryptamine	3.253	<0.001	00.00	<0.001	2.143	<0.001
218.10	11.03	N-Acetylserotonin	3.547	<0.001	1.890	0.001	2.862	<0.001
208.08	11.09	L-Kynurenine	0.479	<0.001	00.00	<0.001	0.381	<0.001
204.08	11.89	L-Tryptophan	1.611	0.0001	00.00	<0.001	1.579	<0.001
191.05	12.46	5-Hydroxyindoleacetate	0.399	0.0004	00.00	<0.001	0.531	<0.001
		Miscellaneous						
260.02	15.91	D-Fructose 6-phosphate	51.691	<0.001	9.658	<0.001	29.954	<0.001
134.05	16.43	Deoxyribose	1.396	0.001	0.471	<0.001	1.015	ns
132.05	15.29	L-Asparagine	34.331	0.03	0.0007	0.02	12.886	ns

131.09	11.54	L-Isoleucine	1.488	<0.001	00.00	<0.001	2.274	<0.001
131.09	11.11	L-Leucine	1.403	0.0008	00.00	<0.001	2.211	<0.001
117.07	12.73	L-Valine	1.271	0.0005	00.00	<0.001	1.659	<0.001
174.01	14.04	L-Dehydroascorbate	587.05	<0.001	1549.676	<0.001	4484.27	<0.001
190.01	15.31	Oxalosuccinate	1384.9	<0.001	1370.447	<0.001	736.5	<0.001
240.02	16.04	L-Cystine	0.782	0.01	00.00	<0.001	2.879	<0.001
301.05	14.70	N-Acetyl-D-glucosamine 6-phosphate	3106.3	<0.001	2200.174	<0.001	1867.13	<0.001
121.01	13.68	L-Cysteine	2.223	<0.001	0.0001	<0.001	1.670	0.0004
105.04	15.83	L-Serine	0.590	<0.001	00.00	<0.001	1.375	<0.001
142.07	14.51	Ectoine	1.295	0.016	00.00	<0.001	1.104	ns
180.06	26.38	D-Galactose	2.441	0.0003	4.64	<0.001	4.574	<0.001
161.06	13.15	N-Methyl-L-glutamate	3.400	0.0013	00.00	<0.001	36.20	<0.001
149.05	11.74	L-Methionine	1.660	<0.001	00.00	<0.001	1.486	<0.001
190.04	23.19	3-Dehydroquinate	1.283	0.0004	0.650	0.0001	0.970	ns
264.11	10.98	alpha-N-Phenylacetyl-L-glutamine	0.766	0.0089	0.0001	<0.001	0.518	<0.001

The data demonstrated in Table 2.1 showed the most significant *($p < 0.05$)* changed metabolites among all groups compared to Exo(M1), where the most affected pathways found to be Arginine and proline metabolism, Pyrimidine metabolism, Purine metabolism, and Tryptophan metabolism.

To investigate the non-polar metabolites produced by the exosome groups, an ACE 5 C18-AR column was used. Multivariate analysis of this data set was performed (Figure 2.10). The PCA-model showed that pooled samples were clustered around the centre of the model which indicates that the analysis performed was valid, and the instrument maintained its stability throughout the run (Figure 2.10.A). In the OPLS-DA model, a clear separation between exosome groups was observed, however, no significant difference of was detected between groups using *P* CV-ANOVA (Figure 2.10.B).

C18-AR

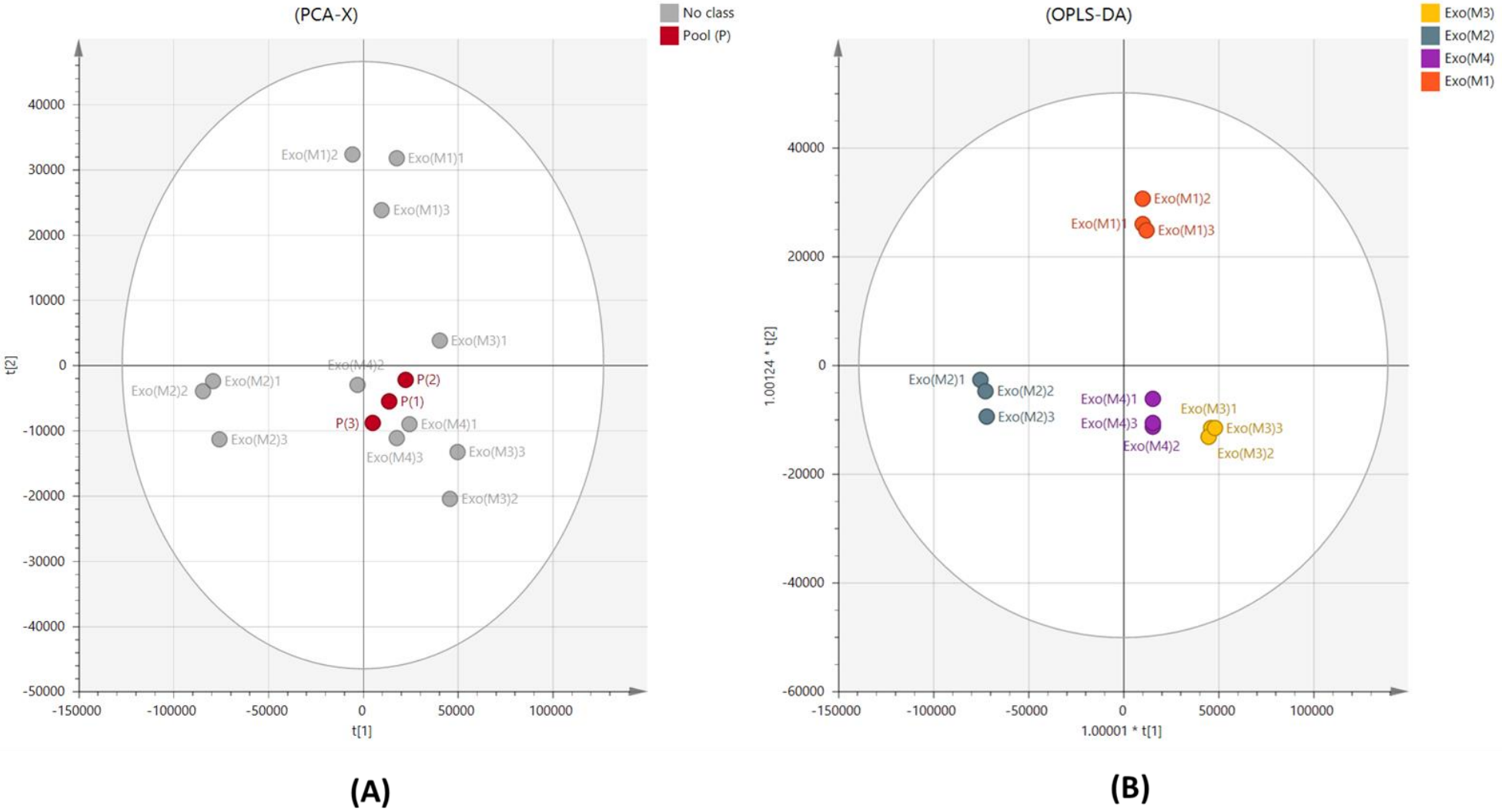

Figure 2.10: (A) PCA-X vs (B) OPLS-DA score plot of HepG2-Exo using C18-AR.

(A) plot shows the clustering of pooled samples (P) compared to HepG2-Exo (grey-No class) collected from different media, PCA-x score plot (A) has R2 = 0.831, Q2= 0.772. (B) plot shows a clear separation and distribution of 12 observations based on readings of 81 non-polar putative metabolites.The observations classified into four groups: Exo(M1), Exo(M2), Exo(M3), and Exo(M4), OPLS-DA score Plot (B) has R2 = 0.921, Q2=0.726.

For in-depth lipidomic profiling, further analysis was implemented employing a reversed-phase (RP) ACE C4 column, owing to its high sensitivity, low retention time, and low hydrophobicity. The purpose of using this column is to enhance the chance of detecting a wider range of metabolites. The multivariate analysis of this run showed that pooled samples were clustered in the PCA model (Figure 2.11.A). While in the OPLS-DA model, exosomes were significantly separated using *P* CV-ANOVA = 0.0021 (Figure 2.11.B). However, all non-polar metabolites of both C18-AR and C4 columns and the calculated ratio can be reviewed in Table 2.2.

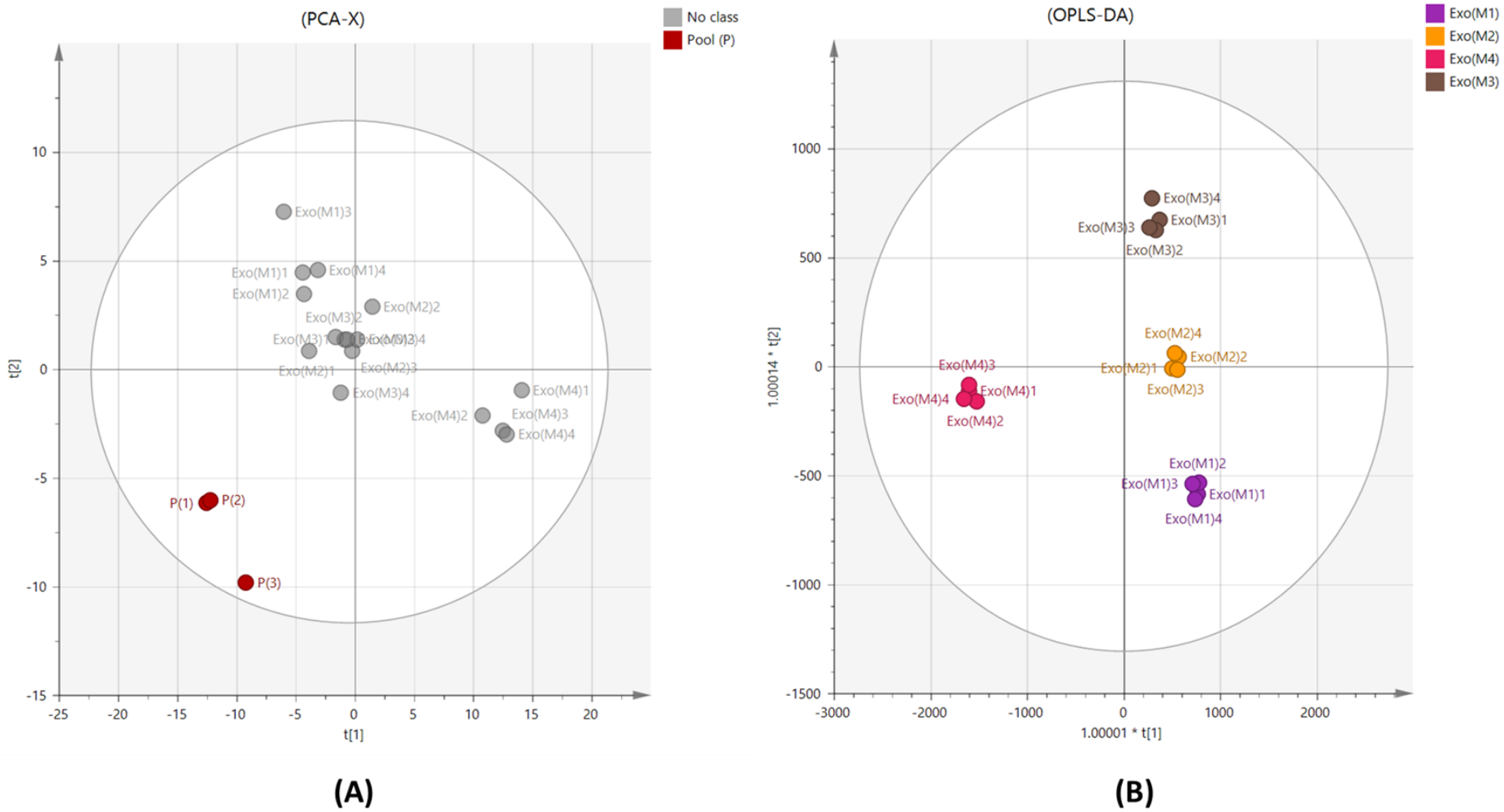

Figure 2.11: (A) PCA-X vs (B) OPLS-DA score plot of HepG2-Exo using ACE C4.

(A) plot shows the clustering of pooled samples (P) compared to isolated HepG2-Exo (grey-No class) from different media, PCA-x score plot (A) has R2 = 0.772, Q2= 0.57. (B) plot shows a clear separation and distribution of 16 observations based on readings of 110 non-polar putative metabolites.The observations classified into four groups: Exo(M1), Exo(M2), Exo(M3), and Exo(M4), OPLS-DA score Plot (B) has R2 = 0.948, Q2=0.905.

Table 2.2: Significantly changed non-polar metabolites detected by.C18-AR and ACE C4 columns.

Mass	Rt	Putative Metabolite	Exo(M1) vs Exo(M2)		Exo(M1) vs Exo(M4)		Exo(M1) vs Exo(M3)	
			Ratio	*p* value	Ratio	*p* value	Ratio	*p* value
		Fatty Acids and metabolites						
243.15	18.74 (-)	Tridecanedioic acid$^{C18\text{-}AR}$ (-)	0.569	0.0001	0.652	0.0026	0.595	0.0002
245.17	29.46	Tridecanedioic acid $^{C18\text{-}AR}$ (+)	0.796	0.003	0.831	0.008	0.732	0.001
229.14	17.14	Dodecanedioic acid $^{C18\text{-}AR}$	0.876	ns	0.740	0.01	0.744	0.01
104.04	2.44	2S-Hydroxy-butanoic acid	0.578	0.002	0.200	<0.001	0.244	<0.001
200.17	13.86	Dodecanoic acid	1.735	0.005	3.844	0.0007	1.281	0.02
228.20	16.99	Tetradecanoic acid	1.656	ns	2.267	0.002	0.768	ns
228.17	21.10	7-Methoxy-4E-dodecenoic acid	2.489	0.01	2.752	0.001	1.333	ns
300.26	15.07	9-Methoxy-heptadecanoic acid	1.291	ns	1.671	0.008	1.103	ns
298.25	13.53	9-Hydroxy-12Z-octadecenoic acid	1.165	ns	1.542	0.01	1.390	0.04
254.22	18.49	(9Z)-Hexadecenoic acid	1.505	ns	6.962	<0.001	2.336	<0.001
188.14	5.87	10-Hydroxydecanoic acid	1.892	0.001	0.846	ns	0.764	0.04
200.10	3.21	[FA (10:1/2:0)] 4E-Decenedioic acid	0.689	0.002	1.161	ns	0.462	0.0003
160.07	2.42	[FA (7:0/2:0)] Heptanedioic acid	0.699	0.007	0.665	0.003	0.414	0.001

102.06	3.43	Ethyl propionate	0.608	0.01	0.168	<0.001	0.220	<0.001
186.12	6.11	2-Oxodecanoic acid	0.668	0.01	4.314	<0.001	0.744	ns
186.16	11.93	[FA (11:0)] Undecanoic acid	1.737	0.012	1.827	0.0045	1.155	ns
130.09	5.66	[FA (7:0)] Heptanoic acid	0.840	0.03	2.683	<0.001	1.053	ns
88.05	2.78	Formyl propionate	0.777	0.035	0.363	0.0004	0.495	0.0005
174.12	4.61	[FA Hydroxy(9:0)] 2-Hydroxy-nonanoic acid	0.694	0.04	3.538	0.0002	0.818	ns
270.25	21.93	[FA (17:0)] Heptadecanoic acid	1.399	ns	2.453	<0.001	1.323	0.0005
242.22	18.64	Pentadecanoic acid	1.281	ns	3.862	0.023	1.349	ns
280.24	19.33	Linoleate	1.225	ns	2.153	0.001	1.403	0.002
214.19	15.73	[FA (13:0)] Tridecanoic acid	1.196	ns	2.400	<0.001	1.048	ns
102.06	2.43	Pentanoate	1.357	ns	0.486	0.0005	0.628	0.007
282.25	21.27	[FA (18:1)] 9Z-Octadecenoic acid	0.850	ns	1.485	0.004	1.922	<0.001
138.10	4.62	Nona-2,6-dienal	0.839	ns	2.515	0.005	0.664	ns
186.12	3.98	10-Oxodecanoate	0.797	ns	3.636	0.0004	0.774	ns
172.11	3.32	7-Methyl-3-oxooctanoic acid	0.903	ns	5.143	<0.001	1.052	ns
214.15	6.38	[FA Hydroxy (12:1)] 12-Hydroxy-10-Dodecenoic acid	1.170	ns	0.608	0.0025	1.362	0.02
240.20	17.15	[FA Dimethyl (13:0)] 2,5-Dimethyl-2E-Tridecenoic acid	1.319	ns	1.986	0.006	0.991	ns

202.12	4.76	[FA (10:0/2:0)] Decanedioic acid	0.948	ns	4.782	0.0002	1.362	ns
144.07	3.00	2S-Hydroxy-2-Isopropylbutano-3S-lactone	0.935	ns	3.863	<0.001	1.265	0.02
268.24	20.20	Omega-Cyclohexylundecanoic acid	1.157	ns	2.419	<0.001	1.084	ns
188.14	4.92	[FA Hydroxy (10:0)] 3R-Hydroxy-decanoic acid	1.035	ns	0.519	0.002	1.131	ns
214.15	5.79	3-Oxododecanoic acid	0.981	ns	3.486	0.0001	1.185	ns
188.14	4.35	[FA Hydroxy (10:0)] 3-Hydroxy-decanoic acid	0.972	ns	0.321	<0.001	0.662	0.008
172.10	4.75	9-Oxononanoic acid	1.083	ns	2.150	0.007	1.323	ns
		Miscellaneous						
286.04	4.37	[Fv] Luteolin	0.624	ns	0.408	0.007	0.599	ns
172.14	10.18	[PR] p-Menthane-3,8-diol	1.377	0.03	2.335	0.004	1.211	ns
142.07	18.30	Ectoine	1.634	<0.001	1.603	<0.001	1.257	0.0001
189.04	11.46	N-Acetylisatin	0.377	<0.001	0.368	<0.001	0.292	0.0001
166.06	9.12	3-(2-Hydroxyphenyl) propanoate	1.082	ns	2.687	0.002	1.078	ns
94.04	9.12	Phenol	1.070	ns	2.035	0.01	1.020	ns
189.04	14.46	Kynurenate	0.965	ns	2.303	0.0001	0.975	ns
467.97	2.03	dUTP	1.336	ns	0.301	0.0003	0.856	ns
160.07	3.35	Indole-3-acetaldehyde	0.145	0.0002	0.439	0.004	0.108	0.0003

585.31	11.63	Presqualene diphosphate	0.741	0.001	0.708	0.0006	0.860	0.03
595.37	12.20	[PR] 7,8-Didehydroastaxanthin	0.730	0.003	0.854	0.03	0.994	ns
335.22	9.02	Prostaglandin A2	0.629	0.01	0.879	ns	1.008	ns

The data demonstrated in Table 2.2 showed non-polar metabolites (i.e. fatty acids and metabolites) detected by C18-AR and ACE C4 columns that significantly *($p < 0.05$)* changed in all groups compared to Exo(M1).

The separations of the exosome groups in OPLS-DA models obtained by SIMCA software, were studied further by categorising detected metabolites based on their map classification (Figure 2.12). As M1 was considered the standard medium for typical HepG2 cell culture, Exo(M1) group was used as a control to calculate the ratio of detected metabolites in other groups. These pie charts showed a noticeable variation in metabolite detection ratio of each group compared to the control group.

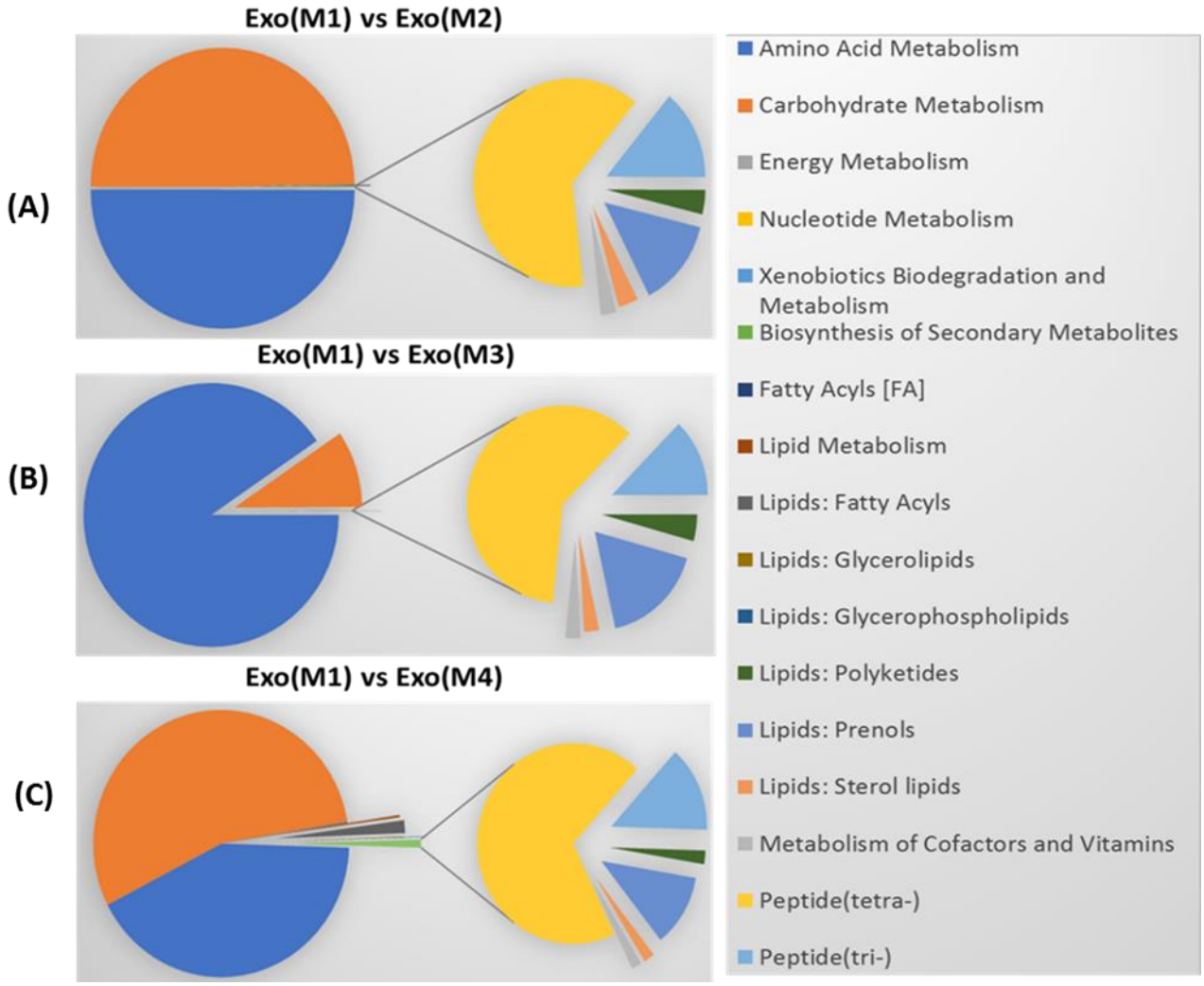

Figure 2.12: Pie chart of HepG2-Exo groups created based on the map classification of the identified metabolites.

Metabolomic profiles of HepG2-Exo groups were compared to Exo(M1) group as a control. (A)shows that Exo(M2) metabolomic profile has shifted compared to Exo(M1) where amino acids and carbohydrates make equal compartments. Whereas (B) demonstrates significantly higher amino acids content in Exo(M3) compared to carbohydrates content. (C) represents slightly higher carbohydrates content that amino acids.

2.3.7. Analysis of miRNA expression in exosomes

This analysis was carried out to investigate miRNAs from the HepG2-Exo and to detect any modifications in gene expression levels.

A detailed analysis of small RNA expression profiles of all exosome groups was obtained by RNA-Seq. After deep sequencing, identified miRNAs (hsa-mir) were detected while non-identified or the so-called (novel miRNAs) were predicted based on their architectural feature using miRDeep2 tool [229] (Table 2.3).

Table 2.3: Total number of novel miRNAs and identified hsa-miRNAs detected in each group of exosomes

	Exo(M1)	Exo(M2)	Exo(M3)	Exo(M4)
Novel miRNAs	1885	1332	1540	1967
hsa-miRNAs (Identified)	396	269	702	330

After normalising the RNA-sequencing data, the expression levels of novel and hsa-miRNAs were evaluated using transcripts per million (TPM) (Figure 2.13) where the quantity of specific miRNAs and novel miRNAs, has changed from one group to another. A heatmap was created by BGI-Tech company based on the significant difference *($p < 0.05$)* in the expression of 44 hsa-mir genes, between exosome groups (Figure 2.14) that demonstrates the degree of change in miRNAs expressions between groups according to the change in colour intensity.

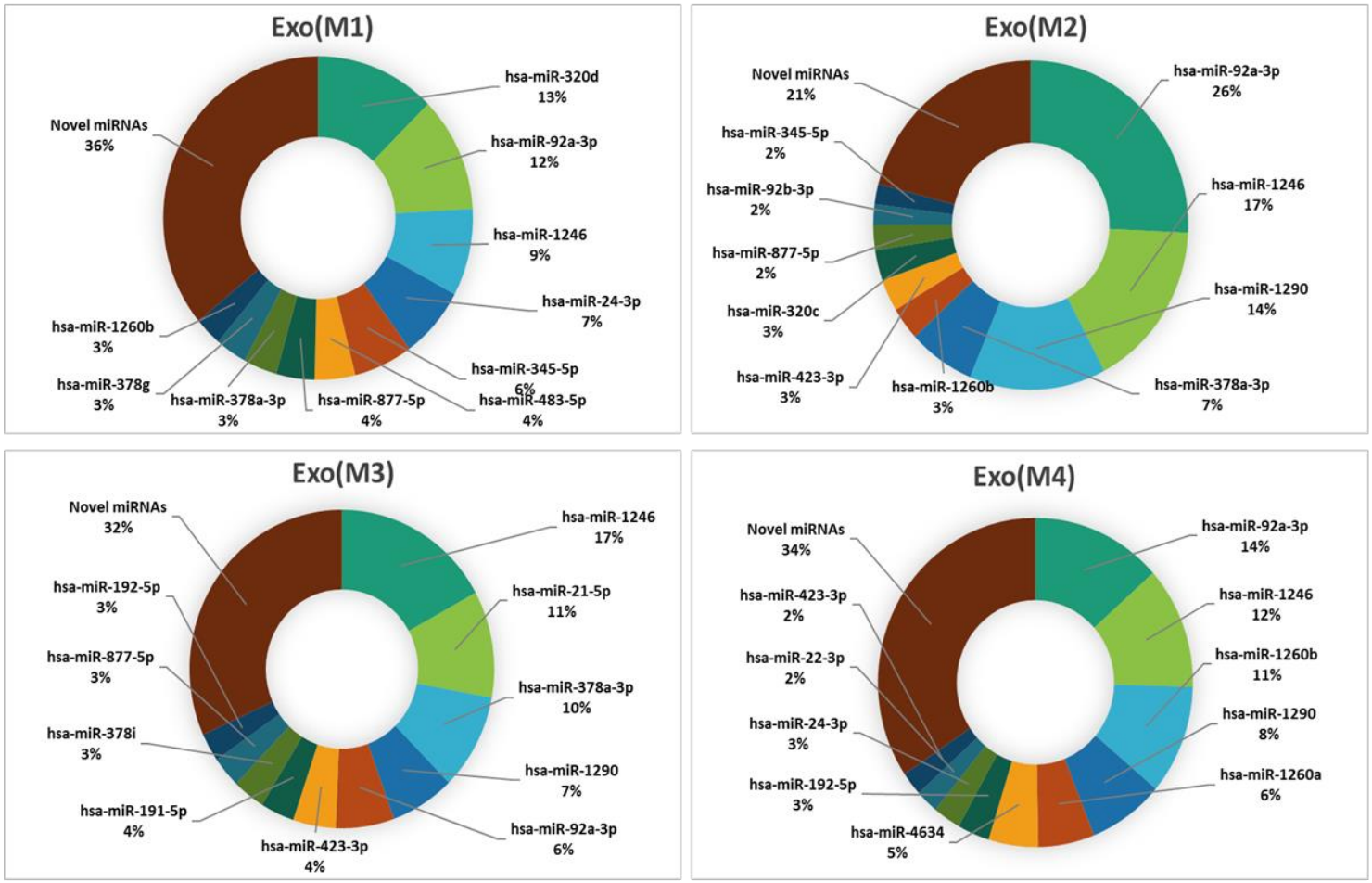

Figure 2.13: Donut pie charts represented the difference in the most abundant miRNAs in each exosome group, according to TPM.

Gene expressions have varied significantly between groups. Hsa-mir-92a-3p was observed in all groups, however, it has recorded the highest expression in Exo(M2), compared to other groups.

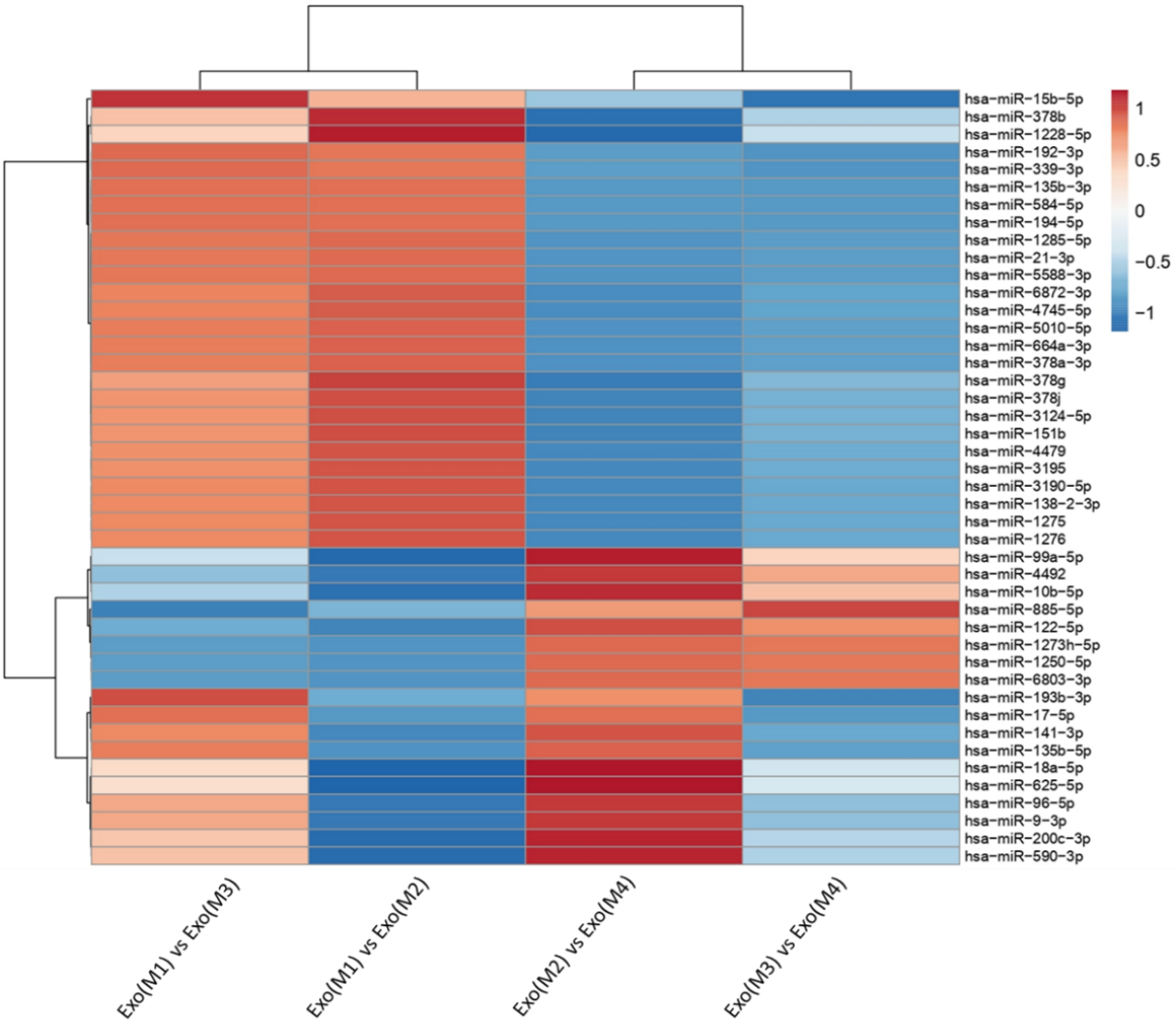

Figure 2.14: Heatmap of all hsa-miRNAs (44) that significantly up-regulated and down-regulated between all exosome groups.

Each row represents a differentially expressed gene while each column represents a pairwise comparison. Genes are clustered based on the expression patterns, which can be correlated to the functional classification of the genes. Branches at the left of the diagram indicates gene clusters. The differences in colour shades represent the difference in intensity of expressed genes, where blue was assigned for down-regulation and red for up-regulation. The data are displayed on a log2 scale.

2.3.8. Validating the expression of mir-21-5p in exosomes using RT-qPCR

These miRNAs: hsa-miR-23a-3p, hsa-miR-26a-5p, and hsa-miR-423-5p, were chosen as internal reference genes based on two studies that investigated reference gene selection for RT-qPCR studies on EVs [230,231]. Hsa-miR-21-5p was considered the gene of interest, due to its constant expression level in all HepG2-Exo groups. Moreover, exosomal miRNA-21 found to play a role in cancer progression through modifying hepatocyte stellate cells to cancer-associated fibroblasts [232].

Recorded cycle threshold (Ct) values of all the candidate reference genes examined were submitted to RefFinder, an online tool created by Xie and Zhang to identify the most stable candidate reference gene (Figure 2.15.A) [233]. According to RefFinder, hsa-miR-26a-5p was the most stable gene amongst the others, hence, hsa-miR-26a-5p was used as the reference gene to validate the expression of hsa-miR-21-5p in all groups of exosomes using the Delta-Delta cycle threshold (ΔΔCt) method (Figure 2.15.B). The relative gene expression of hsa-miR-21-5p was expressed significantly different *($p < 0.05$)* from one group to another, where Exo(M4) represents significantly *($p < 0.05$)* the highest fold change followed by Exo(M2), and Exo(M3), compared to the calibrator (control) sample, Exo(M1).

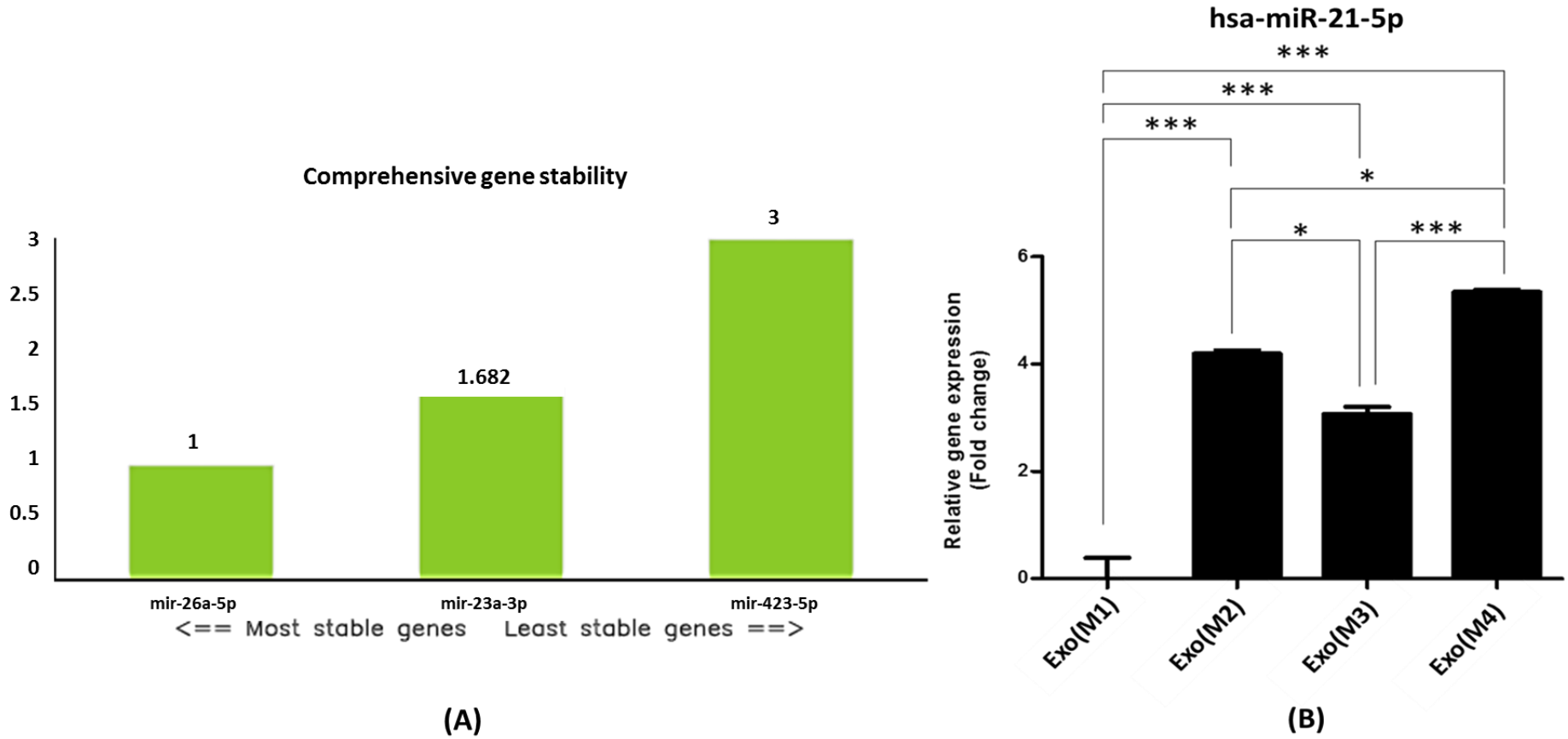

Figure 2.15: Validation of mir-21-5p expression using RT- qPCR.

(A)Stability of Reference Genes analysed using RefFinder tool. Most stable genes are towards the left hand side of the graph while least stable genes are shown to the right hand side of the graph. (B) Relative gene expression of hsa-miR-21-5p in exosome groups using Exo(M1) as a calibrator (Control) sample. This bar graph created by applying the Delta-Delta Ct (ΔΔCt) method using hsa-miR-26a-5p Ct values. The graph represents changes in the expression level of hsa-miR-21-5p between groups. All values are representative of mean ± SEM where *p < 0.05, **p< 0.01, ***p< 0.001 n=3.

2.4. Discussion

Exosomes are known to be crucial contributors in normal physiology and disease conditions by mediating intercellular communications [234]. As such, researchers have been exploring exosome composition, their involvement in cancer progression, and their potential role as diagnostic biomarkers and therapeutic nanodevices [21,103,235]. In order to achieve purity of these exosomes produced using cell culture and to investigate their role without contamination from growth medium sources, this comparative study was designed to investigate the best applicable approach for maintaining successful cell culture and producing a high yield of exosomes with minimal contamination from serum supplementation, using the HepG2 cancer cell line.

The results of cell viability experiment indicated that serum supplemented media: M1 (FBS) and M2 (Dep-FBS) were found to be able to maintain successful cell culture of HepG2 cells, however, serum free ones: M3 (SF) and M4 (SF) could not maintain cell viability/survival *($p > 0.05$)* (Figure 2.2.). This indicates that M2 offered similar growth conditions to M1 (the standard HepG2 medium) despite the difference in serum versions. This was found to be in line with a comparative study performed on different FBS preparations and serum deprivation by Abramowicz *et al.* (2018) who reported that serum deprivation for the last 24 h of incubation of cell cultures, caused significant *($p > 0.05$)* reduction in cell viability while media containing standard FBS, and Dep-FBS maintained cell viability with no significant difference detected [204]. Moreover, Paszkiet *et al*. (2016) proven that cell culture medium supplemented with Dep-FBS maintained cell viability of different cell lines [236] while Rashid and Coombs (2018) confirmed also that serum reduction affect cell viability, morphology, and protein expression compared to medium supplemented with FBS, where no changes were observed [237]. Thus, M2 could

potentially be an efficient replacement to M1, with the advantage of minimal contamination with FBS derived EVs or exosomes while SF versions: M3 and M4 should be avoided.

However, in the literature, it was reported that depleting EVs from FBS using overnight ultracentrifugation has a negative impact on cell growth, viability, migration, and differentiation. For instance, Shelke *et al*. (2014) and Eitan *et al*. (2015) found that EV-depleted FBS has affected the cell behaviour where the migration and growth rate was significantly reduced [219,238]. Also, Aswad *et al*. (2016) confirmed that cell proliferation and differentiation were affected in the absence of FBS derived EVs [239]. Moreover, Lehrich *et al*. (2018) found that FBS depleted of EVs offered suboptimal environment for cell growth and viability [240]. This indicates that the applied technique in depleting FBS from EVs such as ultracentrifugation, is critical in maintaining successful cell culture. Hence, an optimisation study is always required for growing cells in conditioned media using different versions of FBS.

FBS is an essential supplement in cell culture that is important for cell survival and proliferation as it contains growth factors, nutritional and macromolecular factors, and EVs, where BSA and bovine exosomes are the major components [241].

In Micro BCA analysis, protein quantification showed a significant *($p > 0.05$)* increase in Exo(M1) compared to other groups of exosomes, which indicates that Exo(M1) contained the highest protein concentration. For further exosomal characterisation and quantification, this was followed by bead-assisted flow cytometry which offer a semi-quantitative analysis to estimate the amount of exosomes or EVs, and a higher detection limit and a higher sensitivity more than BCA assay, using specific exosomal biomarker such as CD63 [242] (section (2.2.5)). The flow cytometer histograms showed no difference, however, the % of fluorescence revealed a significant *($p > 0.05$)* difference between all exosome groups (Figure 2.5 (B)), where Exo(M1)

represent significantly *(p > 0.05)* the highest percentage of fluorescence compared to all groups. This was followed by Exo(M2), Exo(M3), and Exo(M4) (Figure 2.9 (B)). The obtained findings of these two experiments suggested that Exo(M1) sample containing FBS constituents such as BSA and bovine exosomes [241], where M1 supplemented with standard FBS. This was confirmed by Lötvall *et al*. (2014) study where they observed that BSA is an extracellular protein that is found to be co-isolating with exosomes [80]. These results also tie well with previous findings in the literature showed that Dep-FBS had a much lower protein content than standard FBS, applying electrophoresis and Coomassie blue staining [204]. Also, Kornilov *et al*. (2018) using sliver staining, found that the protein content of FBS was significantly higher than Dep-FBS sample [218].

In Micro BCA, protein quantification implies that Exo(M1) showed high protein content due to FBS in M1, which means that the protein content of Exo(M2), Exo(M3), and Exo(M4) is mainly derived from HepG2-Exo. Therefore, to deliver a better understanding of these findings, a fresh medium containing no serum can be evaluated along with exosome groups. Whereas in flow cytometry, % of fluorescence suggests that the number of exosomes detected in each group is different from the other due to the effect of the media and its composition on the parent cell, consequently, its exosome production. This is found to be consistent with Abramowicz *et al.* (2018), Aswad *et al.* (2016), and Paszkiet *et al.* (2016) findings, as they all reported that FBS contains high amounts of serum proteins and EVs including exosomes [204,236,239].

Thus, using standard FBS in cell culture media is not preferable as it may hinder the detection of the actual number of exosomes of interest, where the presence of high protein content such BSA can impairs the quantitation applying this technique. However, to improve the outcomes of flow cytometry, SEC isolation technique was found to be highly effective in eliminating protein contaminants from exosomes or EVs samples [242].

Tetraspanins or exosome biomarkers are found to be highly enriched in TEX [49], due to their role in promoting cancer progression and metastasis (Chapter 1, section 1.4.2.1.1). However, tetraspanins expression varied among different tumour cell lines [167]. Moreover, cell culture conditions and isolation technique can influence the tetraspanins expression and cargo of cell line derived exosomes [164].

In regard to HepG2-Exo groups derived from M1, M2, M3, and M4, western blot analysis has shown bands of detection of CD63 and CD81 while among the tetraspanins kit (CD63, CD9, and CD81) provided by ExoView, the assessment showed that HepG2 subpopulations have only expressed CD63 and CD9 on their surface. However, the % of CD81 expression in western blot was significantly low in serum free groups: Exo(M3) and Exo(M4), compared to Exo(M1) (Figure 2.6 (B)) using densitometry. This was also found to be in line with ExoView analysis where no capturing or binding was observed with CD81.This suggests that the difference in tetraspanins expressions between ExoView and western blot analysis, can be influenced by the dilution factor used to prepare samples (section 2.2.4 and 2.2.5), the difference in antibody sensitivity used in each assay, and different using antibodies of different manufacturers. However, in literature, CD63, CD81 [160], and CD9 [243] were found to be expressed in liver cancer cell and on the surface of HepG2-Exo.

On the other hand, the difference of tetraspanins expression in between HepG2-Exo groups (Exo(M1), Exo(M2), Exo(M3), and Exo(M4)), indicated that it was mainly driven by HepG2-Exo harvesting media. For instance, in western blot, the intensity of detected bands of CD63 and CD81 varied from one group to another. This difference in band intensities of each group can be interpreted by findings in the literature reported that media containing FBS showed a CD63 band while no band was detected for Dep-FBS [204,236]. This suggests that Exo(M1) bands signals were also expressing FBS-exosomes. While in Exoview, the expression of CD63 and CD9 and the

fluorescence particle count (section 2.3.5), were found to be significantly *(p > 0.05)* increased in Exo(M4), compared to Exo(M1), Exo(M2), and Exo(M3).

Significantly, in western blot, the serum free version exosome groups: Exo(M3) and Exo(M4) showed stronger bands in the CD63 films compared to Exo(M1) and Exo(M2) while Exo(M4) in ExoView analysis has recorded the highest particle count with double binding of anti-CD63 and anti-CD9 to CD63 and CD9 spots amongst all groups (Figure 2.8). These findings showed that the process of exosome biogenesis, exosomes production, and surface markers or tetraspanins expression are strongly affected by HepG2 cell culture conditions which confirms previous findings of Zou *et al.* (2019) who found that maintaining cells in serum starvation mode stimulated exosome production and induced intracellular levels of exosome markers CD63, ALIX, and TSG101 [244]. It was also reported that serum deprivation induced protein expression in released exosomes, including tetraspanins [222]. Moreover, exosome isolation technique found to play a role in the expression of tetraspanins [245]. Collectively, this suggested that maintaining cells in serum starvation mode can influence the expression level of surface exosomal tetraspanins and increases exosome production. Therefore, serum-reduced cell cultures should be carried out with caution.

The expression or the absence of specific tetraspanin found to be critical where tetraspanins have been found to mediate the selective uptake of exosomes through interacting with acceptor cell ligands [246,247]. For instance, the expression of CD63 in liver cancer cell was confirmed by Zhu *et al*. (2014) [248] which found to be involved in immunosuppression and metastasis [249,250]. Whereas Lin *et al*. (2018) validated CD9 expression and its metastatic capacity in HCC [251] and its released exosomes [243] . Also, CD9 has been found to be associated with tumour angiogenesis and suppression [252]. However, the function of CD9 and CD63 are dependent on their association with other tetraspanins or other partner proteins (integrins) [249,252].

Moreover, the overexpression of CD81 is also found to be mediating cancer proliferation, growth, and metastasis [253,254].

On the other hand, the expression of CD63, CD9, and CD81 can be very promising in therapeutics, due to their association with cancer and their role in target selection [46,247,255], where alterations in the expression of tetraspanins can take place to exploit their therapeutic potentials in supressing cancer progression and metastasis.

HepG2-Exo can express other tetraspanins on their surface, however, these tetraspanins were not assessed yet.

MS in combination with chromatographic methods such as HPLC, is a useful approach that offer profiling and characterising EVs content including exosomes, due to the high sensitivity and small sample volumes required for running the analysis [256,257]. LC-MS results showed consistency in separation between exosome groups on all SIMCA models of different columns (Figure 2.9, 2.10, and 2.11) and significant *($p > 0.05$)* difference in the metabolic profiling between the exosome groups compared to the Exo(M1) group (Table 2.1 and 2.2). For instance, arginine, proline, glutamine, glutamate, serine, asparagine, valine, leucine, isoleucine, and tryptophan reported in Table (2.1), are found to be detected in high levels in cancer derived exosomes [258]. However, these metabolites detected in different levels among all HepG2-Exo groups compared to Exo(M1) which implies that cell culture condition can noticeably change the metabolite profiles of EV or exosome [165] (Figure 2.12). These findings were found to be in total agreement with previous observations in this study (section 2.3.4 and 2.3.5), and with previous findings of Haraszti *et al.* (2019), and Zou *et al.* (2019) who reported that stressing the parent cells through serum starvation can change cell derived exosome lipid and protein composition, and induce production of high levels of exosomal marker proteins [222,244].

Moreover, a recent comparative analysis performed by Shin *et al*. (2019) has approved that cancer cells maintained in media containing FBS, found to be secreting higher levels of proteins compared to SF media [259]. Also, it has been found that the isolation technique used for EVs or exosomes collection, can cause a drastic change in the composition of EV [165,260]. For instance, in this current study TIER was used for exosome isolation purposes. International society for extracellular vesicles (ISEVs) has reported in their minimal information for studies of extracellular vesicles 2018 (MISEV2018) recommendations that using precipitation kits containing PEG, or low molecular weight cutoff centrifugal filters may result in the isolation of EVs bound to or mixed with antibodies, beads, and polymers which may influence downstream profiling or functional studies and may also affect the applicability of EVs in therapeutic applications [171]. However, ISEVs stated that conventional methods such as ultracentrifugation is not optimal operation for separating EVs [171].

Therefore, detected metabolites of this current studies were found to mainly influenced by two major factors which are cell culture conditions, and applied isolation technique. Hence, for therapy developers, applying exosomes in therapeutic approaches should be performed with caution through characterising exosomes at all levels, and understanding that the influence of production conditions can highlight novel techniques to alter their innate content.

On the other hand, metabolite cargo of cancer derived exosomes including amino acids, lipids, and TCA-cycle intermediates, can modulate cancer cell metabolism, consequently, promote tumour growth under nutrient deprivation or nutrient stressed conditions, via intercellular communication [258]. Potentially, a therapeutic approach can be developed through inhibiting this crosstalk via targeted methods.

To characterise RNA cargo of exosomes, profiling of miRNAs was essential to investigate in different studies associated with many pathologies, and to detect novel and highly promising biomarkers [261].

The results of RNA-seq showed variation in the total number of identified and novel miRNAs between all exosome groups (Table 2.3). It was also observed that TPM of detected miRNAs varied from one group to another, as shown in (Figure 2.13). Moreover, in Figure 2.14, the heatmap showed significant *($p > 0.05$)* changes in the expression of 44 hsa-miRNAs detected between groups. Moreover, the analysis of acquired data set has also demonstrated differences in the expression of 4 important potential biomarkers between HepG2-Exo groups which are: hsa-miR-18a-5p, hsa-miR-193b-3p, and hsa-miR-21-3p, and hsa-miR-122-5p that specifically expressed in liver cancer [262]. These findings of this study have strongly indicated that using different conditioned media to harvest exosomes from the same cell line, can exert an effect on miRNA content of produced HepG2-Exo. This is found to be in line with the results observed in this current study that reported variation in the exosome groups' composition (section 2.3.6). Also, the findings of Wei *et al*. (2016) study confirmed that culturing the same cell line in different media exhibit distinct profiles of exosomal RNA, and supplementing media with FBS causes an enrichment of exosomal RNA of FBS-derived EVs [220]. For instance, hsa-mir-92a-3p in Figure 2.14, recorded the highest TPM in Exo(M2) which found to be promoting the proliferation of esophageal cancer cells via intercellular communication by targeting PTEN [263]. Li *et al*. (2019) has confirmed also that exosomal hsa-mir-92a-3p induces the proliferation, migration, and invasion of esophageal squamous cell cancer by regulating PTEN [264]. Another study by Casadei *et al*. (2017) has also reported that exosome-derived hsa-mir-92a-3p stimulates liposarcoma progression [265]. This suggests that growing HepG2 cell line in M2 has

induced the expression of hsa-mir-92a-3p in cells, consequently their secreted exosomes. Targeting hsa-mir-92a-3p can be exploited for therapeutic purposes.

On the other hand, a high similarity observed in between RNA profiles of FBS-derived EVs and EVs isolated from different human cell lines and body fluids [219,266,267]. For instance, miRNA analysis of this study demonstrated the expression of hsa-miR-122-5p which is a specific miRNA abundantly expressed in liver tissue [268,269], and not expressed in glioblastoma tumours and cultured glioma cells [220,270]. However, miR-122 is found to be abundant in FBS [220] which indicates that FBS-derived RNAs are falsely interpreted as human RNAs in Exo(M1) sample, where M1(FBS) is the media used for collection. However, depleting FBS from EVs and RNAs do not offer a complete elimination of FBS-derived RNAs, where miR-122 are still detectable [219,220,236]. This implies that M2(Dep-FBS) media is not free of FBS-derived RNA, which means that RNA content of Exo(M2) is still contaminated with FBS-derived RNAs.

However, serum starvation is not recommended as it can lead to cellular stress which is found to be strongly affecting RNA content of cell-derived EVs [271]. This indicates that the RNA content of Exo(M3) and Exo(M4) that isolated from SF media (M3 and M4), has changed.

These findings reported 4 biomarkers that can be utilised as efficient diagnostic tools in liver cancer, and highlighted the effect of different media combination with FBS on RNA content of HepG2-Exo, the inevitable interference of FBS-derived RNA with cell line-derived exosomes despite following different depletion protocols, and the effect of serum starvation on cells and their produced exosomes, therefore, a standard method for harvesting exosomes should be developed to allow the analysis of exosomes of interest without the possibility of any interference with FBS-derived RNAs, or inducing any adverse changes.

To validate the miRNA results, qPCR was performed to assess the expression of hsa-miR-21-5p in the HepG2-Exo groups, as it was detected in all groups with insignificant variation in expression, and for its key role in proliferation in cancer, and as a potential therapeutic and diagnostic target in liver cancer patients [232,262,272]. The results of this experiment confirmed that hsa-miR-26a-5p was the most stable reference gene among others using the RefFinder tool [230,233]. Thus, the expression of hsa-miR-21-5p was determined using hsa-miR-26a-5p Ct values, applying the Delta-Delta Ct (ΔΔCt) method which revealed that the relative gene expression (fold change) has significantly ($p > 0.05$) changed between groups (Figure 2.15), where Exo(M4) recorded significantly ($p > 0.05$) the highest fold change followed by Exo(M2), and Exo(M3), compared to the calibrator sample, Exo(M1). This difference in fold change was expected according to the previous findings of RNA-seq of each group and previous studies mentioned in section (2.3.7). However, the expression of hsa-miR-21-5p was found not limited only to cancer derived-exosomes where Mannerström *et al*. (2019) observed high levels of hsa-miR-21-5p in standard FBS-derived EVs and FBS depleted by ultracentrifugation, and ultrafiltration, and commercially depleted FBS. Also, they demonstrated low levels of hsa-miR-21-5p in SF media [273]. This indicates that no media is free of either vesicular RNA due to serum supplementation or non- vesicular RNA found in SF media which implies that the relative gene expression of hsa-miR-21-5p in Figure 2.15 (B), do not represent only miRNA of HepG2-Exo.

2.5. Conclusion

In this chapter, the influence of different conditioned medium used for collecting HepG2-Exo was studied through supplying media with either standard FBS or Dep-FBS, or complete absence of serum, to monitor cell viability and analyse the released exosomes of each media. In terms of cell viability, M2 media supplemented with commercially prepared Dep-FBS, found to successfully maintained cell culture of HepG2 despite previous findings reported that depleting

FBS derived EVs using ultracentrifugation affect cell behaviour and growth [219,238–240]. This highlighted that the technique used to deplete FBS has major effects on cell cultures.

In terms of exosome analysis, each different media found to exert different effect on exosomes. However, Exoview study has shown that all HepG2-Exo groups are only expressing CD63 and CD9, which suggested that these tetraspanins can be targeted for therapeutic purposes in HCC. Metabolomic profiling of exosome groups has shown that media used for collecting HepG2-Exo can cause significant changes in the composition of exosomes through affecting metabolites ratios.

Depleting FBS from its EVs and RNAs content found to be insufficient in eliminating bovine contaminants. On the other hand, SF growth conditions are not contaminant free and found to affect cell viability, and protein and RNA content of released exosomes. Therefore, this work suggests that conditioning media either by supplementing media with standard or depleted FBS, or using SF media instead, is not ideal to be applied in exosome studies where misinterpretation of the results and misleading conclusions can be developed as proposed earlier in the literature [262,279,289,307].

Chapter 3

The Influence of HepG2-Exo on cancer and normal cell lines

Abstract

Introduction: Cancer progression and metastasis can be stimulated via cancer-derived exosomes, as they induce changes in the recipient cells through modifying their proteomic and genomic composition. These exosomes have therapeutic potentials as they can be re-purposed or their contents modified to deliver particular signals that cause inhibition or suppression of tumours. In this study, different concentrations of HepG2-Exo were prepared to demonstrate their effect on the biological processes and the metabolomes of melanoma (A375), non-small lung cancer (A549), and normal (PNT2A) cell lines.

Methods: Exosome samples were harvested and isolated from HepG2 cells cultured in medium supplemented with Dep-FBS. Different concentrations of HepG2-Exo were prepared: 25, 50, 100, 200, 400, and 800 µg/ml. The assessment of A375, A549, and PNT2A cell lines under these concentrations, was evaluated using MTT cell proliferation assay, migration, adhesion, and invasion assays, then followed by LC-MS analysis.

Results: The MTT assay showed that all cell lines were affected under the influence of HepG2-Exo, where A375, A549, and PNT2A recorded the highest proliferation rate at 100, 50, 200 µg/ml of HepG2-Exo, respectively. This result showed that each cell line reached their optimum proliferation rate at a specific concentration of HepG2-Exo, which indicates that cells respond to HepG2-Exo differently. The migration assay revealed no difference in any cell line, whereas the adhesion and invasion assays showed significant *($p< 0.05$)* difference at 50 µg/ml for A549. PNT2A has showed significant difference at 50 µg/ml in the invasion assay only, while no significant findings were observed for A375 at 100 µg/ml in all assays. These results indicate that A549 was consistently influenced by HepG2-Exo, however, the cellular communication of other cell lines with HepG2-Exo is limited by three factors: cell line, exosome origin, and concentration

of exosomes. LC-MS findings demonstrated a clear significant separation *($p< 0.05$)*, and changes in metabolite ratios of OXPHOS (ATP), and purine and pyrimidine metabolism pathways, between all groups of treatments versus controls, where A375 was the most affected cell line at 100 µg/ml followed by A549 at 50 µg/ml and PNT2A at 50 and 100 µg/ml. This shows that cancer cells such as A375 are subjected to changes by cancer-derived exosomes rather than normal cell line at the same concentration such as PNT2A at 100 µg/ml which explains the increase in proliferative activity of A375 at 100 µg/ml.

Conclusion: Cell behaviour and metabolome of different cancer cell lines were found to be affected by HepG2-Exo under different concentrations. However, high concentrations of HepG2-Exo can either induce a cytotoxic effect or enhance the metabolic and proliferative activity of the recipient cell as observed in A375, therefore, employing HepG2-Exo in therapeutics should be carried out with caution. HepG2-Exo could represent a promising tool in terms of developing lung cancer therapeutics.

3.1. Introduction

Cancer-derived exosomes are key mediators of intercellular communication in the tumour microenvironment, as they carry and transfer modified malignant information and molecules such as lipids, proteins, and nucleic acids, from cancer cells to the recipient cells, or to the peripheral circulation [274,275]. These exosomes play multiple roles to regulate cancer progression, through stimulating the process of angiogenesis, inducing cancer cell migration and invasion, inhibiting immune system responses, and promoting the formation of the metastatic niche [103].

Cancer metastasis is mainly driven and mediated by TEX through inducing the aggressiveness of tumour cells, triggering the process of EMT; stimulating angiogenesis and inducing vascular permeability; modulating immune responses by inducing immunosuppression or releasing immunosuppressive factors; transforming non-neoplastic cells by releasing oncogenic proteins; and reprogramming energy metabolism by modifying metabolic pathways [4]. For instance, in the tumour microenvironment, fibroblasts are transformed into cancer associated fibroblasts (CAFs) that release exosomes containing metabolic cargo that are then transferred into cancer cells and induce remodelling of recipient cell metabolism via cell-to-cell communication [258]. Thus, the effect of cancer-derived exosomes on other cell lines is inevitable and it has been well documented in the literature. For instance, it was reported that cancer cell-derived exosomes were found to induce cell proliferation and chemoresistance in recipient cells *in vitro* and *in vivo* as observed in colon cancer cell-derived exosomes [276]. Moreover, two studies performed by Qu *et al.* (2009) and Li *et al.* (2015), using exosomes revealed that gastric cancer cell line (SGC7901) derived exosomes caused significant increase in the proliferation of two other gastric cancer cell lines (SGC7901 and BGC823) [277,278].

Furthermore, O'Brien *et al.* (2013) performed a study on exosomes derived from triple negative breast cancer (TNBC) cell lines [Hs578T and its modified invasive Hs578Ts(i)8 version was found to induce the proliferation, migration, and invasion significantly of three different recipient breast cancer cell lines (SKBR3, MDA-MB-231 and HCC1954). Moreover, the invasiveness of the parent Hs578T cells increased due to Hs578Ts(i)8-derived exosomes. Also, it was reported that exosomes derived from sera of TNBC patients increased cell invasion compared with control healthy sera derived exosomes [279]. Another study carried out by Zhang *et al.* (2018), using exosomes derived from the metastatic breast cancer cell line MDA-MB-231, revealed that the proliferation of MDA-MB-231 and ZR-75-1, breast cancer cell lines, increased significantly. These two cell lines were also treated with exosomes derived from the noncancerous mammary epithelial line MCF-10A and no significant effect was detected [280]. A study by Yang *et al.* (2013) using exosomes derived from the bladder cancer cell line T24, reported that proliferation of two-recipient bladder cancer cell lines T24 and 5637 increased significantly [281].

Cancer cell-derived exosomes are key players of metastasis, tumour progression and angiogenesis. For example, melanoma (B16-F10), TNBC (Hs578T) and HCC (HepG2) cell line-derived exosomes, caused stimulation of HUVEC tube formation [160,279,282]. Ovarian cancer-derived exosomes were found to promote HUVEC proliferation, migration, and induce the formation of a premetastatic niche [161,283]. Chowdhury *et al*. (2015) studied the effect of PC cell line (DU145)-derived exosomes on BMMSCs by adding exosomes into BMMSCs conditioned media. They found that the levels of pro-angiogenic factor such as VEGF and hepatocyte growth factor (HGF) increased. Also, BMMSC were induced to differentiate into myofibroblasts, and HUVEC proliferation, migration, and tubule-formation were enhanced [284].

In liver carcinoma, HepG2-Exo were found to be strongly involved in tumour progression, metastasis and angiogenesis, through HUVECs stimulation. For instance, Huang *et al.* (2015),

found that HepG2-Exo containing VASN (a type I transmembrane protein), delivered a metastatic signal to the surrounding endothelial cells which resulted in stimulation of HUVECs migration [162]. Moreover, the conversion of fibroblasts into CAFs, found to be associated with HepG2-Exo promoted tumour progression. For example, Luo *et al.* (2017), revealed that HepG2-Exo can induce differentiation of human adipose-derived MSC into CAF, which in turn stimulate the migration of the HepG2 cancer cell line [285]. Furthermore, Fang *et al.* (2017), found that HCC cell line-derived exosomes including HepG2, secrete exosomal miR-1247-3p that induce the conversion of normal fibroblasts to CAFs, promote tumour progression, and stimulate the formation of the premetastatic niche in the lung [286].

Another example of the effect of HepG2-Exo on normal cell lines or tissues was performed on adipocytes by Wang *et al.* (2018). They found that adding HepG2-Exo to adipocytes, changes the transcriptome of adipocytes and cytokine secretion which convert adipocytes into tumour-promoting cells [287].

Furthermore, cancer derived exosomes have been found to cause changes in the metabolism of recipient cells. For instance, Zhao *et al*. (2016) found that CAF-derived exosomes induce glycolysis and glucose uptake in PC through the inhibition of mitochondrial oxidative phosphorylation (OXPHOS). Also, they reported high levels of different amino acids, carboxylic acids, and fatty acids in different types of CAFs-derived EVs, which suggested that EVs are carriers of metabolites that intensify cancer cell metabolism [258]. Moreover, under nutrient-deprived stress conditions, Achreja *et al*. (2017) demonstrated that CAFs-derived EVs enhanced pancreatic ductal adenocarcinoma (PDAC) cell proliferation, regulate glycolysis pathway fluxes by supplying lactate, and provide up to 35% of the tricarboxylic acid (TCA) cycle fluxes via supply of TCA intermediates and glutamine [288]. Earlier, Beckler *et al*. (2013), revealed that the content of EVs released from CRC mutant KRAS-expressing cells, regulate metabolism, glycolysis,

and increase the growth of wild type KRAS cells [289]. In metastatic PC, Valentina *et al*. (2017) found that patients' plasma-derived EVs contribute to stroma activation, angiogenesis, and tumour progression by shifting the target normal fibroblasts metabolism. Also, glutaminase and lactate dehydrogenase (LDH) levels found to be upregulated by EVs [290].

In breast cancer, Zhou *et al*. (2014) demonstrated that fibroblast metabolism influenced via breast cancer cell-derived EVs expressing high levels of miR-122, lowered glucose uptake in the surrounding normal cells via PKM2 and GLUT1 downregulation. Consequently, the availability of glucose for cancer cells increases, causing an increase in cell proliferation and promotion of metastasis [291]. Also, Sansone *et al*. (2017) found that mitochondrial DNA of CAFs-derived EVs can influence breast cancer cell metabolism, stimulate oestrogen receptor-independent OXPHOS and mediate escape from therapy-induced metabolic dormancy [292].

Therefore, in this chapter, HepG2-Exo were further investigated in terms of their effect on other cancer (A375 and A549) and normal (PNT2A) cell lines and their ability to modify the metabolic activity of these cells in a dose-dependent manner.

3.2. Methodology

3.2.1. Cell Culture

Cell lines used for biological assays and metabolomics included: human melanoma (A375) (passage number (no). 31), non-small lung cancer (A549) (passage no. 25), and human normal prostate epithelium (PNT2A) (passage no. 42). A375 and A549 cell lines were maintained in DMEM-high glucose with pre-added supplements by the manufacturer (2.2.1). PNT2A was maintained in Gibco™ RPMI 1640 Medium. All cell cultures were supplemented with 10 % (v/v) of standard FBS and supplemented with 0.584 mg/ml of L-glutamine (200 mM), 0.11 mg/ml of sodium pyruvate (100 mM), 100 I.U./mL penicillin and 100 (µg/mL) streptomycin, and

NEAA(often 10 mM; 100X), that is aseptically added to the medium for a final concentration of 0.1 mM each, and carried out at 37°C in the presence of a mixture of 95% air 5% CO2 with 100% humidity.

3.2.2. Exosome sample preparation

Referring to findings in Chapter 2, HepG2 cell culture was carried out in M2 media. After cells reached confluency, the preparation of exosome sample was performed following steps in section 2.2.8.3.

3.2.3. MTT proliferation assay

Cells were seeded at a density of 5×10^3 cells/well in a 96 well plate. After 24 h, the media were removed and cells were washed three times with HBSS; then serum-free medium was added to each well. After 48 h, six concentrations of HepG2-Exo were prepared and added to each well: 25, 50, 100, 200, 400, and 800 µg/ml. These concentrations were determined using a Micro BCA assay (section 2.2.5). The manufacturer's protocol for cell proliferation Kit I (MTT) was followed for the measurement steps. Cell proliferation was determined using a SpectraMax M5 plate reader at 570 nm and a reference wavelength of 690 nm. The measured absorbance values were corrected by subtracting readings recorded at 690 nm.

After analysing these results, two concentrations were selected for the following assays based on the highest effect induced by HepG2-Exo in the MTT assay on the cancer cell lines. Also, these concentrations were tested on the normal cell line to demonstrate their effect, and to initiate a comparison of the effect HepG2-Exo on cancer and normal cell lines.

3.2.4. Migration, adhesion, and invasion assays

A CytoSelect™ 24-well Cell Migration assay (8 µm, colorimetric format), CytoSelect™ 48-Well Cell Adhesion assay (Collagen I-Coated, colorimetric format), and CytoSelect™ 24-well Cell Invasion assay (8 µm, colorimetric format), were used following the manufacturer's instructions for the staining and extraction steps. The absorbance of extracted cells was measured at 560 nm using a SpectraMax M5 plate reader.

3.2.5. Liquid chromatography–mass spectrometry (LC-MS) analysis

3.2.5.1. Metabolite Extraction

A375, A549, and PNT2A cell lines were seeded in a 6-well plate at a density of 3×10^5 cells/well. After 24 h, the medium was replaced with serum free medium, following 3 washes with HBSS. HepG2-Exo (50 µg/ml) were added to A549 and PNT2A, and (100 µg/ml) to A375 and PNT2A. After 96 h, cell extraction was performed by removing the medium and washing the cells with 3 ml warmed up PBS to 37˚C. Extraction of the cells was performed at a cell density of 1×10^6 cells/well, by adding ice cold extraction solution, methanol: acetonitrile: water (50:30:20) (v/v). After that, the cells were scraped, and the lysates were transferred to microcentrifuge tubes for mixing using a Thermomixer at 4°C for 15 min. The samples were then centrifuged at 0°C for 10,000 × g for 10 min. Supernatants were collected and transferred into auto-sampler HPLC vials. The samples were kept at -20°C until required for the analysis by LC-MS.

3.2.5.2. LC-MS conditions

The HPLC column used was ZIC-pHILIC column (150 × 4.6 mm, 5 µm) following the same running conditions in section 2.2.8.2.

3.2.5.3. Data Extraction and analysis

The extraction and analysis of LC-MS data was performed following steps in section 2.2.8.3.

3.2.6. Statistical Analysis

All experiment values were representative of at least three independent experiments and are displayed as mean ± SEM, where *p< 0.05,**p< 0.01, ***p< 0.001 significant difference, n=3. One-way ANOVA followed by Dunnett's test, and two-way ANOVA followed by Bonferroni post-tests, were used to assess statistical significance between cells. The statistical analysis was performed using GraphPad Prism software version 5.00.

3.3. Results

3.3.1. The effect of HepG2-Exo on cell proliferation

The MTT Kit was used to assess cell proliferation under the influence of HepG2-Exo. The proliferation rate of different cell lines was measured based on the metabolism of MTT (yellow colour) to form formazan crystals (purple in colour) by viable cells. The cell proliferation rate has increased in all cell lines, where the highest proliferation rate for A375 was detected at 100 µg/ml, A549 at 50 µg/ml, and PNT2A at 200 µg/ml (Figure 3.1(A),(B) and(C)). Statistically, a significant *(p>0.05)* inhibition in proliferation at 800 µg/ml was observed in A375 and A549 cell lines, compared to 0 µg/ml. Whereas in PNT2A, cell proliferation rate has increased significantly *(p>0.05)* at 25, 50, 100, 200, and 400 µg/ml of HepG2-Exo (Figure 3.1(A),(B) and(C)). However, 100 and 50 µg/ml were chosen to be applied to the respective cancer cell lines, and on PNT2A as the normal cell line for further assessment.

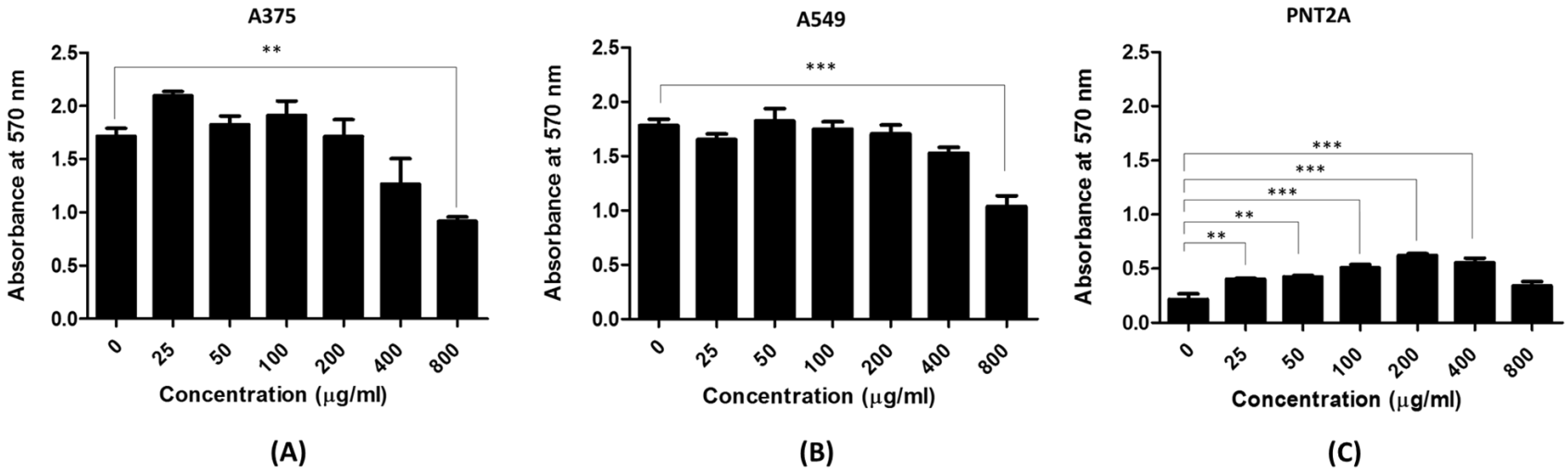

Figure 3.1: MTT Cell Proliferation assay of (A) A375, (B) A549 and (C) PNT2A cells.

All values are representative of mean ± SEM where *p < 0.05, **p< 0.01, ***p< 0.001 n=3.

3.3.2. The effect of HepG2-Exo on cell migration

The migration assay was used to determine the effect of HepG2-Exo on the migration rate of A375, A549, and PNT2A cells. Statistical analysis showed no significant change at both concentrations for each cell line.

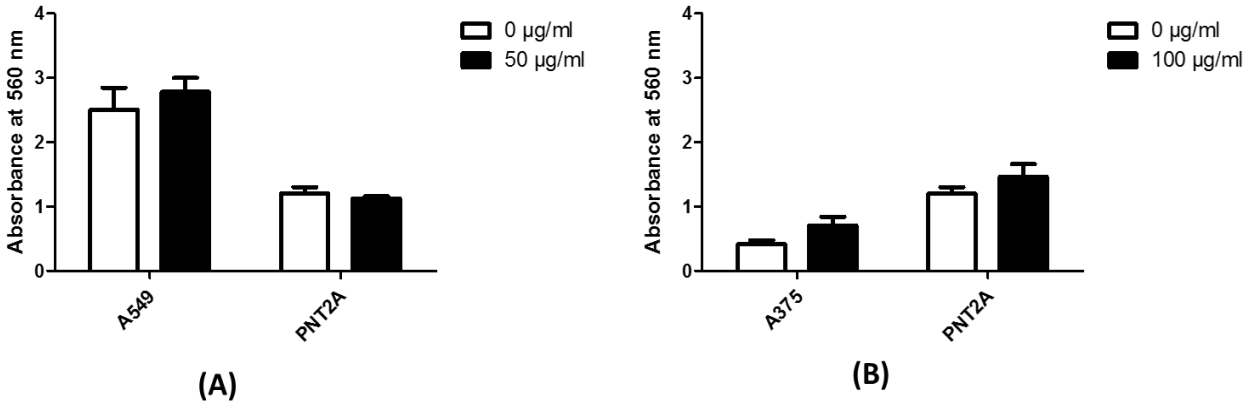

Figure 3.2: 48-well Migration assay.

(A) A549 and PNT2A cells at 50 µg/ml of HepG2-Exo and (B) A375 and PNT2A cells at 100 µg/ml of HepG2-Exo. All values are representative of mean ± SEM, n=3

3.3.3. The effect of HepG2-Exo on cell adhesion

The adhesion assay was used to investigate the adhesion activity of the cells, under the effect of HepG2-Exo. A significant *(p>0.05)* increase in cell adhesion rate was detected in A549 and PNT2A at 50 µg/ml compared to no treatment, 0 µg/ml (Figure 3.3.A). However, no significant difference was observed for A375 and PNT2A at 100 µg/ml (Figure 3.3.B).

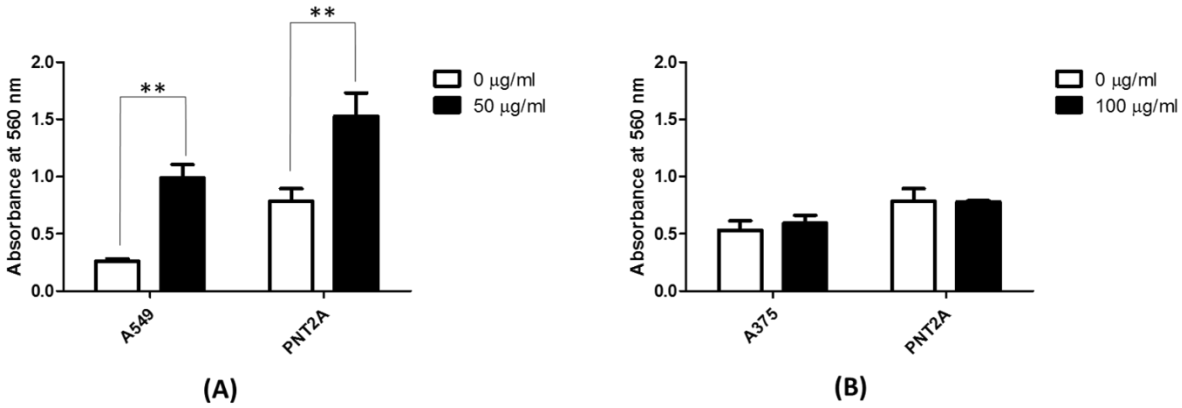

Figure 3.3: Collagen I - 48 well Adhesion assay.

(A) A549 and PNT2A cells at 50 µg/ml of HepG2-Exo. (B)A375 and PNT2A cells at 100 µg/ml of HepG2-Exo. All values are representative of mean ± SEM where **p< 0.01, n=3.

3.3.4. The effect of HepG2-Exo on cell invasion

The invasion assay was performed to assess the effect of HepG2-Exo on the cell invasion rate of A375, A549, and PNT2A. A significant increase *(p>0.05)* was observed only in A549 at 50 µg/ml, while no changes were detected at 100 µg/ml (Figure 3.4).

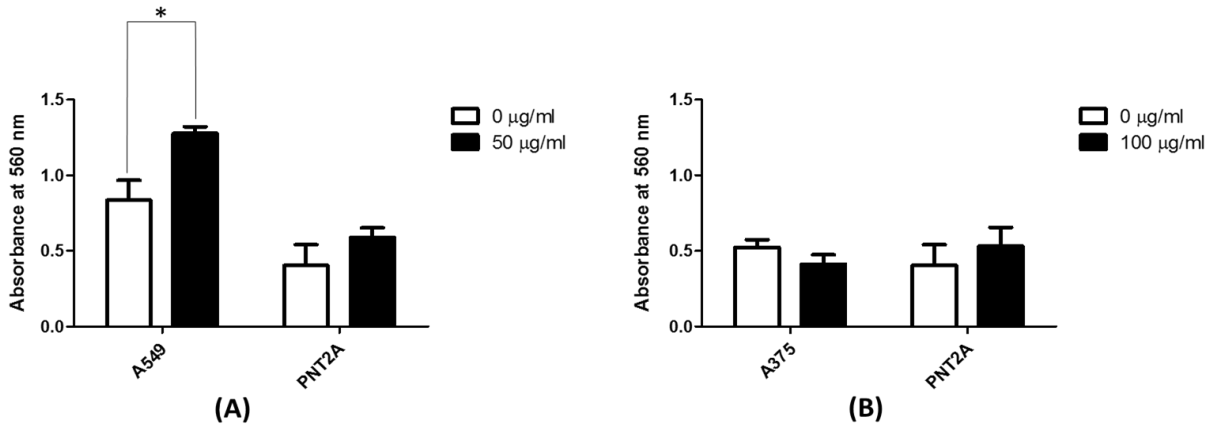

Figure 3.4: 48 well Invasion Assay.

(A) A549 and PNT2A cells at 50 µg/ml of HepG2-Exo. (B) A375 and PNT2A cells at 100 µg/ml of HepG2-Exo. All values are representative of mean ± SEM where *p< 0.05, n=3.

3.3.5. The effect of HepG2-Exo on cancer and normal cell lines

Metabolomics profiling of cancer cell lines (A375 and A549), and normal cell line (PNT2A) was carried out to study the effect of HepG2-Exo on the cell metabolome, and to compare two different concentrations: 50 and 100 µg/ml of the exosomes. Acquired data were processed using SIMCA software to create two models: PCA and OPLS-DA, to assess the separation efficiency of a ZIC-pHILIC column for polar metabolites, the quality of prepared samples, and the difference between HepG2-Exo treatments (Figure 3.5). Quality control samples (P) were clustered around the centre of the plot of the PCA model which validates the efficiency of the analysis and indicates maintained instrument performance and precision throughout the run on the column (Figure 3.5.A). While on the OPLS-DA model, a clear and significant separation was detected between A375, A549, and PNT2A cell lines between the control and treatment groups and between the cell lines with *P* CV-ANOVA= 0.002. Detected metabolites in each cell line were reviewed individually (Table 3.1). A heatmap was created by Clustvis, a web tool for visualising clustering [293], based on the significant difference ($p < 0.05$) observed in 27 metabolites plotted (Figure 3.6) which demonstrates the degree of change in metabolites before and after exosome treatments in each cell line according to the change in colour intensity.

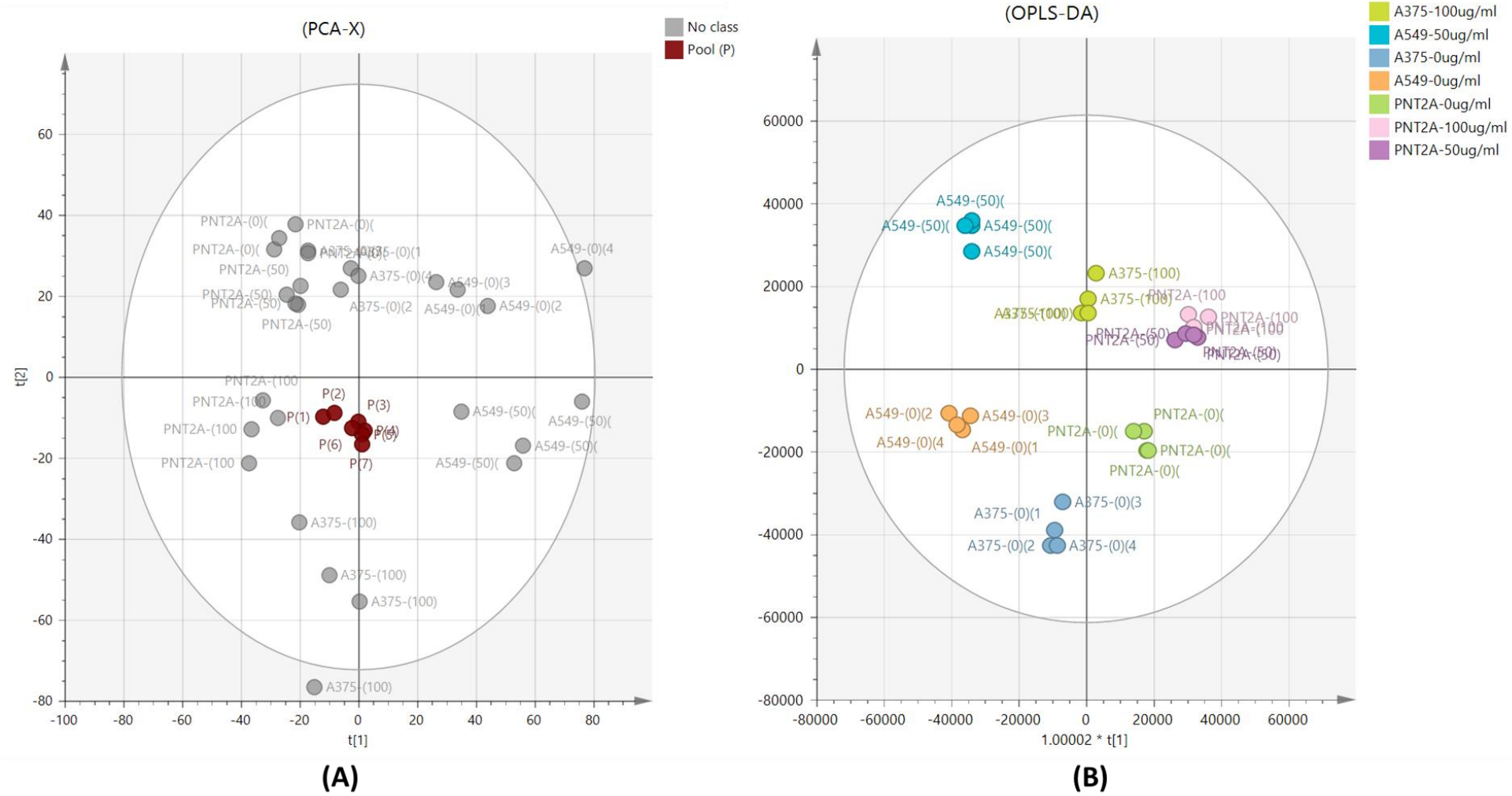

Figure 3.5: (A) PCA-X vs (B) OPLS-DA score plot of A375, A549, and PNT2A cell lines using ZICpHILIC.

(A)plot shows the clustering of pooled samples (P) compared to A375, A549, AND PNT2A control and treated samples with HepG2-Exo (grey-No class), PCA-x score plot (A) has R2 = 0.844, Q2= 0.71. (B) plot shows a clear separation and distribution of 28 observations based on readings of 365 identified polar putative metabolites.The observations classified into seven groups: A375-0µg/ml, A375-100µg/ml, PNT2A- 100µg/ml, A549-0µg/ml, A549-50µg/ml, and PNT2A-50µg/ml, 0OPLS-DA score Plot (B) has has R2 = 0.944, Q2=0.914.

Table 3.1. Significantly changed metabolites within A549, A375, and PNT2A cells treated with different concentrations of HepG2-Exo, compared to untreated cells.

Mass	Rt	Putative Metabolite	A549 (0µg/ml) vs A549 (50µg/ml)		A375 (0µg/ml) vs A375 (100µg/ml)		PNT2A (0µg/ml) vs PNT2A (50µg/ml)		PNT2A (0µg/ml) vs PNT2A (100µg/ml)	
			Ratio	*p* value	Ratio	*p* value	Ratio	*p* value	Ratio	*p* value
		Pyrimidine metabolism								
243.06	12.32	Uridine	0.098	<0.001	0.189	0.001	0.013	<0.001	0.039	<0.001
322.04	15.98	CMP	0.545	0.021	3.870	0.032	0.744	ns	0.676	0.012
482.96	19.15	UTP	0.713	0.006	0.641	ns	0.296	0.007	0.136	0.002
305.01	15.93	2',3'-Cyclic UMP	1.081	ns	5.412	0.0006	1.162	ns	1.208	ns
228.09	13.96	Deoxycytidine	0.667	ns	1.721	<0.001	1.155	ns	1.764	ns
565.04	17.32	UDP-glucose	0.740	0.030	0.388	0.006	0.444	0.001	0.320	0.000
323.02	17.35	UMP	0.707	0.010	0.283	0.002	0.420	0.001	0.284	0.000
402.99	20.54	UDP	0.914	ns	1.286	ns	0.551	0.012	0.275	0.000
		Purine metabolism								
328.04	14.39	3',5'-Cyclic AMP	0.844	ns	0.517	0.024	0.277	0.000	0.243	0.000
346.05	17.54	AMP	0.903	ns	4.282	0.000	1.348	0.034	1.266	ns
362.05	17.56	GMP	0.282	0.028	0.029	<0.001	1.393	ns	0.782	ns
76.03	16.22	Glycine	1.329	0.034	3.133	0.01	1.906	0.04	2.599	0.000
		Oxidative phosphorylation (OXPHOS)								

664.11	14.04	NADH	0.856	ns	0.813	ns	0.973	ns	1.284	ns
662.10	14.41	NAD+	0.937	ns	0.550	0.016	0.450	0.012	0.369	0.007
505.98	17.50	ATP	0.904	ns	4.443	0.000	1.240	ns	0.995	ns
426.02	14.40	ADP	0.897	ns	0.571	0.043	0.376	0.002	0.318	0.001
		Miscellaneous								
194.08	4.76	Phenylacetylglycine	1.067	ns	2.668	0.020	1.539	0.011	2.099	0.000
371.01	13.92	D-Sedoheptulose 1,7-bisphosphate	1.067	ns	0.707	0.031	0.081	0.000	0.158	0.001
289.03	17.12	Sedoheptulose 7-phosphate	0.726	ns	0.249	<0.001	0.607	0.002	0.862	ns
90.054	15.14	L-Alanine	1.360	0.022	1.977	0.019	0.987	ns	1.149	ns
606.07	15.92	UDP-N-acetyl-D-glucosamine	0.858	ns	4.152	0.002	1.052	ns	0.919	Ns
611.14	18.18	Glutathione disulfide	0.332	0.000	1.041	ns	1.055	ns	0.693	0.025
300.04	15.93	N-Acetyl-D-glucosamine 6-phosphate	1.433	0.039	6.379	0.000	1.004	ns	1.073	ns
221.05	17.71	L-Cystathionine	1.941	0.004	3.228	ns	1.847	0.044	1.644	Ns
579.02	20.53	UDP-glucuronate	1.075	ns	1.197	ns	0.677	ns	0.262	0.000
308.09	13.90	N-Acetyl Neuraminate	0.279	0.014	3.360	ns	1.832	0.008	2.125	0.009
744.08	18.33	NADPH	1.619	0.002	1.432	ns	1.113	ns	0.588	0.021

The data demonstrated in Table 3.1 showed the most significant *($p < 0.05$)* changed polar metabolites after exosome treatment where the most affected pathways found to be Pyrimidine metabolism, Purine metabolism, and OXPHOS in A375.

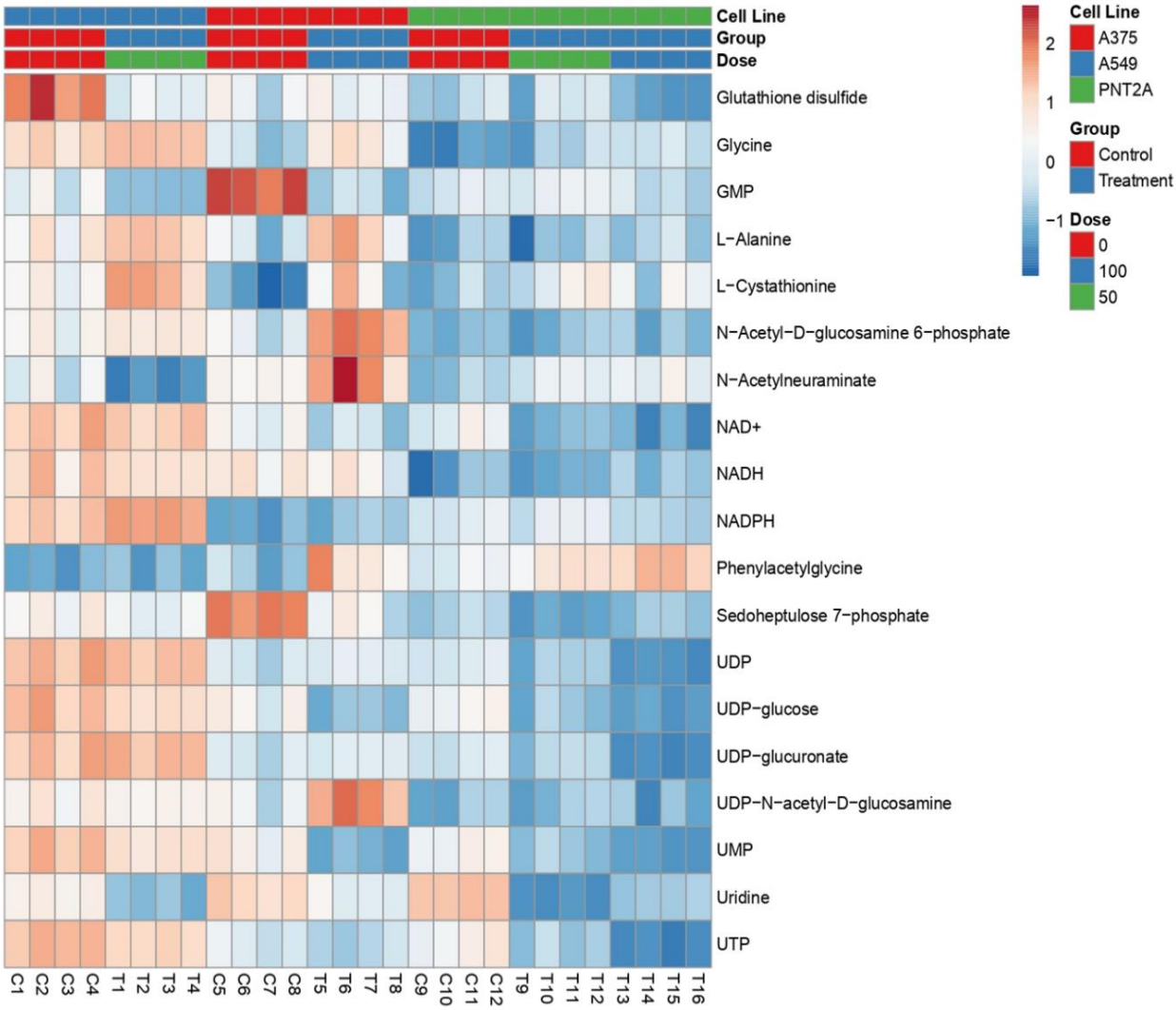

Figure 3.6: Heatmap showing the top 27 significant putative metabolites among controls (C) and treatments (T) of A375, A549 and PNT2A.

The data are displayed on a log2 scale. The differences in colour shades represent intensities of the metabolites vs. sample observations.

3.4. Discussion

Tumour progression and metastasis are carried out through exchanging information using signalling pathways between cells, which involve secreting cytokines, chemokines, and EVs such as exosomes [7]. In the literature, several studies have reported the role of exosomes as mediators in cell-to-cell communication in the tumour microenvironment for cancer development and progression, metastasis, and angiogenesis [7,274,283,294–296]. In order to investigate the influence of HepG2-Exo on other cell lines, this study was designed to monitor the effect of cancer-derived exosomes on biological stages of cancer progression and metastasis, namely proliferation, migration, adhesion and invasion.

The results of the MTT assay showed that HepG2-Exo induce the cell proliferation of all cell lines whereas the proliferation rate of PNT2A has significantly ($p < 0.05$) increased at 25, 50, 100, 200, and 400 µg/ml due to the effect of HepG2-Exo (Figure 3.1). The highest proliferation rate observed for each cell lines: 100 µg/ml (A375), 50 µg/ml (A549), and 200 µg/ml (PNT2A). However, a significant decrease ($p < 0.05$) was observed at 800 µg/ml, in A375 and A549.

This indicates that HepG2-Exo enhance the proliferation activity of both cancer and normal cell lines at specific concentrations, which supports previous findings In the literature that confirmed the role of HCC exosomes such as HepG2-Exo, in promoting the proliferation of cancer cell and the formation of lung metastases [297,298]. In general, TEX were found to contribute to cancer progression and metastasis through stimulating the proliferation of normal and cancer cell lines [281,287,299,300]. On the other hand, the reduction in proliferation rate in the cell lines examined at 800 µg/ml of HepG2-Exo, suggests that these exosomes exerted a cytotoxic effect at higher concentrations which means that higher concentrations of cancer-derived exosomes could work as a therapeutic approach to inhibit cancer cell proliferation. However, this should be applied with high caution using the safest approach available.

Migration, adhesion, and invasion assays were carried out following findings observed in section 3.3.1.

The results of these assays showed that no significant effect was observed in A375 cells at 100 µg/ml whereas A549 were found to be significantly ($p < 0.05$) influenced in terms of adhesion and invasion, at 50 µg/ml. However, PNT2A showed only significant difference ($p < 0.05$) in adhesion at 50 µg/ml of HepG2-Exo.

In spite of not detecting a significant difference in the migration assay for either cell line, a slight increase in migration rate was observed after adding HepG2-Exo in all the cell lines tested (Figure 3.2) which indicates that HepG2-Exo can induce migration in other cancer and normal cell lines. This concurs well with previous studies that reported HepG2-Exo could stimulate angiogenesis through activating the migration of endothelial cells and HCC cells via the expression of HSP70 and miR-210 [160,162,301–306].

The adhesion assay was performed on collagen type I coated wells, to investigate the effect of HepG2-Exo on collagen binding to discoidin domain receptor 2 (DDR2) expressed in these cell lines: A375 and A549 [307], and PNT2A [308].

Findings from this assay suggest that HepG2-Exo induce the adhesion for cancer and normal cells as observed in A549 and PNT2A at 50 µg/ml, which confirms previous finding by Fu *et al*. (2018). They stated that primary tumour exosomes such as HepG2-Exo play a key role in lung metastasis through enhancing cell adhesion of cancer cells [297].

In Invasion assay, the results indicate that HepG2-Exo significantly ($p < 0.05$) increased the invasion rate of A549 at 50 µg/ml only, while an insignificant slight increase was observed in PNT2A at 50 and 100 µg/ml. This matches with previous findings in the literature [309]. Recently,

Yang *et al*. (2020), reported the role of cancer-derived exosomes such as breast cancer-derived exosomes in regulating invasion and metastasis via the delivery of miR-146a to CAFs [310].

However, the overall variations in response to HepG2-Exo doses observed in the assays carried out indicate that the cell line, exosomes origin, and concentration of exosomes play a significant role *in vitro* and in applying therapeutic approaches. In terms of compatibility between the cell line and the origin of exosomes, the observations of Sancho-Albero *et al.* (2019) study confirmed that the response of the recipient cell lines to such cancer cell-derived exosomes is subjective to their origin [311]. In terms of exosomes concentration, Yukawa *et al.* (2018) found that the progression of angiogenesis is dependent on the number of HepG2-Exo produced by HepG2 cell line [288].

However, the findings of these assays collectively confirmed that HepG2-Exo at 50 µg/ml induce the proliferation, migration, adhesion, and the invasion of A549 *in vitro*. Clinically, patients diagnosed with primary liver cancer have been found to develop lung metastasis [312]. This could explain the constant behaviour of A549 towards HepG2-Exo doses. Hence, HepG2-Exo can be targeted and incorporated with specific agents as potential therapeutics for lung cancer.

LC-MS data revealed that the significant ($p < 0.05$) separation observed on the OPLS-DA model between treatment and control groups (Figure 3.5) indicates that HepG2-Exo induced an influence on the metabolome of each cell line.

Moreover, in Table 3.1, the calculated ratio of each metabolite showed a significant ($p < 0.05$) difference at their recorded peak area between HepG2-Exo treatments (50, and 100 µg/ml) for each cell line and control (0 µg/ml). This suggests that cells under HepG2-Exo treatment, developed distinctive metabolic profiles, where multiple metabolic pathways were significantly changed as observed in pyrimidine, purine metabolism, and OXPHOS pathways. Whereas in the

heatmap (Figure 3.6), the change in colour intensity between treatments and control, provided an indication of the degree of variation in cell responses towards treatments.

For further analysis of metabolites in Table 3.1, the OXPHOS metabolic pathway is known to be downregulated in cancer cells which resulted in low generation of ATP molecules [313]. However, after exosome treatments, a significant *($p < 0.05$)* increase in ATP ratio in A375 was observed, which indicates that OXPHOS was induced in A375 cells. This was found to be in complete agreement with Park *et al.* (2019), who found that hypoxic TEX enhanced OXPHOS in macrophages derived from bone marrow [314].

The elevation in intracellular ATP levels in cancer cell lines was reported by Qian *et al.* (2016), Wang *et al.* (2017), and Cao *et al.* (2019) who found that the increase of intracellular ATP is due to the uptake of extracellular ATP through an endocytic pathway called macropinocytosis and others pathways, which in turn induced cell proliferation and drug resistance in tumour cells [315–317]. Whereas, Arslan *et al.* (2013) found that MSC-derived exosomes induce ATP levels in myocardial ischemia [318]. In the literature, the uptake of EVs or exosomes was suggested to be either through fusion with the plasma membrane of the recipient cell, or via endocytic pathways such as macropinocytosis [319,320]. Collectively, findings of these previously mentioned studies suggest that the uptake process of HepG2-Exo may contribute to the increase in intracellular ATP levels, consequently, promote cell proliferation as observed in A375 (section 3.3.1).

Purine and pyrimidine metabolism were found to be strongly affected in A375 followed by A549 and PNT2A cells, after exosome treatment, where a significant ($p < 0.05$) increase was observed in glycine, AMP, UMP, CMP, and 3’5 cyclic AMP levels (Table 3.1) which implies that the cell cycle and metabolome of each cell line was affected, according to the applied concentration of exosomes on each cell line.

This supports previous findings in the literature that stated that proliferating tumour cells exhibit high metabolic activity in which a sufficient supply of nucleotides and other macromolecules are essential to grow and proliferate, therefore, *de novo* nucleotide synthesis pathways are stimulated in cancer cells to form purine and pyrimidine rings to provide an adequate amount of nucleotides to induce nucleic acid and protein synthesis along with maintaining sufficient energy [321–323]. This suggests that the increase in purine and pyrimidine metabolites in cancer cells is due to the increase in the metabolic and proliferative activity of cancer cell line after exosome treatment.

In terms of comparing the same doses on different cell lines, HepG2-Exo showed the strongest effect at 100 µg/ml on A375 cells compared to PNT2A cells, which indicate that cancer cells are more likely to be affected by cancer-derived exosomes (HepG2-Exo) rather than normal cells at the same concentration. This also applies for the comparison of A549 and PNT2A at 50 µg/ml. This proposes that the HepG2-Exo concentration is a critical factor in influencing the targeted cell metabolome.

3.5. Conclusion

In this chapter, studying the effect of HepG2-Exo on cancer and normal cell lines, applying different methods, was found to confirm the role of cancer-derived exosomes in promoting cancer progression and metastasis and induce changes in the metabolic pathways of affected cells. These findings provide a promising platform to employ HepG2-Exo in cancer therapeutics. However, due to their toxic effect, utilising HepG2-Exo in therapy require high caution in terms of applying the appropriate dosage for cancer treatment.

Chapter 4

General Conclusions and Future Work

General conclusion

The aim of this current research project was to optimise the exosome yield of the HepG2 cell line and minimise the contamination with FBS-derived exosomes through applying different approaches for cell culturing, to study the influence of these approaches on their corresponding exosomes, to assess the effective medium to be used for exosome collection and isolation, and to investigate the influence of HepG2-Exo on the biology and the metabolome of cancer and normal cell lines.

Firstly, findings of chapter 2 shown that cell cultures and collected exosomes are influenced by three major factors: media combination, exosome isolation technique, and the duration of serum starvation. In terms of media combination, using standard FBS in media offers the optimum condition for cell growth whereas Dep-FBS found to offer similar condition. However, the applied technique in depleting FBS was found to be a critical factor in cell cultures, where ultracentrifugation induces different effect from commercially depleted FBS, where cell behaviour was affected [219,238–240] (section 2.4.1). However, serum starvation was found to affect cell viability and growth. In terms of studying exosome groups, depleting FBS from EVs, proteins, lipids, and RNAs does not offer a complete elimination of these contaminants, which indicated that exosomes isolated from media supplemented with Dep-FBS as M2 are still contaminated. Moreover, exosomes collected under serum deprivation such as Exo(M3) and Exo(M4), was found to induce a drastic change in exosome traits, count, and composition compared to exosomes isolated from media supplemented with standard FBS (Exo(M1)) or Dep-FBS (Exo(M2)). Furthermore, serum free media are not free of contaminants where non-vesicular RNA observed such as hsa-miR-21-5p [273]. Finally, this work suggested that the probability of misinterpreting exosome of interest and developing misleading conclusions, due to media used in cell cultures, is very high [262,279,289,307].

Overall, the experimental outcomes in this study are encouraging for further exosomes studies to be carried out in developing standard method for harvesting and isolating exosomes that offer production of exosomes of high purity and high yield, or investing in HFBR for large scale production and clinical applications, investigating the therapeutic potentials of HepG2-Exo tetraspanins through modifying their expression, and adjusting exosome composition through applying specific media on the parent cell.

However, exosome studies in chapter 3 were carried out using media supplemented with Dep-FBS (M2) for preparing exosome sample, as it found to be the best available option as it offers the least contamination with FBS derived-EVs and maintains successful cell culture of HepG2 cell line.

Results of chapter 3, revealed that HepG2-Exo effect was inevitable on cancer and normal cell lines, however, the influence of these exosomes is controlled by three parameters: cell line, exosomes origin, and concentration of exosomes. Moreover, using high concentration of cancer derived exosomes should be carried out with caution, as it can stimulate the proliferative activity of the cell such as A375 at 100 µg/ml, A549 at 50 µg/ml, and PNT2A at 200 µg/ml , or induce cytotoxic effect, where A375 and A549 cell proliferation inhibited at 800 µg/ml. However, A549 maintained constant increase in proliferation, migration, adhesion, and invasion rate, after adding 50 µg/ml of HepG2-Exo.

In terms of metabolomics, the effect of 100 µg/ml of HepG2-Exo has induced drastic changes in A375 metabolome, compared to other cell lines, where OXPHOS (ATP), purine and pyrimidine metabolism pathways were strongly influenced. On the other hand, studying HepG2-Exo effect on cancer cell line versus normal cell line using the same concentration, revealed that cancer cell lines are more susceptible to changes rather than normal cell line. After All, this work confirmed

that cancer-derived exosomes play a major role in cancer progression and metastasis, and influencing metabolic pathways of recipient cells.

The findings of this chapter are found to encouraging as they provide a promising platform for the application of HepG2-Exo in lung cancer therapeutics in a clinical setting.

Future work

Based on these promising findings in this thesis, future opportunities have been opened up for investigating and employing cancer-derived exosomes in therapy, *in vivo* through designing animal studies and applying HepG2-Exo, for instance, in HCC bearing mice with lung metastasis such as C57BL6. HepG2-Exo could also be isolated, and loaded with therapeutic agents such as proteins e.g. KRAS or EGFR [333,334] or chemotherapeutics drugs such as Paclitaxel (PTX) or Doxorubicin (DOX) and administered to the mouse [324–326], or modified through altering their tetraspanins expression [49,251]. First, the effect of these loaded or modified exosomes should be monitored *in vitro*. After that, the administration of HepG2-Exo could be either systemically through the intravenous route or nasal route using nebuliser. However, HepG2-Exo are required to be targeted and to avoid any complications, as cancer exosomes are “double edged sword”. Therefore, they require high caution in terms of therapeutic applications.

Another possible approach to be followed, is to use healthy mice and to inject them with HepG2-Exo to track the process of tumour progression and metastasis, and to investigate the tumour pathway, in order to target key proteins or genes involved in cancer progression. Moreover, in terms of cytotoxicity observed at high concentrations of HepG2-Exo, this approach can be followed by targeting these exosomes to induce cytotoxic effects on specific tumour tissue without affecting other organs. Moreover, due to the expression of exosomal mir-92a-3pin HepG2-Exo (Section 2.3.7, Figure 2.14) and its role in cancer progression [263–265] (Section 2.4),

anti-mir-92a-3p, short interfering (si) RNA can be constructed and loaded into nanoparticles or HepG2-Exo to inhibit mir-92a-3p, consequently, supress tumour progression.

For engaging HepG2-Exo *in vivo* in animal studies, more work is required for monitoring and evaluating the appropriate HepG2-Exo dose, the duration of treatment, and side effects or long-term effects on other tissues. Whilst limitations still remain, the application of HepG2-Exo in cancer studies offer a promising future for the development of efficient and non-invasive therapeutic approaches.

References

References

1. Bunggulawa EJ, Wang W, Yin T, *et al.* Recent advancements in the use of exosomes as drug delivery systems. *J. Nanobiotechnology* (2018).

2. Rufino-Ramos D, Albuquerque PR, Carmona V, Perfeito R, Nobre RJ, Pereira de Almeida L. Extracellular vesicles: Novel promising delivery systems for therapy of brain diseases. Available from: J. Control. Release

3. Maltepe E, Penn AA. Development, Function, and Pathology of the Placenta. *Avery's Dis. Newborn*, 40-60.e8 (2018).

4. Wu M, Wang G, Hu W, Yao Y, Yu X-F. Emerging roles and therapeutic value of exosomes in cancer metastasis. *Mol. Cancer*18(1), 53 (2019).

5. Huang T, Deng C-X. Current Progresses of Exosomes as Cancer Diagnostic and Prognostic Biomarkers. *Int. J. Biol. Sci.*15(1), 1–11 (2019).

6. Beit-Yannai E, Tabak S, Stamer WD. Physical exosome:exosome interactions. *J. Cell. Mol. Med.*22(3), 2001–2006 (2018).

7. Li I, Nabet BY. Exosomes in the tumor microenvironment as mediators of cancer therapy resistance. *Mol. Cancer*18(1), 32 (2019).

8. Ståhl A-L, Johansson K, Mossberg M, Kahn R, Karpman D. Exosomes and microvesicles in normal physiology, pathophysiology, and renal diseases. *Pediatr. Nephrol.*34(1), 11–30 (2019).

9. De Broe ME, Wieme RJ, Logghe GN, Roels F. Spontaneous shedding of plasma membrane fragments by human cells in vivo and in vitro. *Clin. Chim. Acta.*81(3), 237–45 (1977).

10. De Broe ME, Borgers M, Wieme RJ. The separation and characterization of liver plasma membrane fragments circulating in the blood of patients with cholestasis. *Clin. Chim. Acta.*59(3), 369–72 (1975).

11. Brocklehurst D, Wilde CE, Doar JW. The incidence and likely origins of serum particulate alkaline phosphatase and lipoprotein-X in liver disease. *Clin. Chim. Acta.*88(3), 509–15 (1978).

12. Brinton LT, Sloane HS, Kester M, Kelly KA. Formation and role of exosomes in cancer. *Cell. Mol. Life Sci.*72(4), 659–71 (2015).

13. Harding C, Stahl P. Transferrin recycling in reticulocytes: pH and iron are important determinants of ligand binding and processing. *Biochem. Biophys. Res. Commun.*113(2), 650–658 (1983).

14. Pan BT, Johnstone RM. Fate of the transferrin receptor during maturation of sheep reticulocytes in vitro: selective externalization of the receptor. *Cell*33(3), 967–78 (1983).

15. Harding C, Heuser J, Stahl P. Receptor-mediated endocytosis of transferrin and recycling of the transferrin receptor in rat reticulocytes. *J. Cell Biol.*97(2), 329–39 (1983).

16. Pan BT, Teng K, Wu C, Adam M, Johnstone RM. Electron microscopic evidence for

externalization of the transferrin receptor in vesicular form in sheep reticulocytes. *J. Cell Biol.*101(3), 942–948 (1985).

17. J. Crenshaw B, Sims B, L. Matthews Q. Biological Function of Exosomes as Diagnostic Markers and Therapeutic Delivery Vehicles in Carcinogenesis and Infectious Diseases. In: *Nanomedicines* (2019)

18. Johnstone RM, Adam M, Hammond JR, Orr L, Turbide C. Vesicle formation during reticulocyte maturation. Association of plasma membrane activities with released vesicles (exosomes). *J. Biol. Chem.*262(19), 9412–9420 (1987).

19. Huotari J, Helenius A. Endosome maturation. *EMBO J.*30(17), 3481–500 (2011).

20. Klumperman J, Raposo G. The Complex Ultrastructure of the Endolysosomal System. *Cold Spring Harb. Perspect. Biol.* (2014).

21. Zhang Y, Liu Y, Liu H, Tang WH. Exosomes: biogenesis, biologic function and clinical potential. *Cell Biosci.*9(1), 19 (2019).

22. Kowal J, Tkach M, Théry C. Biogenesis and secretion of exosomes. *Curr. Opin. Cell Biol.*29C, 116–125 (2014).

23. Abels ER, Breakefield XO. Introduction to Extracellular Vesicles: Biogenesis, RNA Cargo Selection, Content, Release, and Uptake. *Cell. Mol. Neurobiol.*36(3), 301–12 (2016).

24. Frankel EB, Audhya A. ESCRT-dependent cargo sorting at multivesicular endosomes. *Semin. Cell Dev. Biol.*74, 4–10 (2018).

25. Colombo M, Moita C, van Niel G, *et al.* Analysis of ESCRT functions in exosome biogenesis, composition and secretion highlights the heterogeneity of extracellular vesicles. *J. Cell Sci.*126(Pt 24), 5553–65 (2013).

26. Hessvik NP, Llorente A. Current knowledge on exosome biogenesis and release. *Cell. Mol. Life Sci.*75(2), 193–208 (2018).

27. Arenaccio C, Federico M. The multifaceted functions of exosomes in health and disease: An overview. In: *Advances in Experimental Medicine and Biology*, 3–19 (2017)

28. Simpson RJ, Kalra H, Mathivanan S. Exocarta as a resource for exosomal research. *J. Extracell. Vesicles*1(1) (2012).

29. Mathivanan S, Fahner CJ, Reid GE, Simpson RJ. ExoCarta 2012: Database of exosomal proteins, RNA and lipids. *Nucleic Acids Res.*40(D1) (2012).

30. Sagini K, Costanzi E, Emiliani C, Buratta S, Urbanelli L. Extracellular Vesicles as Conveyors of Membrane-Derived Bioactive Lipids in Immune System. *Int. J. Mol. Sci.*19(4) (2018).

31. Urbanelli L, Magini A, Buratta S, *et al.* Signaling pathways in exosomes biogenesis, secretion and fate. *Genes (Basel).*4(2), 152–70 (2013).

32. Subra C, Laulagnier K, Perret B, Record M. Exosome lipidomics unravels lipid sorting at the level of multivesicular bodies. *Biochimie*89(2), 205–212 (2007).

33. Skotland T, Sandvig K, Llorente A. Lipids in exosomes: Current knowledge and the way forward. *Prog. Lipid Res.*66, 30–41 (2017).

34. Vidal M, Sainte-Marie J, Philippot JR, Bienvenue A. Asymmetric distribution of phospholipids in the membrane of vesicles released during in vitro maturation of guinea pig reticulocytes: evidence precluding a role for “aminophospholipid translocase”. *J. Cell. Physiol.*140(3), 455–462 (1989).

35. Laulagnier K, Motta C, Hamdi S, *et al.* Mast cell- and dendritic cell-derived exosomes display a specific lipid composition and an unusual membrane organization. *Biochem. J.*380(Pt 1), 161–171 (2004).

36. Parolini I, Federici C, Raggi C, *et al.* Microenvironmental pH is a key factor for exosome traffic in tumor cells. *J. Biol. Chem.*284(49), 34211–34222 (2009).

37. Simpson RJ, Jensen SS, Lim JWE. Proteomic profiling of exosomes: Current perspectives. *Proteomics*8(19), 4083–4099 (2008).

38. Raimondo F, Morosi L, Chinello C, Magni F, Pitto M. Advances in membranous vesicle and exosome proteomics improving biological understanding and biomarker discovery. *Proteomics*11(4), 709–720 (2011).

39. Andreu Z, Yáñez-Mó M. Tetraspanins in extracellular vesicle formation and function. *Front. Immunol.*5, 442 (2014).

40. Théry C, Regnault A, Garin J, *et al.* Molecular characterization of dendritic cell-derived exosomes: Selective accumulation of the heat shock protein hsc73. *J. Cell Biol.*147(3), 599–610 (1999).

41. Escola JM, Kleijmeer MJ, Stoorvogel W, Griffith JM, Yoshie O, Geuze HJ. Selective enrichment of tetraspan proteins on the internal vesicles of multivesicular endosomes and on exosomes secreted by human B-lymphocytes. *J. Biol. Chem.*273(32), 20121–20127 (1998).

42. Atay S, Gercel-Taylor C, Kesimer M, Taylor DD. Morphologic and proteomic characterization of exosomes released by cultured extravillous trophoblast cells. *Exp. Cell Res.*317(8), 1192–1202 (2011).

43. Hemler ME. Tetraspanin functions and associated microdomains. *Nat. Rev. Mol. Cell Biol.*6(10), 801–811 (2005).

44. Espenel C, Margeat E, Dosset P, *et al.* Single-molecule analysis of CD9 dynamics and partitioning reveals multiple modes of interaction in the tetraspanin web. *J. Cell Biol.*182(4), 765–76 (2008).

45. Charrin S, Jouannet S, Boucheix C, Rubinstein E. Tetraspanins at a glance. *J. Cell Sci.* (2014).

46. Hemler ME. Targeting of tetraspanin proteins--potential benefits and strategies. *Nat. Rev. Drug Discov.*7(9), 747–758 (2008).

47. Chairoungdua A, Smith DL, Pochard P, Hull M, Caplan MJ. Exosome release of beta-catenin: a novel mechanism that antagonizes Wnt signaling. *J. Cell Biol.*190(6), 1079–1091 (2010).

48. Tejera E, Rocha-Perugini V, López-Martín S, *et al.* CD81 regulates cell migration through its association with Rac GTPase. *Mol. Biol. Cell*24(3), 261–73 (2013).

49. Lu J, Li J, Liu S, *et al.* Exosomal tetraspanins mediate cancer metastasis by altering host

microenvironment. *Oncotarget*8(37), 62803–62815 (2017).

50. Saiz ML, Rocha-Perugini V, Sánchez-Madrid F. Tetraspanins as Organizers of Antigen-Presenting Cell Function. *Front. Immunol.*9, 1074 (2018).

51. van Dommelen SM, Vader P, Lakhal S, *et al.* Microvesicles and exosomes: Opportunities for cell-derived membrane vesicles in drug delivery. *J. Control. Release*161(2), 635–644 (2012).

52. Barczyk M, Carracedo S, Gullberg D. Integrins. *Cell Tissue Res.*339(1), 269–80 (2010).

53. Campbell ID, Humphries MJ. Integrin structure, activation, and interactions. *Cold Spring Harb. Perspect. Biol.*3(3) (2011).

54. Théry C, Duban L, Segura E, Véron P, Lantz O, Amigorena S. Indirect activation of naïve CD4+ T cells by dendritic cell-derived exosomes. *Nat. Immunol.*3(12), 1156–1162 (2002).

55. Soung YH, Ford S, Yan C, Chung J. Roles of integrins in regulating metastatic potentials of cancer cell derived exosomes. *Mol. Cell. Toxicol.*15(3), 233–237 (2019).

56. Gonzales PA, Pisitkun T, Hoffert JD, *et al.* Large-scale proteomics and phosphoproteomics of urinary exosomes. *J. Am. Soc. Nephrol.*20(2), 363–379 (2009).

57. Gonzalez-Begne M, Lu B, Han X, *et al.* Proteomic analysis of human parotid gland exosomes by multidimensional protein identification technology (MudPIT). *J. Proteome Res.*8(3), 1304–1314 (2009).

58. Pisitkun T, Shen R-F, Knepper MA. Identification and proteomic profiling of exosomes in human urine. *Proc. Natl. Acad. Sci. U. S. A.*101(36), 13368–13373 (2004).

59. Looze C, Yui D, Leung L, *et al.* Proteomic profiling of human plasma exosomes identifies PPARgamma as an exosome-associated protein. *Biochem. Biophys. Res. Commun.*378(3), 433–438 (2009).

60. Bard MP, Hegmans JP, Hemmes A, *et al.* Proteomic analysis of exosomes isolated from human malignant pleural effusions. *Am. J. Respir. Cell Mol. Biol.*31(1), 114–121 (2004).

61. Mathivanan S, Lim JWE, Tauro BJ, Ji H, Moritz RL, Simpson RJ. Proteomics analysis of A33 immunoaffinity-purified exosomes released from the human colon tumor cell line LIM1215 reveals a tissue-specific protein signature. *Mol. Cell. Proteomics*9(2), 197–208 (2010).

62. Cen J, Feng L, Ke H, *et al.* Exosomal Thrombospondin-1 Disrupts the Integrity of Endothelial Intercellular Junctions to Facilitate Breast Cancer Cell Metastasis. *Cancers (Basel).*11(12) (2019).

63. Xiao X, Mruk DD, Cheng CY. Intercellular adhesion molecules (ICAMs) and spermatogenesis. *Hum. Reprod. Update*19(2), 167–86 (2013).

64. Valadi H, Ekström K, Bossios A, Sjöstrand M, Lee JJ, Lötvall JO. Exosome-mediated transfer of mRNAs and microRNAs is a novel mechanism of genetic exchange between cells. *Nat. Cell Biol.*9(6), 654–659 (2007).

65. Skokos D, Le Panse S, Villa I, *et al.* Mast cell-dependent B and T lymphocyte activation is mediated by the secretion of immunologically active exosomes. *J. Immunol.*166(2), 868–876 (2001).

66. Skokos D, Le Panse S, Villa I, *et al.* Nonspecific B and T cell-stimulatory activity mediated by mast cells is associated with exosomes. In: *International Archives of Allergy and Immunology*, 133–136 (2001)

67. Buschow SI, van Balkom BWM, Aalberts M, Heck AJR, Wauben M, Stoorvogel W. MHC class II-associated proteins in B-cell exosomes and potential functional implications for exosome biogenesis. *Immunol. Cell Biol.*88(8), 851–6 (2010).

68. Long EO. ICAM-1: getting a grip on leukocyte adhesion. *J. Immunol.*186(9), 5021–3 (2011).

69. Segura E, Nicco C, Lombard B, *et al.* ICAM-1 on exosomes from mature dendritic cells is critical for efficient naive T-cell priming. *Blood*106(1), 216–223 (2005).

70. Segura E, Guerin C, Hogg N, Amigorena S, Thery C. CD8+ Dendritic Cells Use LFA-1 to Capture MHC-Peptide Complexes from Exosomes In Vivo. *J. Immunol.*179(3), 1489–1496 (2007).

71. Taverna S, Flugy A, Saieva L, *et al.* Role of exosomes released by chronic myelogenous leukemia cells in angiogenesis. *Int. J. cancer*130(9), 2033–43 (2012).

72. Švajger U, Anderluh M, Jeras M, Obermajer N. C-type lectin DC-SIGN: An adhesion, signalling and antigen-uptake molecule that guides dendritic cells in immunity. *Cell. Signal.*22(10), 1397–1405 (2010).

73. Schiffelers R, Kooijmans S, Vader SM, van Dommelen WW, Van Solinge RM. Exosome mimetics: a novel class of drug delivery systems. *Int. J. Nanomedicine*7, 1525 (2012).

74. Fevrier B, Vilette D, Archer F, *et al.* Cells release prions in association with exosomes. *Proc. Natl. Acad. Sci. U. S. A.*101(26), 9683–9688 (2004).

75. Potolicchio I, Carven GJ, Xu X, *et al.* Proteomic analysis of microglia-derived exosomes: metabolic role of the aminopeptidase CD13 in neuropeptide catabolism. *J. Immunol.*175(4), 2237–2243 (2005).

76. Ji H, Erfani N, Tauro BJ, *et al.* Difference gel electrophoresis analysis of Ras-transformed fibroblast cell-derived exosomes. *Electrophoresis*29(12), 2660–2671 (2008).

77. Zeelenberg IS, Ostrowski M, Krumeich S, *et al.* Targeting tumor antigens to secreted membrane vesicles in vivo induces efficient antitumor immune responses. *Cancer Res.*68(4), 1228–1235 (2008).

78. Hartman ZC, Wei J, Glass OK, *et al.* Increasing vaccine potency through exosome antigen targeting. *Vaccine*29(50), 9361–9367 (2011).

79. Rountree RB, Mandl SJ, Nachtwey JM, *et al.* Exosome targeting of tumor antigens expressed by cancer vaccines can improve antigen immunogenicity and therapeutic efficacy. *Cancer Res.*71(15), 5235–5244 (2011).

80. Lötvall J, Hill AF, Hochberg F, *et al.* Minimal experimental requirements for definition of extracellular vesicles and their functions: a position statement from the International Society for Extracellular Vesicles. *J. Extracell. Vesicles*3 (2014).

81. Mittelbrunn M, Gutiérrez-Vázquez C, Villarroya-Beltri C, *et al.* Unidirectional transfer of microRNA-loaded exosomes from T cells to antigen-presenting cells. *Nat. Commun.*2(1)

(2011).

82. Ratajczak J, Miekus K, Kucia M, *et al.* Embryonic stem cell-derived microvesicles reprogram hematopoietic progenitors: evidence for horizontal transfer of mRNA and protein delivery. *Leuk. Off. J. Leuk. Soc. Am. Leuk. Res. Fund, U.K*20(5), 847–856 (2006).

83. Pegtel DM, Cosmopoulos K, Thorley-Lawson DA, *et al.* Functional delivery of viral miRNAs via exosomes. *Proc. Natl. Acad. Sci.*107(14), 6328–6333 (2010).

84. Wang J-P, Tang Y-Y, Fan C-M, *et al.* The role of exosomal non-coding RNAs in cancer metastasis. *Oncotarget*9(15), 12487–12502 (2018).

85. Dilsiz N. Role of exosomes and exosomal microRNAs in cancer. *Futur. Sci. OA*, FSO465 (2020).

86. Zhao W, Liu Y, Zhang C, Duan C. Multiple Roles of Exosomal Long Noncoding RNAs in Cancers. *Biomed Res. Int.*2019, 1–12 (2019).

87. Xie Y, Dang W, Zhang S, *et al.* The role of exosomal noncoding RNAs in cancer. *Mol. Cancer*18(1), 37 (2019).

88. Bellingham SA, Coleman BM, Hill AF. Small RNA deep sequencing reveals a distinct miRNA signature released in exosomes from prion-infected neuronal cells. *Nucleic Acids Res.*40(21), 10937–10949 (2012).

89. Huang X, Yuan T, Tschannen M, *et al.* Characterization of human plasma-derived exosomal RNAs by deep sequencing. *BMC Genomics*14(1) (2013).

90. Vojtech L, Woo S, Hughes S, *et al.* Exosomes in human semen carry a distinctive repertoire of small non-coding RNAs with potential regulatory functions. *Nucleic Acids Res.*42(11), 7290–7304 (2014).

91. Gajos-Michniewicz A, Duechler M, Czyz M. MiRNA in melanoma-derived exosomes. *Cancer Lett.*347(1), 29–37 (2014).

92. Qin J, Xu Q. Functions and application of exosomes. *Acta Pol. Pharm.*71(4), 537–43 (2014).

93. Rahmati S, Shojaei F, Shojaeian A, Rezakhani L, Dehkordi MB. An overview of current knowledge in biological functions and potential theragnostic applications of exosomes. *Chem. Phys. Lipids*226, 104836 (2020).

94. Ha D, Yang N, Nadithe V. Exosomes as therapeutic drug carriers and delivery vehicles across biological membranes: current perspectives and future challenges. *Acta Pharm. Sin. B*6(4), 287–96 (2016).

95. Heijnen HF, Schiel AE, Fijnheer R, Geuze HJ, Sixma JJ. Activated platelets release two types of membrane vesicles: microvesicles by surface shedding and exosomes derived from exocytosis of multivesicular bodies and alpha-granules. *Blood*94(11), 3791–9 (1999).

96. Ghidoni R, Benussi L, Binetti G. Exosomes: The Trojan horses of neurodegeneration. *Med. Hypotheses*70(6), 1226–1227 (2008).

97. Webber J, Steadman R, Mason MD, Tabi Z, Clayton A. Cancer exosomes trigger fibroblast to myofibroblast differentiation. *Cancer Res.*70(23), 9621–9630 (2010).

98. Rana S, Malinowska K, Zöller M. Exosomal tumor microRNA modulates premetastatic organ cells. *Neoplasia*15(3), 281–95 (2013).

99. Kucharzewska P, Christianson HC, Welch JE, *et al.* Exosomes reflect the hypoxic status of glioma cells and mediate hypoxia-dependent activation of vascular cells during tumor development. *Proc. Natl. Acad. Sci. U. S. A.*110(18), 7312–7 (2013).

100. Liu S-L, Sun P, Li Y, Liu S-S, Lu Y. Exosomes as critical mediators of cell-to-cell communication in cancer pathogenesis and their potential clinical application. *Transl. Cancer Res.*8(1), 298–311 (2019).

101. Sharma A. Role of stem cell derived exosomes in tumor biology. *Int. J. Cancer*142(6), 1086–1092 (2018).

102. Carretero-González A, Otero I, Carril-Ajuria L, de Velasco G, Manso L. Exosomes: Definition, Role in Tumor Development and Clinical Implications. *Cancer Microenviron.* (2018).

103. Osaki M, Okada F. Exosomes and Their Role in Cancer Progression. *Yonago Acta Med.*62(2), 182–190 (2019).

104. Kumar B, Garcia M, Weng L, *et al.* Acute myeloid leukemia transforms the bone marrow niche into a leukemia-permissive microenvironment through exosome secretion. *Leukemia*32(3), 575–587 (2018).

105. Zheng H, Zhan Y, Liu S, *et al.* The roles of tumor-derived exosomes in non-small cell lung cancer and their clinical implications. *J. Exp. Clin. Cancer Res.*37(1), 226 (2018).

106. Nakamura K, Sawada K, Kobayashi M, *et al.* Role of the Exosome in Ovarian Cancer Progression and Its Potential as a Therapeutic Target. *Cancers (Basel).*11(8), 1147 (2019).

107. Morelli AE, Larregina AT, Shufesky WJ, *et al.* Endocytosis, intracellular sorting, and processing of exosomes by dendritic cells. *Blood*104(10), 3257–3266 (2004).

108. De Toro J, Herschlik L, Waldner C, Mongini C. Emerging Roles of Exosomes in Normal and Pathological Conditions: New Insights for Diagnosis and Therapeutic Applications. *Front. Immunol.*6 (2015).

109. Valenti R, Huber V, Iero M, Filipazzi P, Parmiani G, Rivoltini L. Tumor-released microvesicles as vehicles of immunosuppression. *Cancer Res.*67(7), 2912–5 (2007).

110. Liu Y, Gu Y, Cao X. The exosomes in tumor immunity. *Oncoimmunology*4(9), 1–8 (2015).

111. Yang C, Kim SH, Bianco NR, Robbins PD. Tumor-derived exosomes confer antigen-specific immunosuppression in a murine delayed-type hypersensitivity model. *PLoS One*6(8) (2011).

112. Valenti R, Huber V, Filipazzi P, *et al.* Human Tumor-Released Microvesicles Promote the Differentiation of Myeloid Cells with Transforming Growth Factor-β -Mediated Suppressive Activity on T Lymphocytes. *Cancer Res.*66(18), 9290–9298 (2006).

113. Czernek L, Düchler M. Functions of Cancer-Derived Extracellular Vesicles in Immunosuppression. *Arch. Immunol. Ther. Exp. (Warsz).*65(4), 311–323 (2017).

114. Hedlund M, Nagaeva O, Kargl D, Baranov V, Mincheva-Nilsson L. Thermal- and Oxidative Stress Causes Enhanced Release of NKG2D Ligand-Bearing Immunosuppressive Exosomes

in Leukemia/Lymphoma T and B Cells. *PLoS One*6(2), e16899 (2011).

115. Wendler F, Bota-Rabassedas N, Franch-Marro X. Cancer becomes wasteful: emerging roles of exosomes † in cell-fate determination. *J. Extracell. Vesicles*2(1), 22390 (2013).

116. Cho JA, Park H, Lim EH, *et al.* Exosomes from ovarian cancer cells induce adipose tissue-derived mesenchymal stem cells to acquire the physical and functional characteristics of tumor-supporting myofibroblasts. *Gynecol. Oncol.*123(2), 379–86 (2011).

117. Cho JA, Park H, Lim EH, Lee KW. Exosomes from breast cancer cells can convert adipose tissue-derived mesenchymal stem cells into myofibroblast-like cells. *Int. J. Oncol.*40(1), 130–138 (2012).

118. Clayton A, Mitchell JP, Court J, Mason MD, Tabi Z. Human tumor-derived exosomes selectively impair lymphocyte responses to interleukin-2. *Cancer Res.*67(15), 7458–66 (2007).

119. Gross JC, Chaudhary V, Bartscherer K, Boutros M. Active Wnt proteins are secreted on exosomes. *Nat. Cell Biol.*14(10), 1036–1045 (2012).

120. Luga V, Zhang L, Viloria-Petit AM, *et al.* Exosomes mediate stromal mobilization of autocrine Wnt-PCP signaling in breast cancer cell migration. *Cell*151(7), 1542–1556 (2012).

121. Putz U, Howitt J, Doan A, *et al.* The tumor suppressor PTEN is exported in exosomes and has phosphatase activity in recipient cells. *Sci. Signal.*5(243), ra70–ra70 (2012).

122. Wrighton KH. Role of nuclear PTEN revealed. *Nat. Rev. Cancer*11(3), 155–155 (2011).

123. Beloribi S, Ristorcelli E, Breuzard G, *et al.* Exosomal Lipids Impact Notch Signaling and Induce Death of Human Pancreatic Tumoral SOJ-6 Cells. *PLoS One*7(10), e47480 (2012).

124. Sharghi-Namini S, Tan E, Ong LLS, Ge R, Asada HH. Dll4-containing exosomes induce capillary sprout retraction in a 3D microenvironment. *Sci. Rep.*4(1), 1–8 (2014).

125. Ristorcelli E, Beraud E, Mathieu S, Lombardo D, Verine A. Essential role of Notch signaling in apoptosis of human pancreatic tumoral cells mediated by exosomal nanoparticles. *Int. J. Cancer*125(5), 1016–1026 (2009).

126. Wang T, Nasser MI, Shen J, Qu S, He Q, Zhao M. Functions of Exosomes in the Triangular Relationship between the Tumor, Inflammation, and Immunity in the Tumor Microenvironment. *J. Immunol. Res.*2019, 1–10 (2019).

127. Kurywchak P, Tavormina J, Kalluri R. The emerging roles of exosomes in the modulation of immune responses in cancer. *Genome Med.*10(1), 23 (2018).

128. Wolfers J, Lozier A, Raposo G, *et al.* Tumor-derived exosomes are a source of shared tumor rejection antigens for CTL cross-priming. *Nat. Med.*7(3), 297–303 (2001).

129. Admyre C, Johansson SM, Paulie S, Gabrielsson S. Direct exosome stimulation of peripheral humanT cells detected by ELISPOT. *Eur. J. Immunol.*36(7), 1772–1781 (2006).

130. Admyre C, Bohle B, Johansson SM, *et al.* B cell–derived exosomes can present allergen peptides and activate allergen-specific T cells to proliferate and produce TH2-like cytokines. *J. Allergy Clin. Immunol.*120(6), 1418–1424 (2007).

131. Andre F, Schartz NE, Movassagh M, *et al.* Malignant effusions and immunogenic tumour-derived exosomes. *Lancet*360(9329), 295–305 (2002).

132. Lancaster GI, Febbraio MA. Exosome-dependent Trafficking of HSP70: A NOVEL SECRETORY PATHWAY FOR CELLULAR STRESS PROTEINS. *J. Biol. Chem.*280(24), 23349–23355 (2005).

133. Barros FM, Carneiro F, Machado JC, Melo SA. Exosomes and Immune Response in Cancer: Friends or Foes? *Front. Immunol.*9, 730 (2018).

134. Lugini L, Cecchetti S, Huber V, *et al.* Immune Surveillance Properties of Human NK Cell-Derived Exosomes. *J. Immunol.*189(6), 2833–2842 (2012).

135. Muller L, Mitsuhashi M, Simms P, Gooding WE, Whiteside TL. Tumor-derived exosomes regulate expression of immune function-related genes in human T cell subsets. *Sci. Rep.*6(1), 20254 (2016).

136. Mrizak D, Martin N, Barjon C, *et al.* Effect of Nasopharyngeal Carcinoma-Derived Exosomes on Human Regulatory T Cells. *JNCI J. Natl. Cancer Inst.*107(1) (2015).

137. Szajnik M, Czystowska M, Szczepanski MJ, Mandapathil M, Whiteside TL. Tumor-Derived Microvesicles Induce, Expand and Up-Regulate Biological Activities of Human Regulatory T Cells (Treg). *PLoS One*5(7), e11469 (2010).

138. Chalmin F, Ladoire S, Mignot G, *et al.* Membrane-associated Hsp72 from tumor-derived exosomes mediates STAT3-dependent immunosuppressive function of mouse and human myeloid-derived suppressor cells. *J. Clin. Invest.*120(2), 457–471 (2010).

139. Xiang X, Poliakov A, Liu C, *et al.* Induction of myeloid-derived suppressor cells by tumor exosomes. *Int. J. Cancer* (2009).

140. Hong C-S, Sharma P, Yerneni SS, *et al.* Circulating exosomes carrying an immunosuppressive cargo interfere with cellular immunotherapy in acute myeloid leukemia. *Sci. Rep.*7(1), 14684 (2017).

141. Haderk F, Schulz R, Iskar M, *et al.* Tumor-derived exosomes modulate PD-L1 expression in monocytes. *Sci. Immunol.*2(13), eaah5509 (2017).

142. Mosser DM, Edwards JP. Exploring the full spectrum of macrophage activation. Available from: Nat. Rev. Immunol.

143. Mosser DM, Edwards JP. Erratum: Exploring the full spectrum of macrophage activation (Nature Reviews Immunology (2008) 8 (958-969)) [Internet]. [Internet]https://www.nature.com/articles/nri2788Available from: Nat. Rev. Immunol.

144. Quatromoni JG, Eruslanov E. Tumor-associated macrophages: Function, phenotype, and link to prognosis in human lung cancer [Internet]. [Internet]/pmc/articles/PMC3493031/?report=abstractAvailable from: Am. J. Transl. Res.

145. Qian BZ, Pollard JW. Macrophage Diversity Enhances Tumor Progression and Metastasis [Internet]. [Internet]/pmc/articles/PMC4994190/?report=abstractAvailable from: Cell

146. Biswas SK, Mantovani A. Macrophage plasticity and interaction with lymphocyte subsets: Cancer as a paradigm [Internet]. [Internet]https://www.nature.com/articles/ni.1937Available from: Nat. Immunol.

147. Wang F, Li B, Wei Y, *et al.* Tumor-derived exosomes induce PD1+ macrophage population in human gastric cancer that promotes disease progression. *Oncogenesis*7(5), 41 (2018).

148. Yang N, Li S, Li G, *et al.* The role of extracellular vesicles in mediating progression, metastasis and potential treatment of hepatocellular carcinoma. *Oncotarget* (2015).

149. Ludwig N, Whiteside TL. Potential roles of tumor-derived exosomes in angiogenesis. *Expert Opin. Ther. Targets*22(5), 409–417 (2018).

150. Grange C, Tapparo M, Collino F, *et al.* Microvesicles Released from Human Renal Cancer Stem Cells Stimulate Angiogenesis and Formation of Lung Premetastatic Niche. *Cancer Res.*71(15), 5346–5356 (2011).

151. Conigliaro A, Costa V, Lo Dico A, *et al.* CD90+ liver cancer cells modulate endothelial cell phenotype through the release of exosomes containing H19 lncRNA. *Mol. Cancer* (2015).

152. Ludwig N, Yerneni SS, Razzo BM, Whiteside TL. Exosomes from HNSCC Promote Angiogenesis through Reprogramming of Endothelial Cells. *Mol. Cancer Res.*, molcanres.0358.2018 (2018).

153. Tadokoro H, Umezu T, Ohyashiki K, Hirano T, Ohyashiki JH. Exosomes derived from hypoxic leukemia cells enhance tube formation in endothelial cells. *J. Biol. Chem.* (2013).

154. Umezu T, Tadokoro H, Azuma K, Yoshizawa S, Ohyashiki K, Ohyashiki JH. Exosomal miR-135b shed from hypoxic multiple myeloma cells enhances angiogenesis by targeting factor-inhibiting HIF-1. *Blood*124(25), 3748–57 (2014).

155. Mao Y, Wang Y, Dong L, *et al.* Hypoxic exosomes facilitate angiogenesis and metastasis in esophageal squamous cell carcinoma through altering the phenotype and transcriptome of endothelial cells. *J. Exp. Clin. Cancer Res.*38(1), 389 (2019).

156. Liu Y, Luo F, Wang B, *et al.* STAT3-regulated exosomal miR-21 promotes angiogenesis and is involved in neoplastic processes of transformed human bronchial epithelial cells. *Cancer Lett.*370(1), 125–135 (2016).

157. Chan YK, Zhang H, Liu P, *et al.* Proteomic analysis of exosomes from nasopharyngeal carcinoma cell identifies intercellular transfer of angiogenic proteins. *Int. J. Cancer* (2015).

158. Tang MKS, Yue PYK, Ip PP, *et al.* Soluble E-cadherin promotes tumor angiogenesis and localizes to exosome surface. *Nat. Commun.* (2018).

159. Chiba M, Kubota S, Sato K, Monzen S. Exosomes released from pancreatic cancer cells enhance angiogenic activities via dynamin-dependent endocytosis in endothelial cells in vitro. *Sci. Rep.* (2018).

160. Yukawa H, Suzuki K, Aoki K, *et al.* Imaging of angiogenesis of human umbilical vein endothelial cells by uptake of exosomes secreted from hepatocellular carcinoma cells. *Sci. Rep.* (2018).

161. Yi H, Ye J, Yang XM, Zhang LW, Zhang ZG, Chen YP. High-grade ovarian cancer secreting effective exosomes in tumor angiogenesis. *Int. J. Clin. Exp. Pathol.* (2015).

162. Huang A, Dong J, Li S, *et al.* Exosomal transfer of vasorin expressed in hepatocellular carcinoma cells promotes migration of human umbilical vein endothelial cells. *Int. J. Biol.*

Sci. (2015).

163. Whitford W, Guterstam P. Exosome manufacturing status. *Future Med. Chem.*11(10), 1225–1236 (2019).

164. Ludwig N, Whiteside TL, Reichert TE. Challenges in Exosome Isolation and Analysis in Health and Disease. *Int. J. Mol. Sci.*20(19) (2019).

165. Palviainen M, Saari H, Kärkkäinen O, *et al.* Metabolic signature of extracellular vesicles depends on the cell culture conditions. *J. Extracell. vesicles*8(1), 1596669 (2019).

166. Whitford W, Ludlow JW, Cadwell JJS. Continuous Production of Exosomes. *Genet. Eng. Biotechnol. News*35(16), 34–34 (2015).

167. Ludwig N, Razzo BM, Yerneni SS, Whiteside TL. Optimization of cell culture conditions for exosome isolation using mini-size exclusion chromatography (mini-SEC). *Exp. Cell Res.*378(2), 149–157 (2019).

168. Burger D, Turner M, Xiao F, Munkonda MN, Akbari S, Burns KD. High glucose increases the formation and pro-oxidative activity of endothelial microparticles. *Diabetologia*60(9), 1791–1800 (2017).

169. Rice GE, Scholz-Romero K, Sweeney E, *et al.* The Effect of Glucose on the Release and Bioactivity of Exosomes From First Trimester Trophoblast Cells. *J. Clin. Endocrinol. Metab.*100(10), E1280-8 (2015).

170. Garcia NA, Ontoria-Oviedo I, González-King H, Diez-Juan A, Sepúlveda P. Glucose Starvation in Cardiomyocytes Enhances Exosome Secretion and Promotes Angiogenesis in Endothelial Cells. *PLoS One*10(9), e0138849 (2015).

171. Théry C, Witwer KW, Aikawa E, *et al.* Minimal information for studies of extracellular vesicles 2018 (MISEV2018): a position statement of the International Society for Extracellular Vesicles and update of the MISEV2014 guidelines. *J. Extracell. vesicles*7(1), 1535750 (2018).

172. Zhou X, Zhang W, Yao Q, *et al.* Exosome production and its regulation of EGFR during wound healing in renal tubular cells. *Am. J. Physiol. Renal Physiol.*312(6), F963–F970 (2017).

173. Datta A, Kim H, McGee L, *et al.* High-throughput screening identified selective inhibitors of exosome biogenesis and secretion: A drug repurposing strategy for advanced cancer. *Sci. Rep.*8(1), 8161 (2018).

174. Atienzar-Aroca S, Flores-Bellver M, Serrano-Heras G, *et al.* Oxidative stress in retinal pigment epithelium cells increases exosome secretion and promotes angiogenesis in endothelial cells. *J. Cell. Mol. Med.*20(8), 1457–66 (2016).

175. Doyle L, Wang M. Overview of Extracellular Vesicles, Their Origin, Composition, Purpose, and Methods for Exosome Isolation and Analysis. *Cells*8(7), 727 (2019).

176. Livshits MA, Khomyakova E, Evtushenko EG, *et al.* Corrigendum: Isolation of exosomes by differential centrifugation: Theoretical analysis of a commonly used protocol. *Sci. Rep.*6, 21447 (2016).

177. Jeppesen DK, Hvam ML, Primdahl-Bengtson B, *et al.* Comparative analysis of discrete exosome fractions obtained by differential centrifugation. *J. Extracell. vesicles*3, 25011 (2014).

178. Li P, Kaslan M, Lee SH, Yao J, Gao Z. Progress in Exosome Isolation Techniques. *Theranostics*7(3), 789–804 (2017).

179. Yakimchuk K. Exosomes: isolation methods and specific markers. *Mater. Methods*5 (2015).

180. Théry C, Amigorena S, Raposo G, Clayton A. Isolation and characterization of exosomes from cell culture supernatants and biological fluids. *Curr. Protoc. Cell Biol.*Chapter 3, Unit 3.22 (2006).

181. Momen-Heravi F, Balaj L, Alian S, *et al.* Current methods for the isolation of extracellular vesicles. *Biol. Chem.*394(10), 1253–62 (2013).

182. Raposo G, Nijman HW, Stoorvogel W, *et al.* B lymphocytes secrete antigen-presenting vesicles. *J. Exp. Med.*183(3), 1161–1172 (1996).

183. Cantin R, Diou J, Bélanger D, Tremblay AM, Gilbert C. Discrimination between exosomes and HIV-1: purification of both vesicles from cell-free supernatants. *J. Immunol. Methods*338(1–2), 21–30 (2008).

184. Yu L-L, Zhu J, Liu J-X, *et al.* A Comparison of Traditional and Novel Methods for the Separation of Exosomes from Human Samples. *Biomed Res. Int.*2018, 3634563 (2018).

185. de Hoog VC, Timmers L, Schoneveld AH, *et al.* Serum extracellular vesicle protein levels are associated with acute coronary syndrome. *Eur. Hear. journal. Acute Cardiovasc. care*2(1), 53–60 (2013).

186. Oksvold MP, Kullmann A, Forfang L, *et al.* Expression of B-cell surface antigens in subpopulations of exosomes released from B-cell lymphoma cells. *Clin. Ther.*36(6), 847-862.e1 (2014).

187. L B, V L, E C, *et al.* Extracellular Vesicles From Human Cardiac Progenitor Cells Inhibit Cardiomyocyte Apoptosis and Improve Cardiac Function After Myocardial Infarction. *Cardiovasc. Res.*103(4) (2014).

188. Zeringer E, Barta T, Li M, Vlassov A V. Strategies for isolation of exosomes. *Cold Spring Harb. Protoc.* (2015).

189. Zhang M, Jin K, Gao L, *et al.* Methods and Technologies for Exosome Isolation and Characterization. *Small Methods*2(9), 1800021 (2018).

190. Hosseini S, Vázquez-Villegas P, Rito-Palomares M, Martinez-Chapa SO. General overviews on applications of ELISA. In: *SpringerBriefs in Applied Sciences and Technology* (2018)

191. Gheinani AH, Vögeli M, Baumgartner U, *et al.* Improved isolation strategies to increase the yield and purity of human urinary exosomes for biomarker discovery. *Sci. Rep.*8(1), 3945 (2018).

192. Gámez-Valero A, Monguió-Tortajada M, Carreras-Planella L, Franquesa M, Beyer K, Borràs FE. Size-Exclusion Chromatography-based isolation minimally alters Extracellular Vesicles' characteristics compared to precipitating agents. *Sci. Rep.*6(1), 33641 (2016).

193. Zaborowski MP, Balaj L, Breakefield XO, Lai CP. Extracellular Vesicles: Composition, Biological Relevance, and Methods of Study. *Bioscience*65(8), 783–797 (2015).

194. Tauro BJ, Greening DW, Mathias RA, *et al.* Comparison of ultracentrifugation, density gradient separation, and immunoaffinity capture methods for isolating human colon cancer cell line LIM1863-derived exosomes. *Methods*56(2), 293–304 (2012).

195. Zhang W, Yu Z-L, Wu M, *et al.* Magnetic and Folate Functionalization Enables Rapid Isolation and Enhanced Tumor-Targeting of Cell-Derived Microvesicles. *ACS Nano*11(1), 277–290 (2017).

196. Patel GK, Khan MA, Zubair H, *et al.* Comparative analysis of exosome isolation methods using culture supernatant for optimum yield, purity and downstream applications. *Sci. Rep.* (2019).

197. Batrakova E V., Kim MS. Using exosomes, naturally-equipped nanocarriers, for drug delivery. *J. Control. Release*219, 396–405 (2015).

198. Zarovni N, Corrado A, Guazzi P, *et al.* Integrated isolation and quantitative analysis of exosome shuttled proteins and nucleic acids using immunocapture approaches. *Methods*87, 46–58 (2015).

199. Taylor DD, Gercel-Taylor C. MicroRNA signatures of tumor-derived exosomes as diagnostic biomarkers of ovarian cancer. *Gynecol. Oncol.*110(1), 13–21 (2008).

200. Liga A, Vliegenthart ADB, Oosthuyzen W, Dear JW, Kersaudy-Kerhoas M. Exosome isolation: a microfluidic road-map. *Lab Chip*15(11), 2388–2394 (2015).

201. Yáñez-Mó M, Siljander PR-M, Andreu Z, *et al.* Biological properties of extracellular vesicles and their physiological functions. *J. Extracell. Vesicles*4(1), 27066 (2015).

202. Palmisano G, Jensen SS, Bihan M-C Le, *et al.* Characterization of Membrane-shed Microvesicles from Cytokine-stimulated β-Cells Using Proteomics Strategies. *Mol. Cell. Proteomics*11(8), 230–243 (2012).

203. Keerthikumar S, Chisanga D, Ariyaratne D, *et al.* ExoCarta: A Web-Based Compendium of Exosomal Cargo. *J. Mol. Biol.* (2016).

204. Abramowicz A, Marczak L, Wojakowska A, *et al.* Harmonization of exosome isolation from culture supernatants for optimized proteomics analysis. *PLoS One* (2018).

205. Zhou M, Weber SR, Zhao Y, Chen H, Sundstrom JM. Methods for exosome isolation and characterization. *Exosomes*, 23–38 (2020).

206. Pierce Biotechnology. Micro BCA ™ Protein Assay Kit Instructions. *Man. 0011237* (2017).

207. Scientific T. BCA ™ Protein Assay Kit. *BCA Protein Assay Kit* (2007).

208. Soares Martins T, Catita J, Martins Rosa I, A B da Cruz E Silva O, Henriques AG. Exosome isolation from distinct biofluids using precipitation and column-based approaches. *PLoS One*13(6), e0198820 (2018).

209. Franquesa M, Hoogduijn MJ, Ripoll E, *et al.* Update on controls for isolation and quantification methodology of extracellular vesicles derived from adipose tissue

mesenchymal stem cells. *Front. Immunol.*5, 525 (2014).

210. Gallagher S, Winston SE, Fuller SA, Hurrell JGR. Immunoblotting and Immunodetection. *Curr. Protoc. Mol. Biol.* (2004).

211. Szatanek R, Baj-Krzyworzeka M, Zimoch J, Lekka M, Siedlar M, Baran J. The Methods of Choice for Extracellular Vesicles (EVs) Characterization. *Int. J. Mol. Sci.*18(6), 1153 (2017).

212. Schey KL, Luther JM, Rose KL. Proteomics Characterization of Exosome Cargo. *Methods*87, 75 (2015).

213. Rosa-Fernandes L, Rocha VB, Carregari VC, Urbani A, Palmisano G. A Perspective on Extracellular Vesicles Proteomics. *Front. Chem.*5, 102 (2017).

214. Chen S, Datta-Chaudhuri A, Deme P, *et al.* Lipidomic characterization of extracellular vesicles in human serum. *J. Circ. Biomarkers*8, 184945441987984 (2019).

215. Haraszti RA, Didiot M-C, Sapp E, *et al.* High-resolution proteomic and lipidomic analysis of exosomes and microvesicles from different cell sources. *J. Extracell. vesicles*5, 32570 (2016).

216. Santonocito M, Vento M, Guglielmino MR, *et al.* Molecular characterization of exosomes and their microRNA cargo in human follicular fluid: Bioinformatic analysis reveals that exosomal microRNAs control pathways involved in follicular maturation. *Fertil. Steril.* (2014).

217. Schageman J, Zeringer E, Li M, *et al.* The Complete Exosome Workflow Solution: From Isolation to Characterization of RNA Cargo. *Biomed Res. Int.*2013, 1–15 (2013).

218. Kornilov R, Puhka M, Mannerström B, *et al.* Efficient ultrafiltration-based protocol to deplete extracellular vesicles from fetal bovine serum. *J. Extracell. vesicles*7(1), 1422674 (2018).

219. Shelke GV, Lässer C, Gho YS, Lötvall J. Importance of exosome depletion protocols to eliminate functional and RNA-containing extracellular vesicles from fetal bovine serum. *J. Extracell. Vesicles*3(1) (2014).

220. Wei Z, Batagov AO, Carter DRF, Krichevsky AM. Fetal Bovine Serum RNA Interferes with the Cell Culture derived Extracellular RNA. *Sci. Rep.*6 (2016).

221. Lobb RJ, Becker M, Wen Wen S, *et al.* Optimized exosome isolation protocol for cell culture supernatant and human plasma. *J. Extracell. Vesicles*4(1), 27031 (2015).

222. Haraszti RA, Miller R, Dubuke ML, *et al.* Serum Deprivation of Mesenchymal Stem Cells Improves Exosome Activity and Alters Lipid and Protein Composition. *iScience* (2019).

223. Invitrogen NVS a, Invitrogen a S, Invitrogen SRL, *et al.* A Guide to Serum-Free Cell Culture. *Culture* (2003).

224. Fang C-Y, Wu C-C, Fang C-L, Chen W-Y, Chen C-L. Long-term growth comparison studies of FBS and FBS alternatives in six head and neck cell lines. *PLoS One*12(6), e0178960 (2017).

225. Arora M. Cell Culture Media: A Review. *Mater. Methods*3 (2013).

226. Creek DJ, Jankevics A, Burgess KE V, Breitling R, Barrett MP. IDEOM: an Excel interface for

analysis of LC-MS-based metabolomics data. *Bioinformatics*28(7), 1048–9 (2012).

227. Wishart DS, Feunang YD, Marcu A, *et al.* HMDB 4.0: the human metabolome database for 2018. *Nucleic Acids Res.*46(D1), D608–D617 (2018).

228. Kanehisa M, Goto S. KEGG: kyoto encyclopedia of genes and genomes. *Nucleic Acids Res.*28(1), 27–30 (2000).

229. MR F, W C, C A, *et al.* Discovering microRNAs From Deep Sequencing Data Using miRDeep. *Nat. Biotechnol.*26(4) (2008).

230. Gouin K, Peck K, Antes T, *et al.* A comprehensive method for identification of suitable reference genes in extracellular vesicles. *J. Extracell. Vesicles* (2017).

231. Ragni E, Orfei CP, De Luca P, *et al.* Identification of miRNA reference genes in extracellular vesicles from adipose derived mesenchymal stem cells for studying osteoarthritis. *Int. J. Mol. Sci.* (2019).

232. Zhou Y, Ren H, Dai B, *et al.* Hepatocellular carcinoma-derived exosomal miRNA-21 contributes to tumor progression by converting hepatocyte stellate cells to cancer-associated fibroblasts. *J. Exp. Clin. Cancer Res.* (2018).

233. Xie F, Xiao P, Chen D, Xu L, Zhang B. miRDeepFinder: A miRNA analysis tool for deep sequencing of plant small RNAs. *Plant Mol. Biol.* (2012).

234. Isola A, Chen S. Exosomes: The Messengers of Health and Disease. *Curr. Neuropharmacol.* (2016).

235. Mashouri L, Yousefi H, Aref AR, Ahadi AM, Molaei F, Alahari SK. Exosomes: composition, biogenesis, and mechanisms in cancer metastasis and drug resistance. *Mol. Cancer*18(1), 75 (2019).

236. Paszkiet B, Spencer V, Fein J, *et al.* Development of an improved process for the depletion of exosomes from fetal bovine serum. , 92008 (2016).

237. Rashid M, Coombs KM. Serum-reduced media impacts on cell viability and protein expression in human lung epithelial cells. *J. Cell. Physiol.*234(6), 7718–7724 (2019).

238. Eitan E, Zhang S, Witwer KW, Mattson MP. Extracellular vesicle–depleted fetal bovine and human sera have reduced capacity to support cell growth. *J. Extracell. Vesicles*4 (2015).

239. Aswad H, Jalabert A, Rome S. Depleting extracellular vesicles from fetal bovine serum alters proliferation and differentiation of skeletal muscle cells in vitro. *BMC Biotechnol.* (2016).

240. Lehrich BM, Liang Y, Khosravi P, Federoff HJ, Fiandaca MS. Fetal Bovine Serum-Derived Extracellular Vesicles Persist within Vesicle-Depleted Culture Media. *Int. J. Mol. Sci.* (2018).

241. Johnson M. Fetal Bovine Serum. *Mater. Methods*2 (2012).

242. Suárez H, Gámez-Valero A, Reyes R, *et al.* A bead-assisted flow cytometry method for the semi-quantitative analysis of Extracellular Vesicles. *Sci. Rep.*7(1), 11271 (2017).

243. Masyuk AI, Masyuk T V., LaRusso NF. Exosomes in the pathogenesis, diagnostics and therapeutics of liver diseases. *J. Hepatol.*59(3), 621–625 (2013).

244. Zou W, Lai M, Zhang Y, *et al.* Exosome Release Is Regulated by mTORC1. *Adv. Sci.*6(3), 1801313 (2019).

245. Serrano-Pertierra E, Oliveira-Rodríguez M, Rivas M, *et al.* Characterization of Plasma-Derived Extracellular Vesicles Isolated by Different Methods: A Comparison Study. *Bioengineering*6(1) (2019).

246. Malla RR, Pandrangi S, Kumari S, Gavara MM, Badana AK. Exosomal tetraspanins as regulators of cancer progression and metastasis and novel diagnostic markers. *Asia. Pac. J. Clin. Oncol.*14(6), 383–391 (2018).

247. Willms E, Cabañas C, Mäger I, Wood MJA, Vader P. Extracellular Vesicle Heterogeneity: Subpopulations, Isolation Techniques, and Diverse Functions in Cancer Progression. *Front. Immunol.*9, 738 (2018).

248. Zhu L, Qu X-H, Sun Y-L, Qian Y-M, Zhao X-H. Novel method for extracting exosomes of hepatocellular carcinoma cells. *World J. Gastroenterol.*20(21), 6651 (2014).

249. Pols MS, Klumperman J. Trafficking and function of the tetraspanin CD63. *Exp. Cell Res.*315(9), 1584–1592 (2009).

250. Takahashi R, Ochiya T. Small Interfering RNA-Mediated Silencing of the Ribophorin II Gene: Advances in the Treatment of Malignant Breast Cancer. *Nucleic Acid Nanotheranostics*, 27–41 (2019).

251. Lin Q, Peng S, Yang Y. Inhibition of CD9 expression reduces the metastatic capacity of human hepatocellular carcinoma cell line MHCC97-H. *Int. J. Oncol.*53(1), 266–274 (2018).

252. Hemler ME. Tetraspanin proteins promote multiple cancer stages. *Nat. Rev. Cancer*14(1), 49–60 (2014).

253. Mizoshiri N, Shirai T, Terauchi R, *et al.* The tetraspanin CD81 mediates the growth and metastases of human osteosarcoma. *Cell. Oncol.*42(6), 861–871 (2019).

254. Vences-Catalán F, Rajapaksa R, Srivastava MK, *et al.* Tetraspanin CD81 Promotes Tumor Growth and Metastasis by Modulating the Functions of T Regulatory and Myeloid-Derived Suppressor Cells. *Cancer Res.*75(21), 4517–4526 (2015).

255. Vences-Catalán F, Levy S. Immune Targeting of Tetraspanins Involved in Cell Invasion and Metastasis. *Front. Immunol.*9 (2018).

256. Bandu R, Oh JW, Kim KP. Mass spectrometry-based proteome profiling of extracellular vesicles and their roles in cancer biology. *Exp. Mol. Med.*51(3), 30 (2019).

257. Kreimer S, Belov AM, Ghiran I, Murthy SK, Frank DA, Ivanov AR. Mass-Spectrometry-Based Molecular Characterization of Extracellular Vesicles: Lipidomics and Proteomics. *J. Proteome Res.*14(6), 2367–2384 (2015).

258. Zhao H, Yang L, Baddour J, *et al.* Tumor microenvironment derived exosomes pleiotropically modulate cancer cell metabolism. *Elife* (2016).

259. Shin J, Rhim J, Kwon Y, *et al.* Comparative analysis of differentially secreted proteins in serum-free and serum-containing media by using BONCAT and pulsed SILAC. *Sci. Rep.* (2019).

260. Williams C, Palviainen M, Reichardt NC, Siljander PRM, Falcón-Pérez JM. Metabolomics applied to the study of extracellular vesicles. Available from: Metabolites

261. Li M, Zeringer E, Barta T, Schageman J, Cheng A, Vlassov A V. Analysis of the RNA content of the exosomes derived from blood serum and urine and its potential as biomarkers. *Philos. Trans. R. Soc. Lond. B. Biol. Sci.*369(1652) (2014).

262. Berardocco M, Radeghieri A, Busatto S, *et al.* RNA-seq reveals distinctive RNA profiles of small extracellular vesicles from different human liver cancer cell lines. *Oncotarget* (2017).

263. LIU MX, LIAO J, XIE M, *et al.* miR-93-5p Transferred by Exosomes Promotes the Proliferation of Esophageal Cancer Cells via Intercellular Communication by Targeting PTEN. *Biomed. Environ. Sci.*31(3), 171–185 (2018).

264. Li X, Guo S, Min L, Guo Q, Zhang S. MiR-92a-3p promotes the proliferation, migration and invasion of esophageal squamous cell cancer by regulating PTEN. *Int. J. Mol. Med.*44(3), 973–981 (2019).

265. Casadei L, Calore F, Creighton CJ, *et al.* Exosome-derived miR-25-3p and miR-92a-3p stimulate liposarcoma progression. *Cancer Res.*77(14), 3846–3856 (2017).

266. Lässer C, Alikhani VS, Ekström K, *et al.* Human saliva, plasma and breast milk exosomes contain RNA: uptake by macrophages. *J. Transl. Med.*9, 9 (2011).

267. Crescitelli R, Lässer C, Szabó TG, *et al.* Distinct RNA profiles in subpopulations of extracellular vesicles: apoptotic bodies, microvesicles and exosomes. *J. Extracell. vesicles*2 (2013).

268. Landgraf P, Rusu M, Sheridan R, *et al.* A mammalian microRNA expression atlas based on small RNA library sequencing. *Cell*129(7), 1401–14 (2007).

269. Ludwig N, Leidinger P, Becker K, *et al.* Distribution of miRNA expression across human tissues. *Nucleic Acids Res.*44(8), 3865–77 (2016).

270. Agrawal R, Pandey P, Jha P, Dwivedi V, Sarkar C, Kulshreshtha R. Hypoxic signature of microRNAs in glioblastoma: insights from small RNA deep sequencing. *BMC Genomics*15(1) (2014).

271. Li J, Lee Y, Johansson HJ, *et al.* Serum-free culture alters the quantity and protein composition of neuroblastoma-derived extracellular vesicles. *J. Extracell. Vesicles*4 (2015).

272. Pan JH, Zhou H, Zhao XX, *et al.* Role of exosomes and exosomal microRNAs in hepatocellular carcinoma: Potential in diagnosis and antitumour treatments (Review). Available from: Int. J. Mol. Med.

273. Mannerström B, Paananen RO, Abu-Shahba AG, Moilanen J, Seppänen-Kaijansinkko R, Kaur S. Extracellular small non-coding RNA contaminants in fetal bovine serum and serum-free media. *Sci. Rep.*9(1), 5538 (2019).

274. Maia J, Caja S, Strano Moraes MC, Couto N, Costa-Silva B. Exosome-Based Cell-Cell Communication in the Tumor Microenvironment. *Front. cell Dev. Biol.*6, 18 (2018).

275. Ruivo CF, Adem B, Silva M, Melo SA. The Biology of Cancer Exosomes: Insights and New Perspectives. *Cancer Res.*77(23), 6480–6488 (2017).

276. Othman N, Jamal R, Abu N. Cancer-Derived Exosomes as Effectors of Key Inflammation-Related Players. *Front. Immunol.*10, 2103 (2019).

277. Qu JL, Qu XJ, Zhao MF, *et al.* Gastric cancer exosomes promote tumour cell proliferation through PI3K/Akt and MAPK/ERK activation. *Dig. Liver Dis.* (2009).

278. Li C, Liu DR, Li GG, *et al.* CD97 promotes gastric cancer cell proliferation and invasion through exosome-mediated MAPK signaling pathway. *World J. Gastroenterol.* (2015).

279. O'Brien K, Rani S, Corcoran C, *et al.* Exosomes from triple-negative breast cancer cells can transfer phenotypic traits representing their cells of origin to secondary cells. *Eur. J. Cancer* (2013).

280. Zhang P, Zhou H, Lu K, Lu Y, Wang Y, Feng T. Exosome-mediated delivery of MALATI induces cell proliferation in breast cancer. *Onco. Targets. Ther.* (2018).

281. Yang L, Wu XH, Wang D, Luo CL, Chen LX. Bladder cancer cell-derived exosomes inhibit tumor cell apoptosis and induce cell proliferation in vitro. *Mol. Med. Rep.* (2013).

282. Hood JL, Pan H, Lanza GM, Wickline SA. Paracrine induction of endothelium by tumor exosomes. *Lab. Investig.* (2009).

283. Feng W, Dean DC, Hornicek FJ, Shi H, Duan Z. Exosomes promote pre-metastatic niche formation in ovarian cancer. *Mol. Cancer*18(1), 124 (2019).

284. Chowdhury R, Webber JP, Gurney M, Mason MD, Tabi Z, Clayton A. Cancer exosomes trigger mesenchymal stem cell differentiation into pro-angiogenic and pro-invasive myofibroblasts. *Oncotarget* (2015).

285. Luo F, Sun Z, Han Q, Xue C, Bai C. Effect of human hepatocellular carcinoma HepG2 cell-derived exosome on the differentiation of mesenchymal stem cells and their interaction. *Acta Acad. Med. Sin.* (2017).

286. Fang T, Lv H, Lv G, *et al.* Tumor-derived exosomal miR-1247-3p induces cancer-associated fibroblast activation to foster lung metastasis of liver cancer. *Nat. Commun.*9(1), 191 (2018).

287. Wang S, Xu M, Li X, *et al.* Exosomes released by hepatocarcinoma cells endow adipocytes with tumor-promoting properties. *J. Hematol. Oncol.* (2018).

288. Achreja A, Zhao H, Yang L, Yun TH, Marini J, Nagrath D. Exo-MFA – A 13C metabolic flux analysis framework to dissect tumor microenvironment-secreted exosome contributions towards cancer cell metabolism. *Metab. Eng.*43, 156–172 (2017).

289. Beckler MD, Higginbotham JN, Franklin JL, *et al.* Proteomic Analysis of Exosomes from Mutant KRAS Colon Cancer Cells Identifies Intercellular Transfer of Mutant KRAS. *Mol. Cell. Proteomics*12(2), 343 (2013).

290. Minciacchi VR, Spinelli C, Reis-Sobreiro M, *et al.* MYC Mediates Large Oncosome-Induced Fibroblast Reprogramming in Prostate Cancer. *Cancer Res.*77(9), 2306–2317 (2017).

291. Zhou W, Fong MY, Min Y, *et al.* Cancer-secreted miR-105 destroys vascular endothelial barriers to promote metastasis. *Cancer Cell*25(4), 501 (2014).

292. Sansone P, Savini C, Kurelac I, *et al.* Packaging and transfer of mitochondrial DNA via exosomes regulate escape from dormancy in hormonal therapy-resistant breast cancer. *Proc. Natl. Acad. Sci. U. S. A.*114(43), E9066 (2017).

293. Metsalu T, Vilo J. ClustVis: a web tool for visualizing clustering of multivariate data using Principal Component Analysis and heatmap. *Nucleic Acids Res.*43(W1), W566-70 (2015).

294. Tian W, Liu S, Li B. Potential Role of Exosomes in Cancer Metastasis. *Biomed Res. Int.*2019, 1–12 (2019).

295. Osaki M, Okada F. Exosomes and Their Role in Cancer Progression. *Yonago Acta Med.*62(2), 182–190 (2019).

296. Steinbichler TB, Dudás J, Riechelmann H, Skvortsova I-I. The role of exosomes in cancer metastasis. *Semin. Cancer Biol.*44, 170–181 (2017).

297. Fu Q, Zhang Q, Lou Y, *et al.* Primary tumor-derived exosomes facilitate metastasis by regulating adhesion of circulating tumor cells via SMAD3 in liver cancer. *Oncogene*37(47), 6105–6118 (2018).

298. Kogure T, Lin W-L, Yan IK, Braconi C, Patel T. Inter-cellular nanovesicle mediated microRNA transfer: a mechanism of environmental modulation of hepatocellular cancer cell growth. *Hepatology*54(4), 1237 (2011).

299. Whiteside TL. Tumor-Derived Exosomes and Their Role in Cancer Progression. In: *Advances in Clinical Chemistry* (2016)

300. He X, Yu J, Xiong L, *et al.* Exosomes derived from liver cancer cells reprogram biological behaviors of LO2 cells by transferring Linc-ROR. *Gene*719, 144044 (2019).

301. Lv L-H, Wan Y-L, Lin Y, *et al.* Anticancer drugs cause release of exosomes with heat shock proteins from human hepatocellular carcinoma cells that elicit effective natural killer cell antitumor responses in vitro. *J. Biol. Chem.*287(19), 15874–85 (2012).

302. Bruns AF, Yuldasheva N, Latham AM, *et al.* A Heat-Shock Protein Axis Regulates VEGFR2 Proteolysis, Blood Vessel Development and Repair. *PLoS One*7(11) (2012).

303. Lin X-J, Fang J-H, Yang X-J, *et al.* Hepatocellular Carcinoma Cell-Secreted Exosomal MicroRNA-210 Promotes Angiogenesis In Vitro and In Vivo. *Mol. Ther. - Nucleic Acids*11, 243–252 (2018).

304. Kogure T, Lin W-L, Yan IK, Braconi C, Patel T. Intercellular nanovesicle-mediated microRNA transfer: A mechanism of environmental modulation of hepatocellular cancer cell growth. *Hepatology*54(4), 1237–1248 (2011).

305. Wei J, Lv L, Wan Y, *et al.* Vps4A Functions as a Tumor Suppressor by Regulating the Secretion and Uptake of Exosomal MicroRNAs in Human Hepatoma Cells. *Hepatology*61(4), 1284 (2015).

306. Lin X-J, Chong Y, Guo Z-W, *et al.* A serum microRNA classifier for early detection of hepatocellular carcinoma: a multicentre, retrospective, longitudinal biomarker identification study with a nested case-control study. *Lancet Oncol.*16(7), 804–815 (2015).

307. Emonard H, Duca L, Dedieu S. Editorial: Matricellular Receptors As Potential Targets in Anti-

Cancer Therapeutic Strategies. Available from: Front. Pharmacol.

308. Suhovskih A V., Kashuba VI, Klein G, Grigorieva E V. Prostate cancer cells specifically reorganize epithelial cell-fibroblast communication through proteoglycan and junction pathways. *Cell Adh. Migr.*11(1), 39–53 (2017).

309. Soung YH, Nguyen T, Cao H, Lee J, Chung J. Emerging roles of exosomes in cancer invasion and metastasis. *BMB Rep.*49(1), 18 (2016).

310. Yang S-S, Ma S, Dou H, *et al.* Breast cancer-derived exosomes regulate cell invasion and metastasis in breast cancer via miR-146a to activate cancer associated fibroblasts in tumor microenvironment. *Exp. Cell Res.*391(2), 111983 (2020).

311. Sancho-Albero M, Navascués N, Mendoza G, *et al.* Exosome origin determines cell targeting and the transfer of therapeutic nanoparticles towards target cells. *J. Nanobiotechnology* (2019).

312. Wu W, He X, Andayani D, *et al.* Pattern of distant extrahepatic metastases in primary liver cancer: a SEER based study. *J. Cancer*8(12), 2312–2318 (2017).

313. Ashton TM, McKenna WG, Kunz-Schughart LA, Higgins GS. Oxidative Phosphorylation as an Emerging Target in Cancer Therapy. *Clin. Cancer Res.*24(11), 2482–2490 (2018).

314. Park JE, Dutta B, Tse SW, *et al.* Hypoxia-induced tumor exosomes promote M2-like macrophage polarization of infiltrating myeloid cells and microRNA-mediated metabolic shift. *Oncogene*38(26), 5158–5173 (2019).

315. Qian Y, Wang X, Li Y, Cao Y, Chen X. Extracellular ATP a new player in cancer metabolism: NSCLC cells internalize ATP in vitro and in vivo using multiple endocytic mechanisms. *Mol. Cancer Res.* (2016).

316. Wang X, Li Y, Qian Y, *et al.* Extracellular ATP, as an energy and phosphorylating molecule, induces different types of drug resistances in cancer cells through ATP internalization and intracellular ATP level increase. *Oncotarget* (2017).

317. Cao Y, Wang X, Li Y, Evers M, Zhang H, Chen X. Extracellular and macropinocytosis internalized ATP work together to induce epithelial-mesenchymal transition and other early metastatic activities in lung cancer. *Cancer Cell Int.* (2019).

318. Arslan F, Lai RC, Smeets MB, *et al.* Mesenchymal stem cell-derived exosomes increase ATP levels, decrease oxidative stress and activate PI3K/Akt pathway to enhance myocardial viability and prevent adverse remodeling after myocardial ischemia/reperfusion injury. *Stem Cell Res.*10(3), 301–312 (2013).

319. Recouvreux MV, Commisso C. Macropinocytosis: A Metabolic Adaptation to Nutrient Stress in Cancer. *Front. Endocrinol. (Lausanne).*8, 261 (2017).

320. Maacha S, Bhat AA, Jimenez L, *et al.* Extracellular vesicles-mediated intercellular communication: roles in the tumor microenvironment and anti-cancer drug resistance. *Mol. Cancer*18(1), 55 (2019).

321. Villa E, Ali ES, Sahu U, Ben-Sahra I. Cancer Cells Tune the Signaling Pathways to Empower de Novo Synthesis of Nucleotides. *Cancers (Basel).*11(5) (2019).

322. Tong X, Zhao F, Thompson CB. The molecular determinants of de novo nucleotide biosynthesis in cancer cells. *Curr. Opin. Genet. Dev.*19(1), 32–7 (2009).

323. Lane AN, Fan TW-M. Regulation of mammalian nucleotide metabolism and biosynthesis. *Nucleic Acids Res.*43(4), 2466–85 (2015).

324. Saari H, Lázaro-Ibáñez E, Viitala T, Vuorimaa-Laukkanen E, Siljander P, Yliperttula M. Microvesicle- and exosome-mediated drug delivery enhances the cytotoxicity of Paclitaxel in autologous prostate cancer cells. *J. Control. Release*220, 727–737 (2015).

325. Hadla M, Palazzolo S, Corona G, *et al.* Exosomes increase the therapeutic index of doxorubicin in breast and ovarian cancer mouse models. *Nanomedicine*11(18), 2431–2441 (2016).

326. Rao Q, Zuo B, Lu Z, *et al.* Tumor-derived exosomes elicit tumor suppression in murine hepatocellular carcinoma models and humans in vitro. *Hepatology*64(2), 456–472 (2016).